SYNTHESIS AND LABELING STRATEGY FOR INDIRECT DETECTION OF ESTROGEN-DERIVED DNA ADDUCTS USING AQUEOUS QUANTUM DOTS

by

MAUSAM KALITA

M.S. University of Delhi, 2003

AN ABSTRACT OF A DISSERTATION

submitted in partial fulfillment of the requirements for the degree

DOCTOR OF PHILOSOPHY

Department of Chemistry
College of Arts and Sciences

KANSAS STATE UNIVERSITY
Manhattan, Kansas

2010

Abstract

Estrogen-derived DNA adducts in human could be the initiating step of breast and prostate cancer, as the scientific literature suggests. Previous studies demonstrated that 4-hydroxy-estrone (estradiol)-1-N3Adenine and 4-hydroxy-estrone (estradiol)-1-N7Guanine were the most abundant adducts found in urine of human subjects. Sensitive detection of these adducts in urine samples could lead to better breast and prostate cancer risk assessment. The standard adducts were synthesized and characterized by NMR and mass spectrometry. Since these adducts are not fluorescent at room temperature an aminomethyl ($-CH_2NH_2$) linker was introduced at the C-17 position for derivatization with fluorescence label. This linker allowed to attach highly fluorescent water soluble quantum dots (QDs) for indirect adduct detection. A direct gram-scale synthesis of highly fluorescent, photostable water soluble QDs was executed by developing a new class of 4,4'-bipyridinium salt based twin ligands with 85% and 15% of carboxylic acid and maleimide termini, respectively. These ligands not only stabilized the QDs in water but also provided versatile linkers for two labeling strategies. The twin ligands were afforded by a facile synthesis through S_N2 nucleophilic substitution reaction. Labeling of adducts was achieved via a covalent coupling between the ($-CH_2NH_2$) linker and the carboxyl (-COOH) terminal ligand on the QDs. However, ELISA experiments utilizing an IgM antibody didn't reveal any measurable signal from adduct-QD complexes suggesting that one QD is bound to a large number of adducts through –COOH terminal ligands present on QD surface. To explore the binding capabilities of QDs in more detail, a maleimide terminal ligand (a twin partner on the QDs) was synthesized to explore the thiol (-SH) functionality of thiopyrene. Preliminary ELISA showed that these QDs gave detectable fluorescent signal originating from the [pyrene-S-QD]− 8E11 monoclonal antibody (mAb) complex when QD was selectively excited at 470 nm. This clearly indicates that it is necessary to develop a strategy for a distinct 1:1 labeling procedure between QD and the adduct of interest. In addition, IgG (instead of IgM) antibodies should be developed for biosensor application. The latter could afford binding of mAb in upright position, leading to an increase in surface density of mAb and better detection limit.

SYNTHESIS AND LABELING STRATEGY FOR INDIRECT DETECTION OF ESTROGEN-DERIVED DNA ADDUCTS USING AQUEOUS QUANTUM DOTS

by

MAUSAM KALITA

M.S. University of Delhi, 2003

A DISSERTATION

submitted in partial fulfillment of the requirements for the degree

DOCTOR OF PHILOSOPHY

Department of Chemistry
College of Arts and Sciences

KANSAS STATE UNIVERSITY
Manhattan, Kansas

2010

Approved by:

Major Professor
Stefan H. Bossmann

Abstract

Estrogen-derived DNA adducts in human could be the initiating step of breast and prostate cancer, as the scientific literature suggests. Previous studies demonstrated that 4-hydroxy-estrone (estradiol)-1-N3Adenine and 4-hydroxy-estrone (estradiol)-1-N7Guanine were the most abundant adducts found in urine of human subjects. Sensitive detection of these adducts in urine samples could lead to better breast and prostate cancer risk assessment. The standard adducts were synthesized and characterized by NMR and mass spectrometry. Since these adducts are not fluorescent at room temperature an aminomethyl ($-CH_2NH_2$) linker was introduced at the C-17 position for derivatization with fluorescence label. This linker allowed to attach highly fluorescent water soluble quantum dots (QDs) for indirect adduct detection. A direct gram-scale synthesis of highly fluorescent, photostable water soluble QDs was executed by developing a new class of 4,4'-bipyridinium salt based twin ligands with 85% and 15% of carboxylic acid and maleimide termini, respectively. These ligands not only stabilized the QDs in water but also provided versatile linkers for two labeling strategies. The twin ligands were afforded by a facile synthesis through S_N2 nucleophilic substitution reaction. Labeling of adducts was achieved via a covalent coupling between the ($-CH_2NH_2$) linker and the carboxyl (-COOH) terminal ligand on the QDs. However, ELISA experiments utilizing an IgM antibody didn't reveal any measurable signal from adduct-QD complexes suggesting that one QD is bound to a large number of adducts through –COOH terminal ligands present on QD surface. To explore the binding capabilities of QDs in more detail, a maleimide terminal ligand (a twin partner on the QDs) was synthesized to explore the thiol (-SH) functionality of thiopyrene. Preliminary ELISA showed that these QDs gave detectable fluorescent signal originating from the [pyrene-S-QD]− 8E11 monoclonal antibody (mAb) complex when QD was selectively excited at 470 nm. This clearly indicates that it is necessary to develop a strategy for a distinct 1:1 labeling procedure between QD and the adduct of interest. In addition, IgG (instead of IgM) antibodies should be developed for biosensor application. The latter could afford binding of mAb in upright position, leading to an increase in surface density of mAb and better detection limit.

Table of Contents

List of Figures

List of Tables

Acknowledgements

Words cannot explain the intellectual contribution of both of my PhD mentors, Professor Stefan H. Bossmann and Professor Ryszard Jankowiak. Prof. Bossmann always encouraged me to think outside the box and to take the risk of applying new ideas to my bench-work. He inspired me to present talks in many American Chemical Society conferences, contributing to my ability in public speaking. My highly collaborative research was possible due to unrelenting support of both of my professors. Prof. Jankowiak gave me an opportunity to work in the University of Nebraska Medical Center (UNMC), Omaha from June, 2009 to August, 2009, which expanded my research experience. Discussions with him helped me immensely in figuring out research problems. He also has taught me the value of precise measurements.

I would like to express my gratitude to Prof. Ercole Cavalieri, Prof. Eli Rogan and their post-doctoral student Dr. Muhammad Saeed, who mentored me when I worked at UNMC, Omaha. Prof. Kenneth J. Klabunde and his graduate student, Dr. Sreeram Cingarapu deserve acknowledgement for their contributions in synthesizing water soluble quantum dots (QDs) through Solvated Metal Atom Dispersion (SMAD) followed by digestive ripening. ELISA experiments were carried out in Prof. Deryl Troyer's lab in the Department of Anatomy and Physiology, Veterinary Medicine, for which he deserves my high regard. I thank Prof. Dan Higgins and his graduate student Seok Chan Park for helping me in studying the photostability of QDs.

I also like to thank both the Jankowiak and Bossmann group members, especially Dr. Tej B. Shrestha for valuable discussions and for providing me with thiopyrene for use in the ELISA experiment. I thank Katrin Bossmann for her corrections of the general English of my PhD thesis and credit seminars, the Chemistry Department's glass blower James Hodgson and our NMR manager Dr. Leila Maurmann for their contributions during my PhD.

I do thank Roshi, Aditya, Amit, Ola, Sanmitra, Prashant, Lateef, Khem, Bhanu for their wonderful friendship and care during my PhD career.

Finally, I would like to thank my amazing parents for installing my desire for scientific investigation and logical analysis. I also extent my special thanks to my teachers, Subrata Kumar Barua and Jogendra Nath Kalita, who not only taught Organic Chemistry and English literature , respectively, but also inspired me to question everything.

Dedication

To my teachers who contributed and continue to contribute to my intellectual evolution through both direct and indirect interactions

Asato maa sadgamaya

Tamaso maa jyotirgamaya

Mṛityor maa amṛitan gamaya

Om shaanti shaanti shaanti

From the unreal, lead us to the Real;

from darkness, lead us unto Light;

from death, lead us to Immortality.

Om peace, peace, peace.

Preface

In the summer of 2008, Dr. Tej Shrestha, who was a graduate student in the Bossmann group at that time, and I were working on a project to synthesize a photochromic switch. I was involved in introducing a maleimide functionality to 4,4'-bipyridine, which Tej was going to use to synthesize the photochromic spirodihydroindolizine (DHI) switch. This led to the synthesis of maleimide derivative of a 4,4'-bipyridinium salt. At that time, I was also struggling to synthesize a ligand, which can stabilize quantum dots (QDs) in water. The idea of using the maleimide derivative of 4,4'-bipyridinium salt appealed to me. We were able to synthesize CdSe QDs by using this ligand but the QDs were hardly water soluble. This made me develop more synthetic modifications to design a ligand, which is water-soluble before and after nanoparticle surface stabilization. Tej was also involved in synthesizing a carboxylic acid derivative of 4,4'-bipyridinium salt, which was readily dissolved in water. Our conversation convinced me that this compound should make QDs water soluble through carboxyl functional group on this ligand, even after QD surface stabilization through the lone pair of the sp^2-nitrogen on 4,4'-bipyridine. I decided to use about 85% of the carboxylic acid and 15% of the maleimide derivative of the 4,4'-bipyridinium salt ligand. This resulted in the first direct synthesis of water soluble QDs by applying an evaporation-co-condensation-reflux technique with two ligands to be used for double labeling. This was a great learning experience for me in the sense that one molecule can be used to solve more than one research problem.

A similar technique is used by nature to solve biochemical problems. For example, cyclic adenosine monophosphate (cAMP) is a secondary messenger used by bacterium *E. coli* to signal hunger and is recruited by neurons for memory storage. The cAMP pathway is also used by the kidney and the liver to bring about metabolic changes. Thus, evolution does not synthesize an entirely new compound to produce a new adaptive mechanism. The molecular geneticist François Jacob writes," Evolution is not an original engineer that sets out to solve new problems with completely new sets of solutions. Evolution is a tinkerer. It uses the same collection of genes time and again in slightly different ways."

Research in the laboratory offers one solution to more than one problem. Using one molecule to solve multiple problems reduces not only waste in terms of money and time, but also in terms of intellect.

CHAPTER 1 - Introduction

According to the American Chemical Society, breast cancer is the dominant cause of death of women in US.[1] In 2010, 207,090 women will be diagnosed with breast cancer. 39,840 will have to die from this type of cancer. (http://www.cancer.gov/cancertopics/types/breast). The National Cancer Institute estimated that 217,730 men will be diagnosed with and 32,050 men will die of cancer of the prostate in 2010. (http://seer.cancer.gov/statfacts/html/prost.html) Noninvasive diagnosis of breast and prostate cancer risk will be an easy and effective way to enhance the standard of human life and to prolong the patients' life itself. The gender hormone estrogen is known to act as mild carcinogen, probably initiating breast cancer.[2, 3] It is hypothesized that the oxidation of estrogen forms catechol estrogen quinines and estrone (estradiol) quinones [$E_1(E_2)$-Q], which in turn react with DNA initiating breast cancer.[4] Thus, catechol estrogen quinones are endogenous chemical carcinogens which form specific depurinating estrogen-DNA adducts, predominantly, 4-hydroxyestrone(estradiol)-1-N3Adenine [4-$OHE_1(E_2)$-1-N3Ade] and 4-hydroxyestrone(estradiol)-1-N7Guanine [4-$OHE_1(E_2)$-1-N7Gua]. Both are leading to cell transformation.[5, 6, 7] DNA-estrogen adducts are released from the affected cells into the blood stream and finally, are excreted in urine. These adducts are potential biomarkers for both breast and prostate cancer. A diagnosis tool based on monoclonal antibodies (MAbs) has been sought to develop in order to investigate the hypothesis that metabolically activated endogenous estrogens are involved in the initiation of breast and prostate cancers. Highly sensitive detection of various estrogen derived biomarkers in urine samples of breast and prostate cancer patients and healthy control subjects is the objective of this approach. This involves the chemical synthesis of standard estrogen-DNA adducts and their structural modifications of these adducts for the conjugation of fluorescent tags and the N418 antibody in order to target dendritic cell (DC), professional antigen presenting cells to raise IgG antibody against these adducts.[8] In addition, water soluble, highly fluorescent, stable quantum dots (QDs) were synthesized in order to enhance the sensitivity of the biomonitoring technique for cancer risk by improving the limit of detection of estrogen-derived DNA adducts.

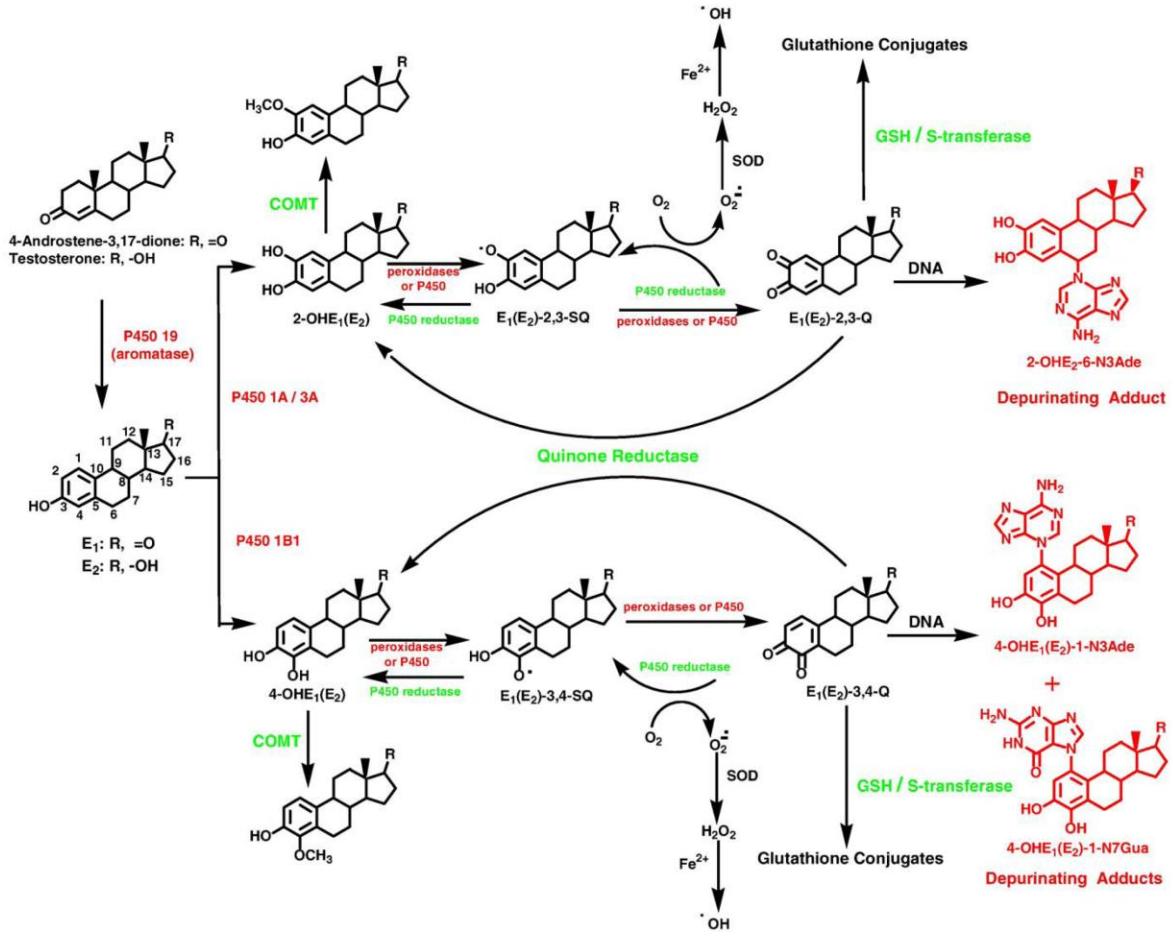

Fig 1.1 Biosynthesis and metabolic activation/deactivation pathways of the estrogens, E_1 and E_2[9]

1.1. Biomarkers of Breast Cancer Risk

Metabolic activation pathways of estrogen lead to the formation of estrogen quinines, which can act as endogeneous chemical carcinogens unless the deactivation pathways are switched on. (Fig 1.1) [9] The quinones react with DNA forming DNA-estrogen adducts that initiate point mutations on the DNA double helix. On the contrary, the deactivation pathway involves methylation of catechol derivatives to form methoxy catechol estrogens,[10] reduction of quinones by quinone reductase [11] and conjugation of quinones with glutathione (GSH).[12]

A study of depurinating estrogen-DNA adducts in the urine of healthy women, high-risk women (Gail Model score >1.66%) and women with breast cancer found that N3Ade and N7Gua adducts of 4-$OHE_1(E_2)$ play a major role, whereas the adducts of 2-$OHE_1(E_2)$ play a minor role. (Fig 1.2)[13] The results of this study are consistent with the hypothesis that DNA-estrogen adducts

are a causative factor in the etiology of breast cancer. The Y-axis of the Figure 2 represents the ratio of depurinating DNA adducts divided by their respective estrogen metabolites and conjugates.

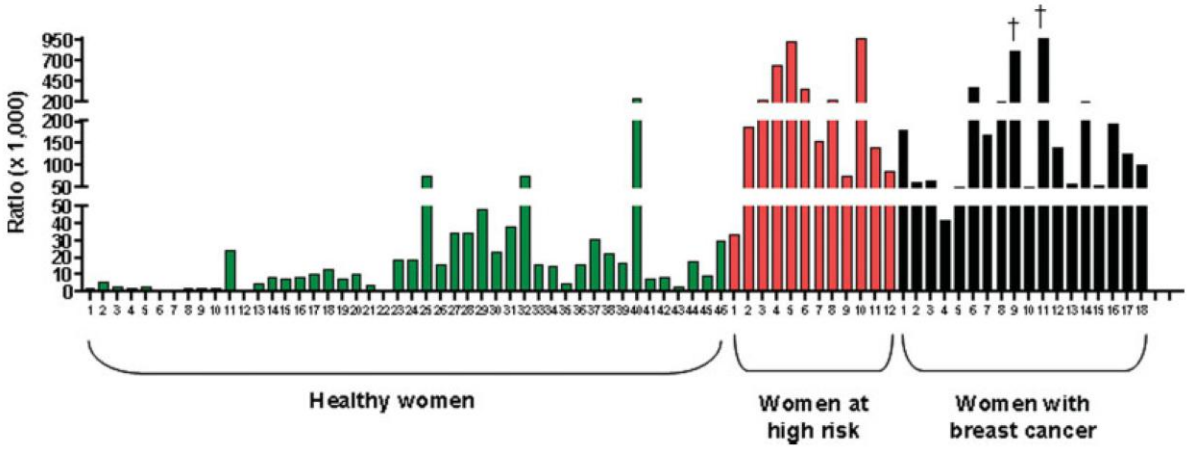

Fig 1.2 N3Ade and N7Gua adducts of 4-OHE$_1$(E_2) and 2-OHE$_1$(E_2) in the urine of healthy women, high risk women and women with breast cancer [13]

1.1.1. Estrogens As Tumor Initiators

The hypothesis that estrogen can act as epigenetic carcinogen was supported by the discovery that specific oxidative metabolites of estrogen can react with DNA resulting in cancer initiation in hormone-dependent and independent tissues.[14, 15, 16, 17] This hypothesis is based on experiments on estrogen metabolism,[18, 19, 20] formation of DNA adducts,[21, 22, 23]carcinogenicity,[24, 25] mutagenicity[14, 15, 16, 17] and cell transformation.[26, 27, 28] Highly reactive CE-3, 4-Q and, to a lesser extent, CE-2, 3-Q, initiate electrophilic substitution reactions at purine bases of DNA leading to point mutations which in turn, initiate breast, prostate cancer.[17]

Similar redox potentials of both 4-OHE$_1$ (E_2) and 2-OHE$_1$ (E_2) suggest that the greater carcinogenicity of 4-OHE$_1$ (E_2) than 2-OHE$_1$(E_2) is attributed to much higher level of depurinating DNA adducts formed by E$_1$(E_2)-3, 4-Q compared to E$_1$(E_2)-2, 3-Q.[29]

Both breast and prostate cancer is preceded by the imbalance estrogen homeostasis as evidenced by overexpression of CYP19 in target tissues[30, 31, 32] and/or the presence of unregulated sulfatase that converts excess stored E$_1$-sulfate to E$_1$. [33, 34] It has also been observed that there is more E_2 present in target tissues than would be predicted from plasma concentrations. A level of

catechol-O-methyltransferase (COMT) activity is responsible for insufficient methylation of 4-$OHE_1(E_2)$, making it susceptible for oxidation into catechol quinones.[35] Paucity of GSH and/or quinone reductase and/or CYP reductase could result in a higher level of $E_1(E_2)$-3, 4-Q, leading to DNA mutation.

A study to compare the levels of estrogen and DNA-derived estrogen metabolites in breast tissue of women with breast cancer and healthy control subjects suggests that higher estrogen hormone levels exist in women with carcinoma than in controls. In addition, the levels of 4-$OHE_1(E_2)$ are four times higher in women with breast cancer than in the control group. (Fig 1.3)[20]

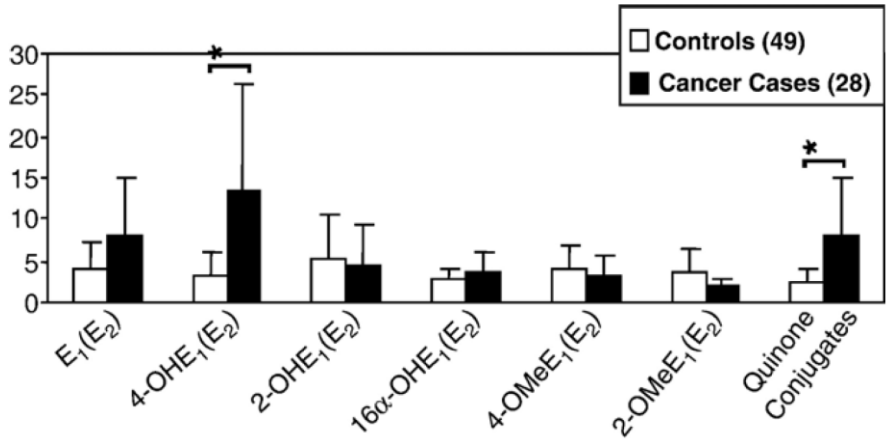

Fig 1.3 Relative abundances of estrogen metabolites in non-tumor breast tissue of women with breast cancer vs. control[20]

1.1.2. In vitro/in vivo evidence of estrogen-induced carcinogenesis

In vivo studies on severely compromised immune-deficient (SCID) mice and in vitro studies on human breast epithelium, ER-α negative MCF-10F cells, respectively, showed that E_2 and its metabolites are mutagenic. Colony efficiency of MCF-10F was used to determine the carcinogenicity of E_2, 2-OHE_2, 4-OHE_2 or 16α-OHE_2 and it was found that colony efficiency and invasiveness of E_2 and 4-OHE_2 treated cells was greater than of the other two.[36] When 0.007 nM or 70 nM doses of E_2 or 4-OHE_2 was administered, ER-α negative MCF-10F cells were transformed exhibiting loss of heterozygosity (LOH) in the region 13q12.3. The same doses also induce a 5-bp deletion in TP53 exon 4 of chromosome 17 in cells.[37] The mutagenic pathway is estrogen receptor pathway independent as anti-estrogen did not prevent any mutation.

1.2. Biomarkers of Prostate Cancer Risk

The relationship between estrogens and prostate cancer is less than concrete.[38] The higher levels of estrogen observed in African American men may be responsible for twofold higher risk of prostate cancer compared with European-American men.[39] Testosterone and estrogen experiments performed on Noble rats showed that 100% of rats had ductal adenocarcinoma of the prostate upon combined treatment but, 40% of rats developing prostate cancer upon only testosterone treatment. However, only 4% incidence of prostate cancer was reported upon treatment with 5α-dihydrotestosterone which cannot be converted to E_2, which is suggested resulting from estrogen induced initiation and testosterone induced promotion of prostate cancer.[40, 41]

Three analytical methods have been used to determine possible biomarkers for human prostate cancer. N7Gua and N3Ade adducts of 4-OHE_1- and 4-OHE_2 are strongly phosphorescent when excited at 257 nm in a high energy laser at 77K, with limit of detection (LOD) in the low femtomole range.[42] Capillary electrophoresis with field amplified sample stacking (FASS) achieved the limit of detection of the estrogen metabolites in ~3 X 10^{-8} M range.[43, 44] A monoclonal antibody (MAb) based technique was used to identify 4-OHE_1-1-N3Ade adduct in human urine samples from men with prostate cancer and healthy men as controls. The urine samples were analyzed using an immunoaffinity column packed with MAb developed against the 4-OHE_1-1-N3Ade adducts. These adducts eluted from the immunoaffinity columns were analyzed by laser-excited 77K luminescence spectroscopy and liquid chromatography interfaced with tandem mass spectrometry (LC/MS/MS). The urine samples were also further analyzed by capillary electrophoresis with FASS and detected by absorbance based electrograms. (Fig 3)[43] MAb based biosensor has the potential to detect the DNA-estrogen adducts in urine samples of prostate and breast cancer making it a possible commercial tool of diagnosis.

LC/MS/MS played an important role in assigning the peaks of the samples eluted from the immunoaffinity columns. The daughter peaks m/z 135.9 and 296.0 were obtained from fragmentation of 4-OHE_1-1-N3Ade adduct parent ion, m/z 420.1 suggesting that this adduct may be a biomarker for the risk of developing prostate cancer. (Fig 1.4)[43]

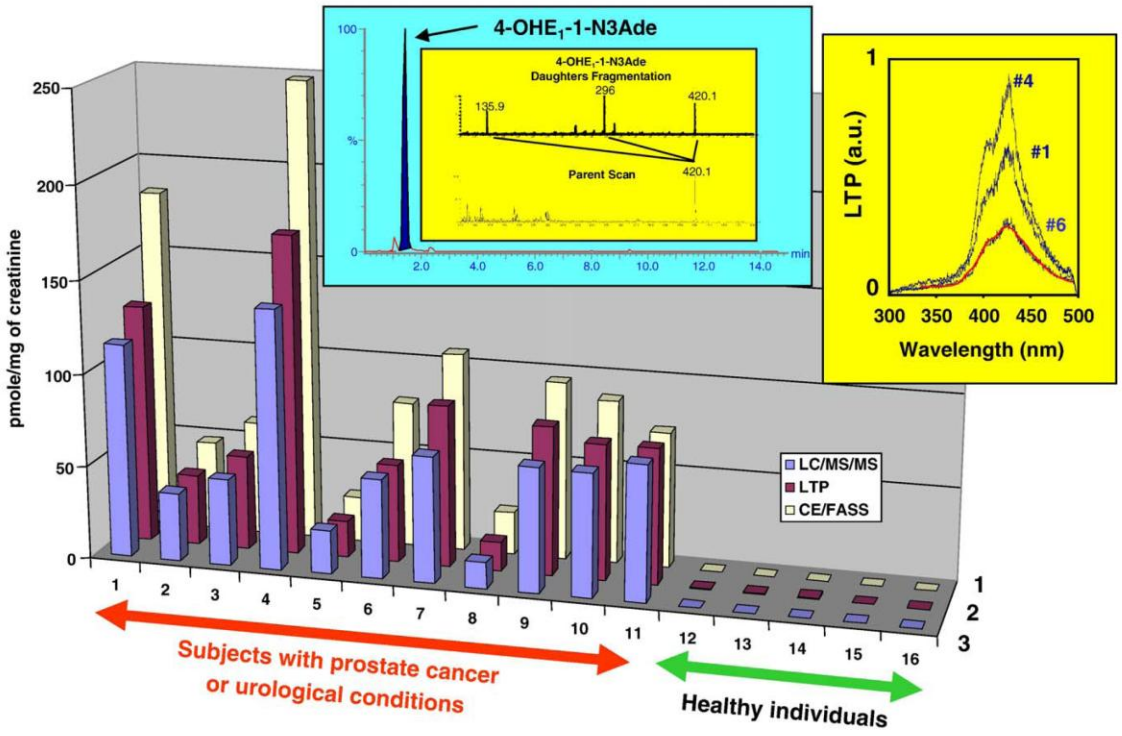

Fig 1.4 Detection of 4-OHE_1-1-N3Ade adduct in human urine samples with prostate cancer and healthy men as controls. Right inset: phosphorescence spectrum for sample 1, 4 and 6 at 77K, Left inset: LC/MS/MS for sample 11 showing the 4-OHE_1-1-N_3Ade peak at m/z 420.1 and its fragmentations[43]

2. Quantum Dots: A Brief Overview

Quantum dots, which form the smallest regime of nanoparticles, are semiconductor nanocrystals of the sizes between 2 and 10 nm. They have size- and composition-tunable electronic and optical properties with sharp, Gaussian-type emission spectra. The following table 1.1 shows the large absorption coefficient of quantum dots across a wide spectral range.[45] These are definite advantages of quantum dots over traditional dyes as imaging agent *in vivo* and *in vitro.*

Quantum dots are semiconductors composed of atoms from groups II-VI or III-V elements of periodic table[46] e.g. CdSe. CdTe, InP etc. Their brightness is attributed to the quantization of energy levels due to confinement of an electron in a three dimensional box. The optical properties of these dots can be manipulated by a shell around it. Such dots are known as core-shell quantum dots. e.g. CdSe-ZnS, InP-ZnS, InP-CdSe etc.

Table 1.1. Size and composition tunable properties of quantum dots (www.evidenttech.com)[45]

Material System	Type	Color	Emission Peak [nm]	Emission Peak Tolerance	Typical FWHM [nm]	Suggested Excitation [nm]	1st Exciton Peak [nm-nominal]	Crystal Diameter[a] [nm-approx.]	Molar Extinction Coefficient at 1st Exciton[b] [10^5]	Molecular Weight[c] [µg/nmol]	Approx. Quantum Yield[d]
CdSe	Core	Forget-me-not Blue	465	+/-10	N/A[e]	<400	445	1.9	0.32	3	N/A
CdSe	Core	Spearmint Green	500	+/-10	N/A	<400	480	2.1	0.45	8.4	N/A
CdSe	Core	Amaranth Green	520	+/-10	<30	<400	510	2.4	0.59	14	N/A
CdSe	Core	Aloe Green	545	+/-10	<30	<400	530	2.6	0.77	20	N/A
CdSe	Core	Hawkweed Orange	570	+/-10	<30	<400	560	3.2	1.3	38	N/A
CdSe	Core	Poppy Red Orange	595	+/-10	<30	<400	585	4.0	2.3	78	N/A
CdSe	Core	Begonia Red	620	+/-10	<30	<400	610	5.2	4.5	200	N/A
CdSe	Core	Aster Red[f]	640	+/-10	<30	<400	635	6.8	9.4	580	N/A
CdSe/ZnS	Core-Shell	Lake Placid Blue	490	+/-10	<40	<400	470	1.9	0.40	2.7	30%-50%
CdSe/ZnS	Core-Shell	Adirondack Green	520	+/-10	<35	<400	505	2.1	0.55	9	30%-50%
CdSe/ZnS	Core-Shell	Catskill Green	540	+/-10	<30	<400	525	2.4	0.72	14	30%-50%
CdSe/ZnS	Core-Shell	Hops Yellow	560	+/-10	<30	<400	545	2.6	0.98	20	30%-50%
CdSe/ZnS	Core-Shell	Birch Yellow	580	+/-10	<30	<400	570	3.2	1.6	38	30%-50%
CdSe/ZnS	Core-Shell	Fort Orange	600	+/-10	<30	<400	590	4.0	2.6	74	30%-50%
CdSe/ZnS	Core-Shell	Maple Red-Orange	620	+/-10	<30	<400	610	5.2	4.5	180	30%-50%
CdTe/CdS[g]	Core-Shell	Macintosh Red	620	+/-10	<40	<450	605	3.7	1.6	100	30%-50%
CdTe/CdS[g]	Core-Shell	Cortland Red	640	+/-10	<35	<450	630	4.0	2	120	30%-50%
CdTe/CdS[g]	Core-Shell	Rome Red	660	+/-10	<35	<450	650	4.3	2.3	150	30%-50%
CdTe/CdS[g]	Core-Shell	Empire Red	680	+/-10	<35	<450	670	4.8	2.9	220	30%-50%

2.1. Electronic and Optical Properties of Quantum Dots

A quantum dot, also often called an artificial atom, represents the electron confinement in a sphere smaller than its exciton (electron-hole) Bohr radius which gives rise to discrete energy levels. The band gap, ΔE, between the valance and conduction band of the semiconductor is a function of the nanocrystal's size. (Fig 1.5)

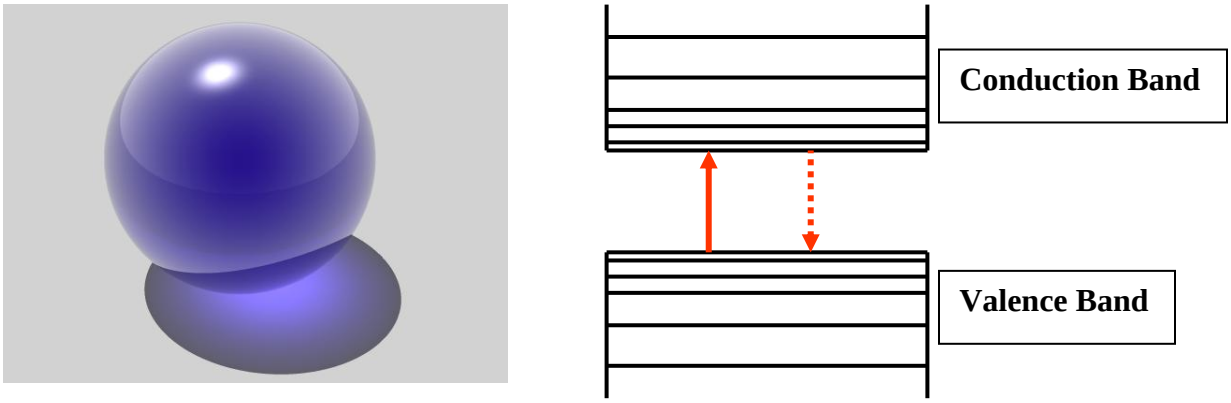

A **B**

Fig 1.5 A. electron confinement in a sphere **B.** a typical semiconductor with band gap, Δ E, between the valance band and conduction band

As the quantum dot size increases, ΔE decreases and there is a red shift in the first excitation peak. The emission can be tuned to even the far-red and near-infrared (NIR) region by increasing the size. Electronic excitations at short wavelengths are possible due to presence of multiple electronic states as the quantum dot size increases.[46] Large molar extinction coefficients across a wide spectral range allow in simultaneous excitation of multiple color Q-dots with single light source. (Fig 1.6)

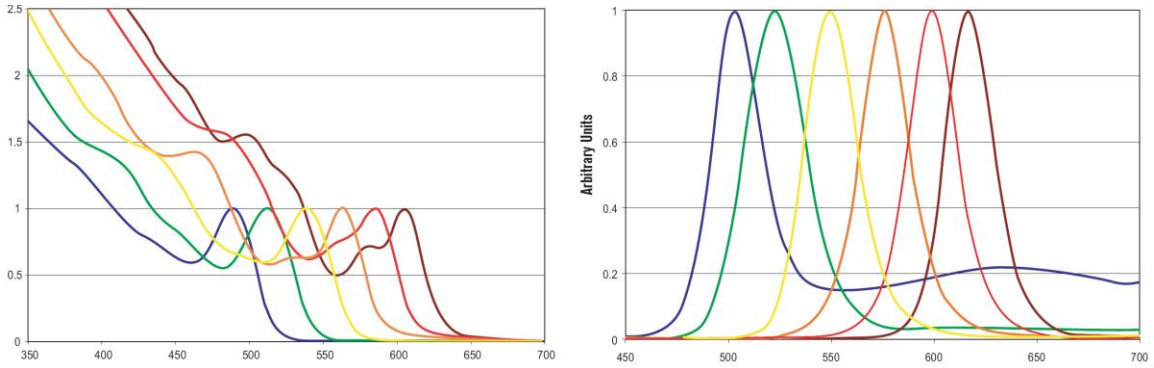

A **B**

Fig 1.6 A. Absorption Spectra and **B.** Emission Spectra of CdSe quantum dots. As the Q-dot size increases the absorption and emission maxima shift to longer Wavelength (or, red shift) (www.evidenttech.com).

These dots have slightly lower quantum yield than the traditional organic dyes, but they have much larger absorption cross-sections and low rate of photobleaching. Molar extinction coefficients of Q-dots are about $10^5 – 10^6$ M^{-1} cm^{-1} which are 10-100 times larger than dyes. [47, 48]

2.2. Surface modification of quantum dots for biocompatibility

Quantum dots are synthesized in organic solvents and therefore, incompatible to use *in vivo* and *in vitro*. Q-dot solubilization in aqueous phase can be achieved by attaching these dots with polar ligands. The tri-(n-octyl) phosphine oxide passivated quantum dot surface can be functionalized by adding a layer of amphiphilic molecules such as cross-linked polymer shell [49], amphiphilic triblock copolymer [50] or phospholipids micelles.[51] (Fig 1.7) [52]

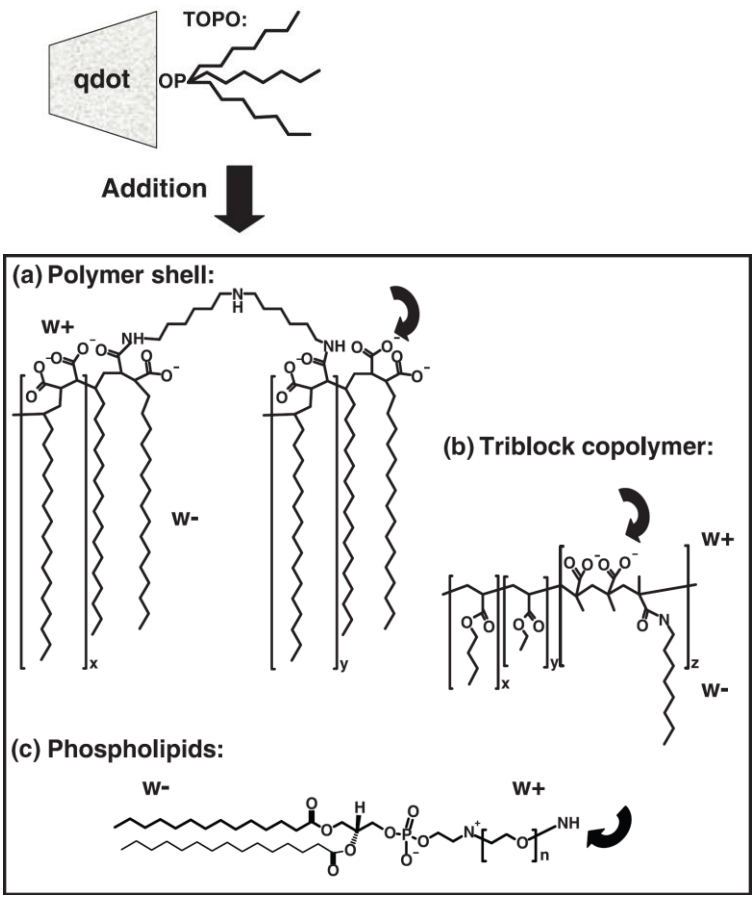

Fig 1.7 Quantum dot functionalization to solubilize in aqueous buffer by adding amphiphilic polymer coat around TOPO passivated Q-dot surface[52]

TOPO exchange with other ligands such as thiol,[53] amine,[54] containing molecules can bring the Q-dot from the nonpolar organic to polar aqueous layer. (Fig 1.8)[52]

The direct synthesis of water soluble QDs is hardly reported in literature. Twin ligands based on a 4,4'-bipyridinium salt were synthesized to use as QD surface stabilizing ligands during quantum dot synthesis by using the Solvated Metal Atom Dispersion (SMAD) technique. Narrowing of QD size distribution was achieved by digestive ripening.

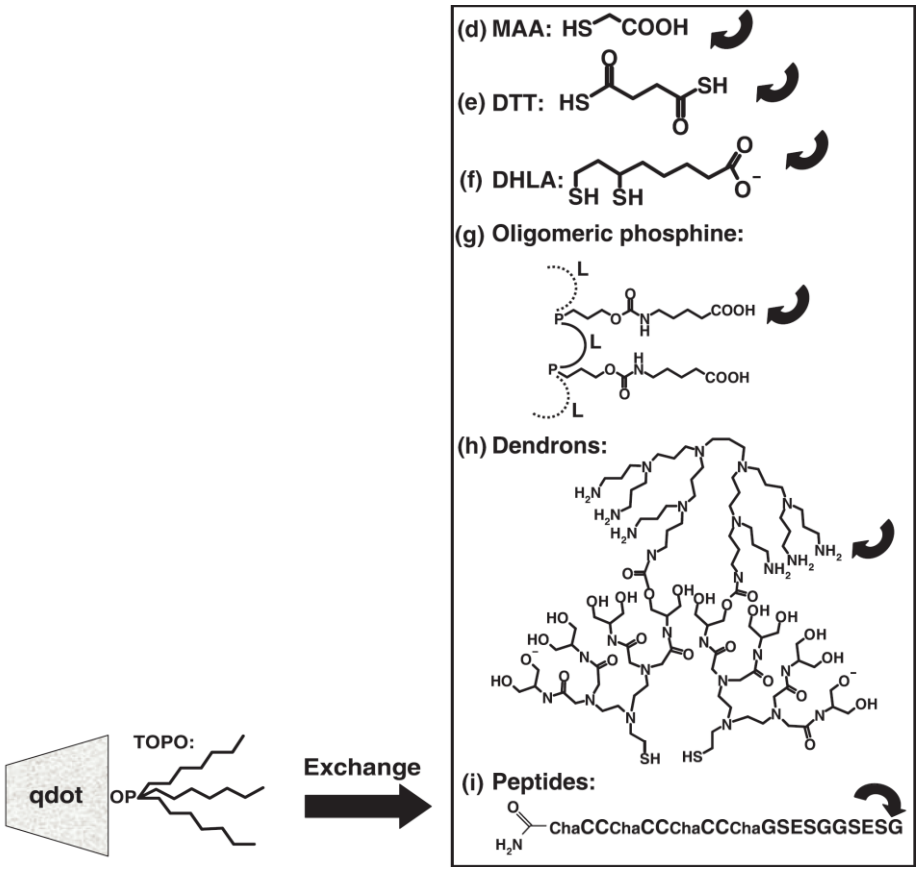

Fig 1.8 Ligand exchange is another way to functionalize the Q-dots to enhance its biocompatibility[52]

Use of amphiphilic poly(acrylic acid) as a primary coat on Q-dots followed by methoxy-terminated poly-(ethylene glycol) (mPEG) coating makes them biocompatible for *in vivo* imaging of lymph nodes, liver, spleen and bone marrow of mice.[55] PEGylation of Q-dots reduces its uptake by reticuloendothelian system and thereby increases circulating lifetime. Other ligands such as streptavidin to detect Her2 cancer markers,[56] secondary antibodies to detect the integrin α_v subunit in SK-N-SH human neuroblastoma cells[57] and recognition peptides for protein recognition[57] are also used to link the quantum dots.

3. Research Plans and Executions

The chemical synthesis of DNA-estrogen adducts is essential for indirect detection of these adducts present in women of high-risk and breast cancer subjects. Two structural modifications of the DNA-derived estrogen adducts are important for (a) labeling of water soluble QDs through

aminomethyl (-CH_2NH_2) linker for fluorescent imaging in order to lower the limit of detection of these adducts and (b) labeling of N418 MAbs through carboxyl linker (-COOH) for DC targeted immunological response in host animal in an attempt to generate MAbs against DNA-estrogen adducts. (Figure 1.9)

A **B**

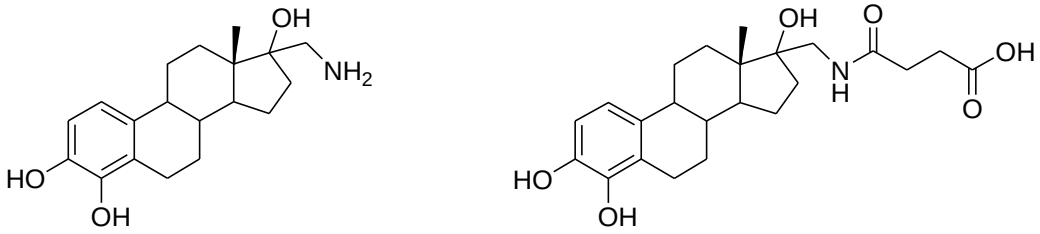

Fig 1.9 (A) 4-OH-E_2-17-aminomethane for labeling of QDs through –CH_2NH_2 group; (B) 4-OH-E_2-17-amidopropanoic acid for N418 MAb labeling through carboxylic acid group (-COOH)

The challenges of synthesizing water soluble QDs are met with the synthesis of novel twin ligands based on a 4,4'-bipyridinium salt. (Fig 1.10) These ligands are used to stabilize the surface of CdSe and CdTe QDs and to make them water soluble. This direct synthesis of aqueous QDs is carried out by using solvated metal atom dispersion (SMAD) followed by narrowing of size distribution through digestive ripening.[58] DNA-estrogen adducts are labeled with these QDs covalently and sought to use them for a biomonitoring technique.

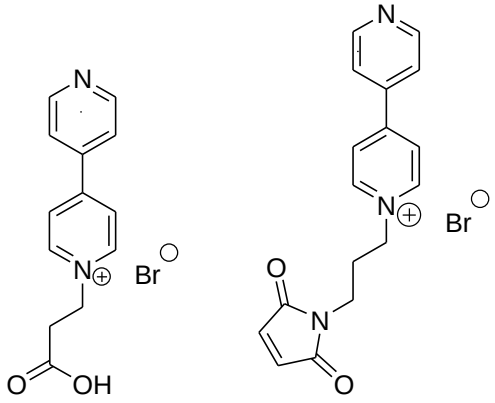

Fig 1.10 A new class of 4,4'-bipyridinium salt based ligands has been synthesized to obtain aqueous QDs

Future direction of this research involves the use of QD labeled DNA-derived estrogen adducts to develop MAb based biosensors on glass, polymer and/or silicon wafer substrates with multiple patches on the surfacefor sensitive and selective detection of estrogen derived biomarkers based

on a novel “first-come-first-serve” approach. This approach will provide excellent methodology for identification of estrogen derived biomarkers and cost-effective devices for future clinical applications.

References

1. Cancer Facts and Figures 2010, American Cancer Society; www.cancer.org
2. Key, T.; Appleby, P.; Barnes, I.; Reeves, G. *J. National Cancer Institute*, **2002**, *94*, 606-616.
3. Kaaks, R.; Berrino, F.; Key, T.; Rinaldi, H.; Dossus, L.; Biessy, C.; Secreto, G.; Amiano, P.; Bingham, S.; Boeing, H.; Bueno de Mesquita, H. B.; Chang-Claude, *J. National Cancer Institute*, **2005**, *97*, 755-765.
4. Cavalieri, E.; Chakravarti, D.; Guttenplan, J.; Hart, E.; Ingle, J.; Jankowiak, R.; Muti, P.; Rogan, E.; Russo, J.; Santen, R.; Sutter, T. *Biochem Biophys Acta*, **2006**, *1766*, 63-78.
5. Cavalieri, E.; Stack, D. E.; Devanesan, P. D.; Todorovic, R.; Dwivendy, I.; Higginbotham, S.; Johansson, S. L.; Patil, K. D.; Gross, M. L.; Gooden, J. K.; Ramanathan, R.; Cerny, R. L. *Proc. Natl. Acad. Sci. USA*, **1997**, *94*, 10937-10942.
6. Li, K. M.; Todorovic, R.; Devanesan, P.; Higginbotham, S.; Kofeler, H.; Ramanathan, R.; Gross, M. L.; Rogan, E. G.; Cavalieri, E. L. *Carcinogenesis*, **2004**, *25*, 289-297.
7. Zahid, M.; Kohli, E.; Saeed, M.; Rogan, E.; Cavalieri, E. *Chem. Res. Toxicol.* **2006**, *19*, 164-172.
8. Gaikwad, N. W.; Yang, L.; Muti, P.; Meza, J. L.; Pruthi, S.; Ingle, J. N.; Rogan, E. G.; Cavalieri, E. L. *Int. J. Cancer*, **2008**, *122*, 1949-1957.
9. Berry, J. D.; Licea, A.; Popkov, M.; Cortez, X.; Fuller, R.; Elia, M.; Kerwin, L.; Kubitz, D.; Barbas III, C. F. *Hybridoma and Hybridomics*, **2003**, *22(1)*, 23-31.
10. Mannisto, P. T.; Kaakkola, S. *Pharmacol. Rev.* **1999**, *51*, 593-628.
11. Cavalieri, E. L.; Kumar, S.; Todorovic, R.; Higginbotham, S.; Badawi, A. F.; Rogan, E. G. *Chem. Res. Toxicol.* **2001**, *14*, 1041-1050.
12. Gaikwad, N. W.; Rogan, E. G. Cavalieri, E. L. *Free Radic. Biol. Med*. **2007**, *43*, 1289-1298.
13. Gaikwad, N. W.; Yang, L.; Muti, P.; Meza, J. L.; Pruthi, S.; Ingle, J. N.; Rogan, E. L.; Cavalieri, E. L. *Int. J. Cancer*, **2008**, *122*, 1949-1957.
14. Chakravarti, D.; Mailander, P. C.; Li, K. –M.; Higginbotham, S.; Zhang, H. L.; Gross, M. L.; Meza, J. L.; Cavalieri, E. L.; Rogan, E. G. *Oncogene*, **2001**, *25*, 289-297.
15. Chakravarti, D.; Mailander, P. C.; Higginbotham, S.; Cavalieri, E. L.; Rogan, E. G. *Proc. Am. Assoc. Cancer Res.* **2003**, *44*, 180.

16. Guttenplan, J. B. U. S. Army Breast Cancer Research Program Era of Hope Meeting, June 8-11, **2005**.
17. Zhao, Z.; Kosinska, W.; Khmelnitsky, M.; Cavalieri, E. L.; Rogan, E. G.; Chakravarti, D.; Sacks, P.; Guttenplan, J. B. *Chem. Res. Toxicol.* **2006**, *19*, 475-479.
18. Cavalieri, E. L.; Kumar, S.; Todorovic, R.; Higginbotham, S.; Badawi, A. F.; Rogan, E. G. *Chem. Res. Toxicol.* **2001**, *14*, 1041-1050.
19. Cavalieri, E. L.; Devanesan, P.; Bosland, M. C.; Badawi, A. F.; Rogan, E. G. *Carcinogenesis*, **2002**, *23*, 329-333.
20. Rogan, E. G.; Badawi, A. F.; Devanesan, P. D.; Meza, J. L.; Edney, J. A.; West, W. W.; Higginbotham, S. M.; Cavalieri, E. L. *Carcinogenesis*, **2003**, *24*, 697-702.
21. Cavalieri, E. L.; Stack, D. E.; Devanesan, P. D.; Todorovic, R.; Dwivedy, I.; Higginbotham, S.; Johansson, S. L.; Patil, K. D.; Gross, M. L.; Gooden, J. K.; Ramanathan, R.; Cerny, R. L.; Rogan, E. G. *Proc. Natl. Acd. Sci. U. S. A.* **1997**, *94*, 10937-10942.
22. Cavalieri, E.; Frenke, K.; Liehr, J. G.; Rogan, E.; Roy, D. *JNCI Monograph 27: Estrogens as Endogenous Carcinogens in the Breast and Prostate*, Oxford Press, **2000**, 75-93.
23. Jankowiak, R.; Rogan, E. G.; Cavalieri, E. L. *J. Phys. Chem. B* **2004**, *108*, 10266-10283.
24. Li, J. J.; Li, S. A. *Fed. Proc.* **1987**, *46*, 1858-1863.
25. Newbold, R. R.; Liehr, J. G. *Cancer Res.* **2000**, *60*, 235-237.
26. Russo, J.; Lareef, M. H.; Tahin, Q.; Hu, Y. F.; Slater, C.; Ao, X.; Russo, I. H. *J. Steroid Biochem. Mol. Biol.* **2002**, *80*, 149-162.
27. Russo, J.; Lareef, M. H.; Balogh, G.; Guo, S.; Russo, I. H. *J. Steroid Biochem. Mol. Biol.* **2003**, *87*, 1-25.
28. Lareef, M. H.; Garber, J.; Russo, P. A.; Russo, I. H.; Heulings, R.; Russo, J. *Int. J. Oncol.* **2005**, *26*, 423-429.
29. Zahid, M.; Kohli, E.; Saeed, M.; Rogan, E.; Cavalieri, E. L. *Chem. Res. Toxicol*. **2005**, *19*, 164-172.
30. Miller, W. R.; O'Neill, J.; *Steroids*, **1987**, *50*, 537-548.
31. Simpson, E. R.; Mahendroo, M. S.; Means, G. D.; Kilgore, M. W.; Hinshelwood, M. M.; Graham-Lorence, S.; Amarneh, B.; Ito, Y.; Fisher, C. R.; Michael, M. D.; Mendelson, C. R.; Bulun, S. E. *Endocrine Rev*. **1994**, *15*, 342-355.

32. Jefcoate, C. R.; Liehr, J. G.; Santen, R. J.; Sutter, T. R.; Yager, J. D.; Yue, W.; Santner, S. J.; Tekmal, R.; Demers, L.; Pauley, R.; Naftolin, F.; Mor, G.; Bernstein, L. *JNCI Monograph 27: Estrogens as Endogenous Carcinogens in the Breast and Prostate*, Oxford Press, **2000**, 95-112.
33. Santner, S. J.; Feil, P D.; Santen, R. J. *J. Clin. Endocrinol. Metab*. **1984**, *59*, 29-33.
34. Pasqualini, J. R.; Chetrite, G.; Blacker, C.; Feinstein, M. C.; Delalonde, L.; Talbi, M.; Maloche, C. *J. Clin. Endocrinol. Metab*. **1996**, *81*, 1460-1464.
35. Mitrunen, K.; Hirvonen, A. Mutat. Res. **2003**, *544*, 9-41.
36. Russo, J.; Calaf, G.; Russo, I. H. *CRC Crit. Rev. Oncog.* **1993**, *4*, 403-417.
37. Fernandez, S. V.; Russo, I. H.; Russo, J. *Int. J. Cancer*, **2006**, *118*, 1862-1868.
38. Bosland, M. C. *J. Natl. Cancer Inst. Monogr*. **2000**, *27*, 39-66.
39. Ross, R.; Bernstein, L.; Judd, H.; Hanisch, R.; Pike, M.; Henderson, B. *J. Natl. Cancer Inst.* **1986**, *76(1)*, 45-48.
40. Leav, I.; Merck, F. B.; Kwan, P. W.; Ho, S. M. *Prostate*, **1989**, *15(1)*, 23-40.
41. Bosland, M. C.; Ford, H.; Horton, L. *Carcinogenesis*, **1995**, *16(6)*, 1311-1317.
42. Markushin, Y.; Zhong, W.; Cavalieri, E. L.; Rogan, E. G.; Small, G. J.; Yeung, E. S.; Jankowiak, R. *Chem. Res. Toxicol*. **2003**, *16*, 1107-1117.
43. Jankowiak, R.; Markushin, Y.; Cavalieri, E. L.; Small, G. J. *Chem. Res. Toxicol*. **2003**, *16*, 304-311.
44. Markushin, Y.; Kapke, P.; Saeed, M. Zhang, H.; Dawoud, A.; Rogan, E. G.; Cavalieri, E. L.; Jankowiak, R. *Chem. Res. Toxicol*. **2005**, *18*, 1520-1527.
45. www.evidenttech.com
46. Chan, W.; Maxwell, D. J.; Gao, X.; Bailey, R. E.; Han, M.; Nie, S. *Anal. Biotechnol.* **2002**, *13*, 40-46.
47. Murray, C. B.; Norris, D. J.; Bawendi, M. G. *J. Am. Chem. Soc.* **1993**, *115*, 8706-8715.
48. Dabbousi, B. O.; Rodriguez-Viejo, J.; Mikulec, F. V.; Heine, J. R.; Mattoussi, H.; Ober, R.; Jensen, K. F.; Bawendi, M. G. *J. Phys. Chem. B.* **1997**, *101*, 9463-9475.
49. Pellegrino, T.; Manna, L.; Kudera, S.; Liedl, T.; Koktysh, D.; Rogach, A. L.; Keller, S.; Radler, J.; Natile, G.; Parak, W. J. Nano Lett. 2004, 4, 703-707.
50. Gao, X.; Cui, Y.; Levenson, R. M.; Chung, L. W. K.; Niw, S. Nat. Biotechnol. 2004, 22, 969.

51. Dubertret, B.; Skourides, P.; Norris, D. J.; Noireaux, V.; Brivanlou, A. H.; Libchaber, A. Science, 2002, 298, 1259-1262.
52. Michaler, X.; Pinaud, F. F.; Bentolia, L.A.; Tsay, J. M.; Doose, S.; Li, J. J.; Sundaresan, G.; Wu, A. M.; Gambhir, S. S.; Weiss, S. *Science*, **2005**, *307*, 538-544.
53. Chan, W. C. W.; Nie, S. *Science*, **1998**, *281*, 2016.
54. Pinaud, F.; King, D.; Moore, H.-P.; Weiss. *J. Am. Chem. Soc.* **2004**, *126*, 6115.
55. Ballou, B.; Lagerholm, C.; Ernst, L. A.; Bruchez, M. P.; Waggoner, A. S. *Bioconjuate Chem.* **2004**, *15*, 79-86.
56. Wu, Xingyong; Liu, Hongjian; Liu, Jianquan; Haley, Kari N.; Treadway, Joseph A.; Larson, J. Peter; Ge, Nianfeng; Peale, Frank; Bruchez, Marcel, P.; *Nat. Biotechnol*. **2003,** *21*, 41-46.
57. Winter, J. O.; Liu, T. Y. ; Korgel, B.A.; Schmidt, C. E. *Avd. Mater*, **2001**, *13*, 1673.
58. Lin, S.; Franklin, M. T.; Klabunde, K. J. *Langmuir*, **1986**, *2*, 259-260.

CHAPTER 2 - Synthesis of Estrogen-Derived DNA Adducts and Their Structural Modifications for Conjugation

ABSTRACT

A variety of experimental evidence led to the hypothesis that catechol estrogen-3, 4-quinones (CE-3, 4-Q) react with DNA to initiate cancer. CE-3, 4-Q reacts with DNA purine bases to form depurinating adducts: N3-adenine and N7-guanine adducts of 4-hydroxyestrone (estradiol) [4-$OHE_1(E_2)$-1-N3Ade and 4-$OHE_1(E_2)$-1-N7Gua]. These depurinating estrogen-derived DNA adducts are released and found in urine of women at high risk and women with breast cancer making these adducts potential biomarkers. It is feasible that by inhibiting formation of estrogen-derived DNA adducts, one could prevent initiation of breast cancer. Therefore new methodologies for detection of these adducts need to be developed. The organic synthesis of the standard adducts and their structural modifications to conjugate with highly fluorescent quantum dots (QDs) and to form a hapten for monoclonal antibody (mAb) generation are described in this chapter.

2.1. Introduction

The hypothesis that certain estrogen metabolites reacts with purine bases of DNA to induce point mutation on the double helix initiating breast cancer is based on experiments on estrogen metabolism,[1, 2, 3] formation of estrogen derived DNA adducts,[4, 5, 6] carcinogenicity,[7, 8, 9] mutagenicity[10, 11, 12] and cell transformation.[13, 14, 15]

Estrogen can undergo enzymatic activation through P450 1B1 to form catechol estrogens (CE), particularly 4-CE which in turn oxidizes to endogenous carcinogenic catechol estrogen-3,4-quinones (CE-3,4-Q). (Fig 1) CE-3,4-Q initiates 1,4-Michael addition with both purine bases of DNA forming estrogen-derived DNA adducts; 4-$OHE_1(E_2)$-1-N3Ade and 4-$OHE_1(E_2)$-1-N7Gua. A competing deactivation pathway is switched on when ubiquitous catechol-O-methyltransferase (COMT) catalyzes O-methylation of 4-$OHE_1(E_2)$. Another deactivation pathway involves redirection of quinones either to glutathione (GSH) conjugates in presence of GSH/S-transferase or CE through quinone reductase. (Fig 2.1)[16]

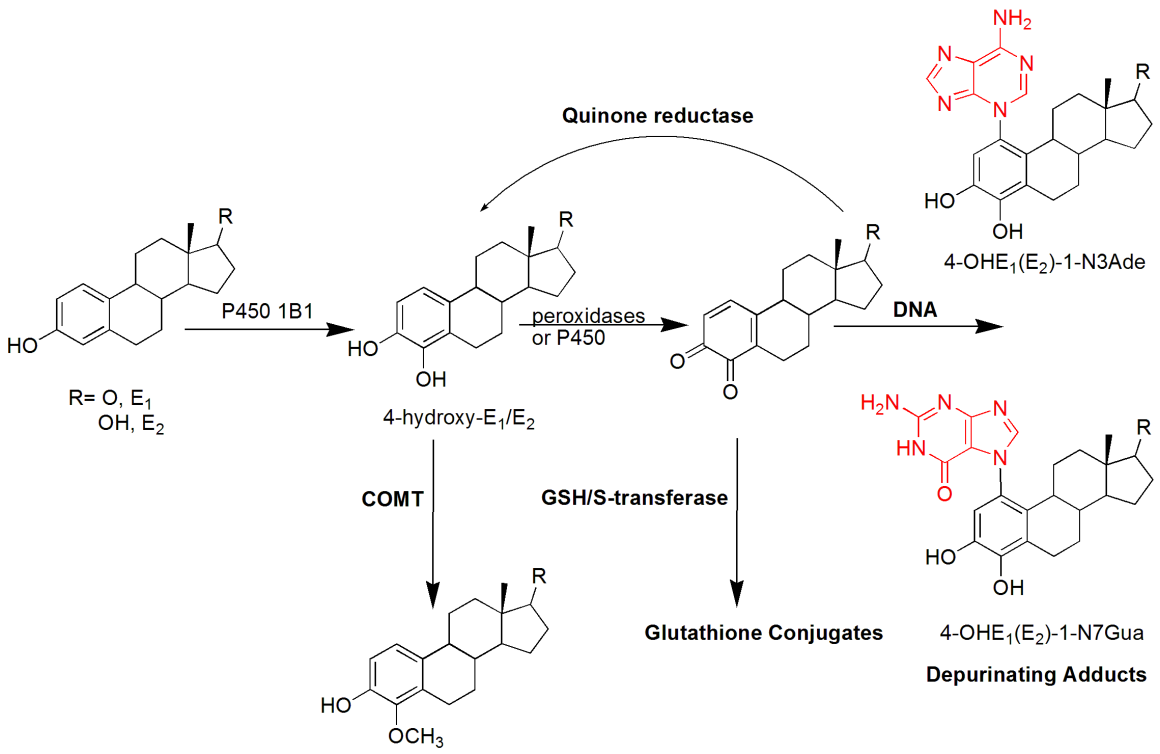

Fig 2.1 Enzymatic activation and deactivation pathway for 4-hydroxylated estrogen[16]

If the deactivation pathways are switched off, CS-3,4-quinones reaction with purine bases of DNA resulting depurinating adducts. These adducts are shed from DNA by breaking the glycosyl bond and finally, expressed in the urine of women at high-risk or with breast cancer.

2.2. Synthesis of Standard Estrogen-Derived DNA Adducts

In order to determine the estrogen-derived DNA adducts in human urine samples through indirect method, standard adducts were synthesized.[16] The first step of synthesis of DNA-estrogen adduct involves the nitration of estrone (E_1). 4-NO_2-E_1 recrystallizes and 2-NO_2-E_1 remains in the solution making the separation easier. (Scheme 2.1)

Scheme 2.1 Nitration of estrone (E_1)

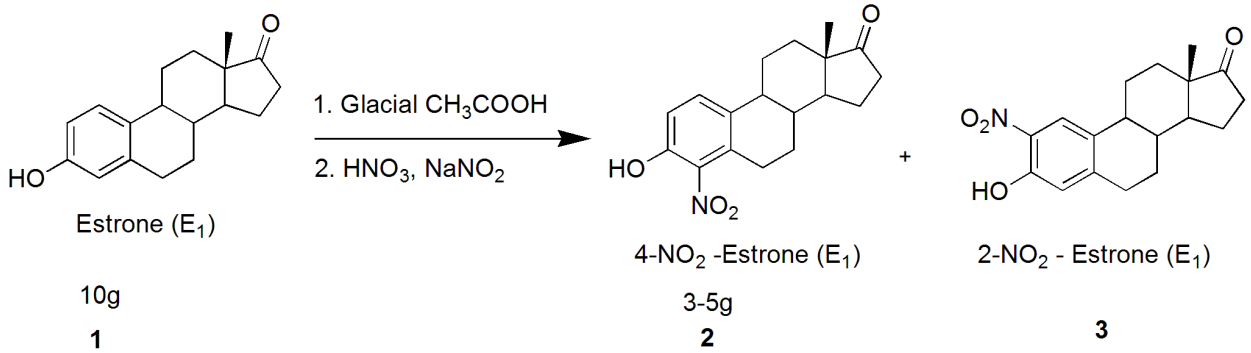

One possible explanation for the solubility of 2-NO_2-E_1 is its enhanced salvation with water through N-O^- while there is steric hindrance to rotation about N-C bond in 4-NO_2-E_1 making it locked into intramolecular H-bonding. This resulted in hindered solvation of compound **2** with water and, therefore in crystallization of it from aqueous solution. (Fig 2.2)[17]

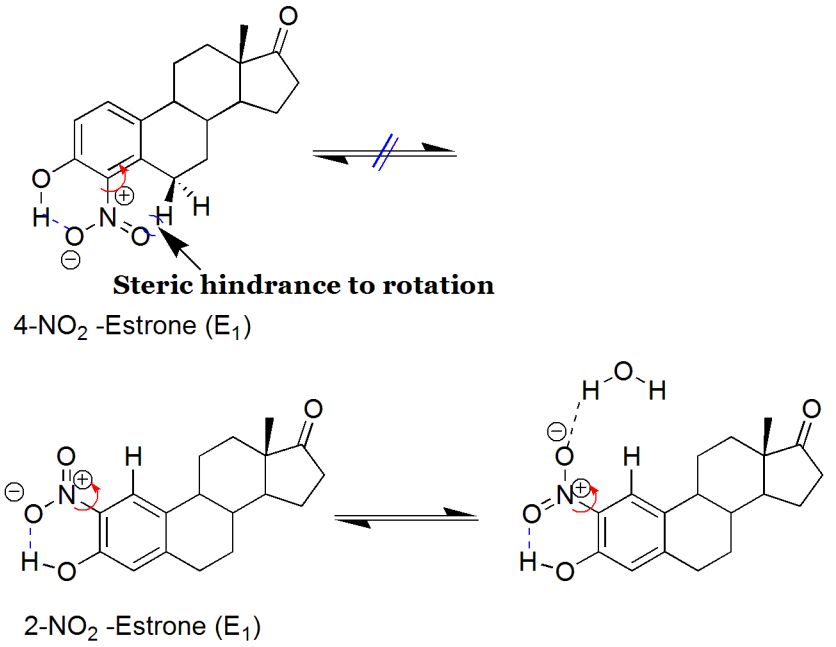

Fig 2.2 2-NO_2-E_1 remained soluble in solvent due to enhanced solvation through N-O bond

Carbonyl group (-C=O) of 4-NO_2-E_1 (**2**) was enantio-selectively reduced by sodium borohydride ($NaBH_4$) to form 4-NO_2-17β-estradiol (**4**) which was treated with $Na_2S_2O_4$ to form 4-NH_2-17β-estradiol (**5**) in 98% yield. In the final step, 4-NH_2-17β-estradiol (**5**) was converted into 4-OHE_2 on treatment with $NaIO_4$-KI couple with 28.3% yield. (Scheme 2.2)

Scheme 2.2 Synthesis of 4-hydroxyestradiol (4-OHE_2)

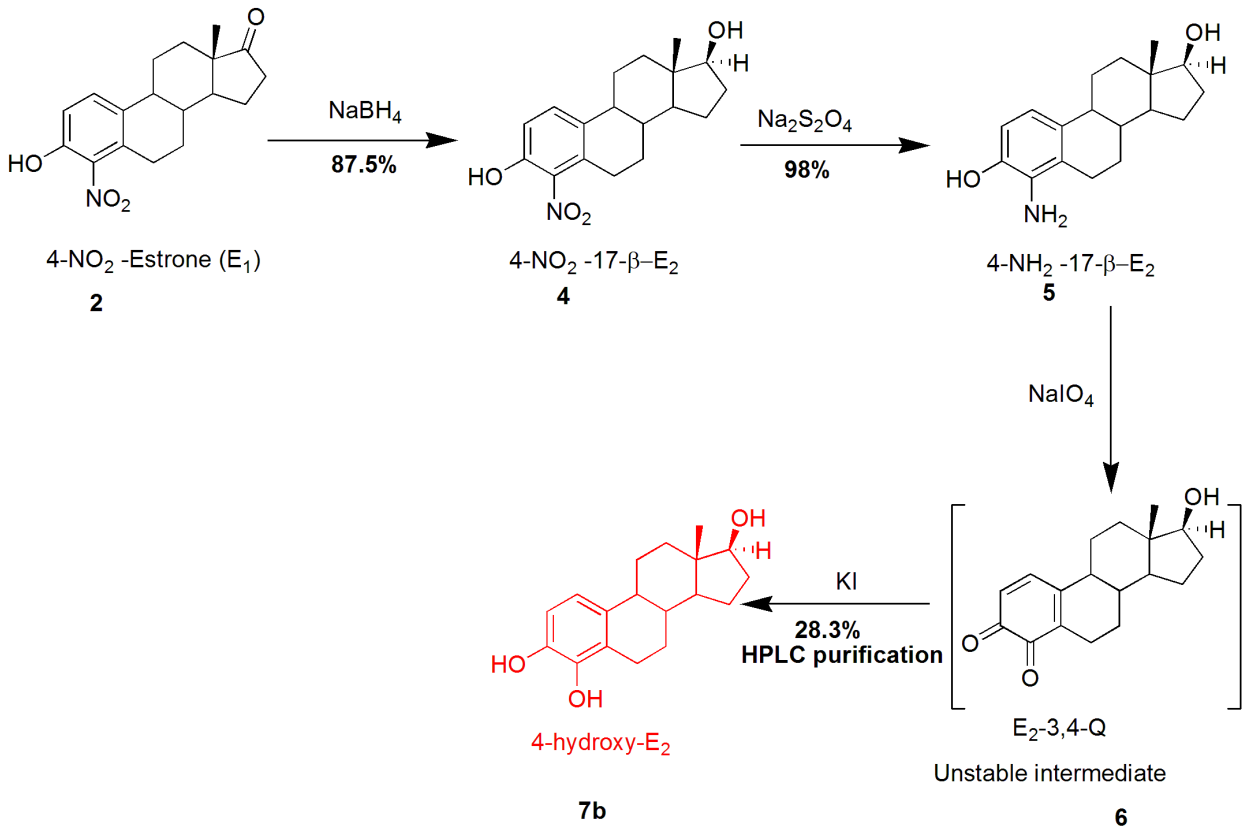

The synthesis of 4-OHE_1 was carried out in similar fashion except that the ketonic C=O was not reduced. (Scheme 2.3)

Scheme 2.3 Synthesis of 4-hydroxyestrone (4-OHE_1)

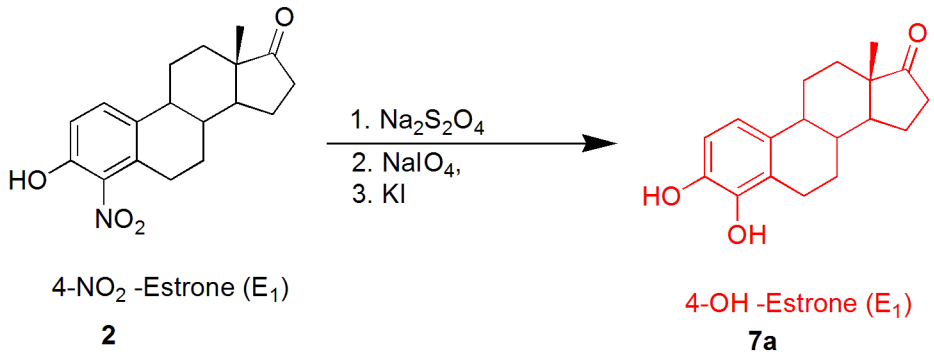

4-OH-E_2 (**7a**) was converted into a quinone by treatment with MnO_2. The quinone was a substrate for 1,4-Michael addition by 2'-deoxyguanosine(dG) and adenine to yield 4-OHE_1(E_2)-1-N7Gua and 4-OHE_1(E_2)-1-N3Ade respectively. (Scheme 2.4) An attempt to use 2'-deoxyadenosine (dA) was failed on account of steric hindrance offered by deoxyribose group at N9 while the electrophile E_1(E_2)-3,4-Q approached the N3 of dA.[16]

Scheme 2.4 Estrogen derived DNA adduct synthesis

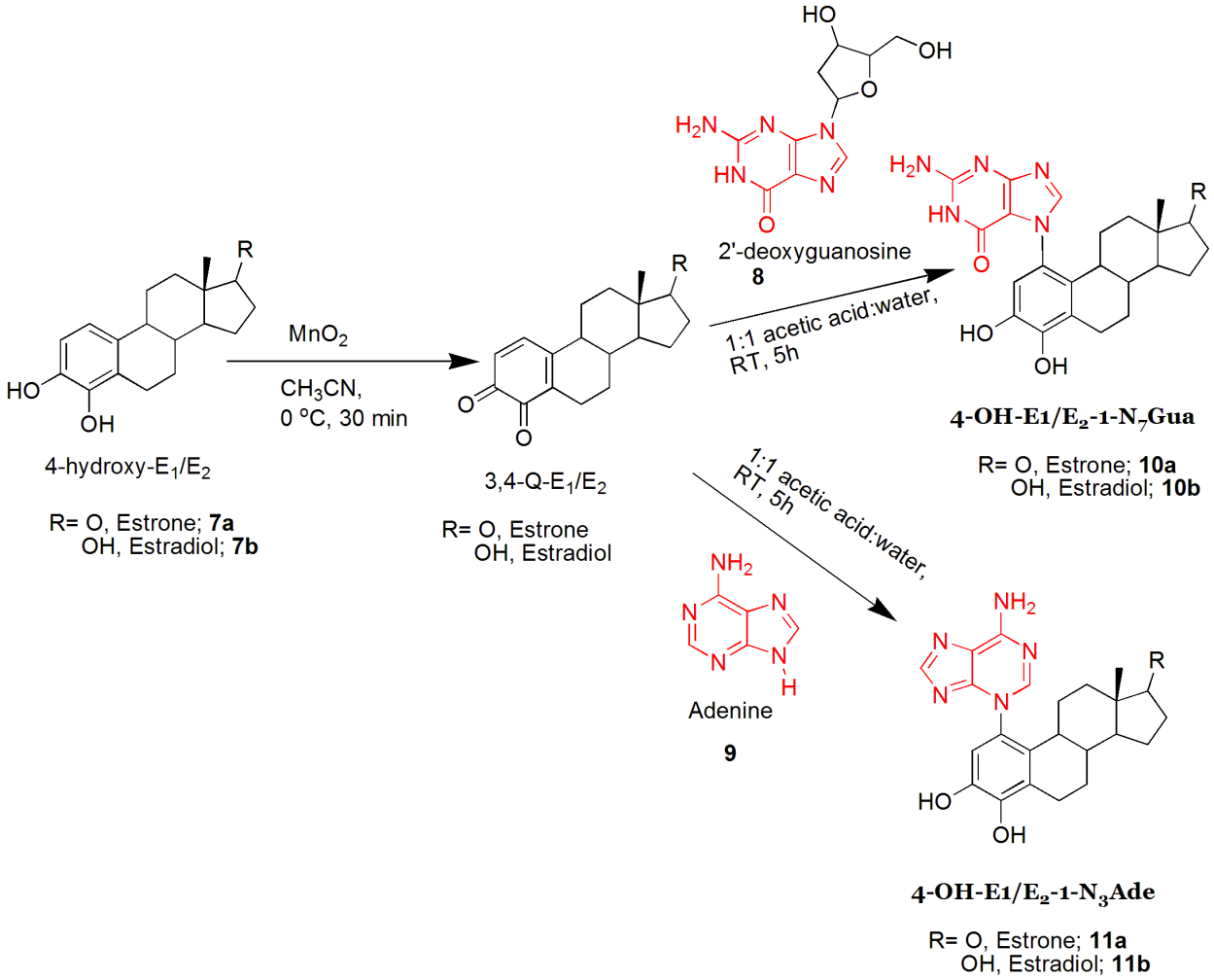

2.3. Synthesis of Aminomethyl Linker at C-17 Position of DNA-Estrogen Adducts

The labeling strategy for estrogen-derived DNA adducts required to synthesize a linker. A primary amine (RNH_2) linker was selected to serve the purpose of labeling through carboxylic acid (-COOH) in a coupling reaction. Highly fluorescent, photostable aqueous quantum dots (QDs) synthesized in our lab can be conjugated by this strategy. Keeping this in mind, an aminomethyl ($-CH_2NH_2$) group was attached to 4-OHE_2-1-N3Ade and 4-OHE_2-1-N7Gua. (Scheme 2.5)

Scheme 2.5 Synthesis of aminomethyl (-CH_2NH_2) linker on 4-OHE_2

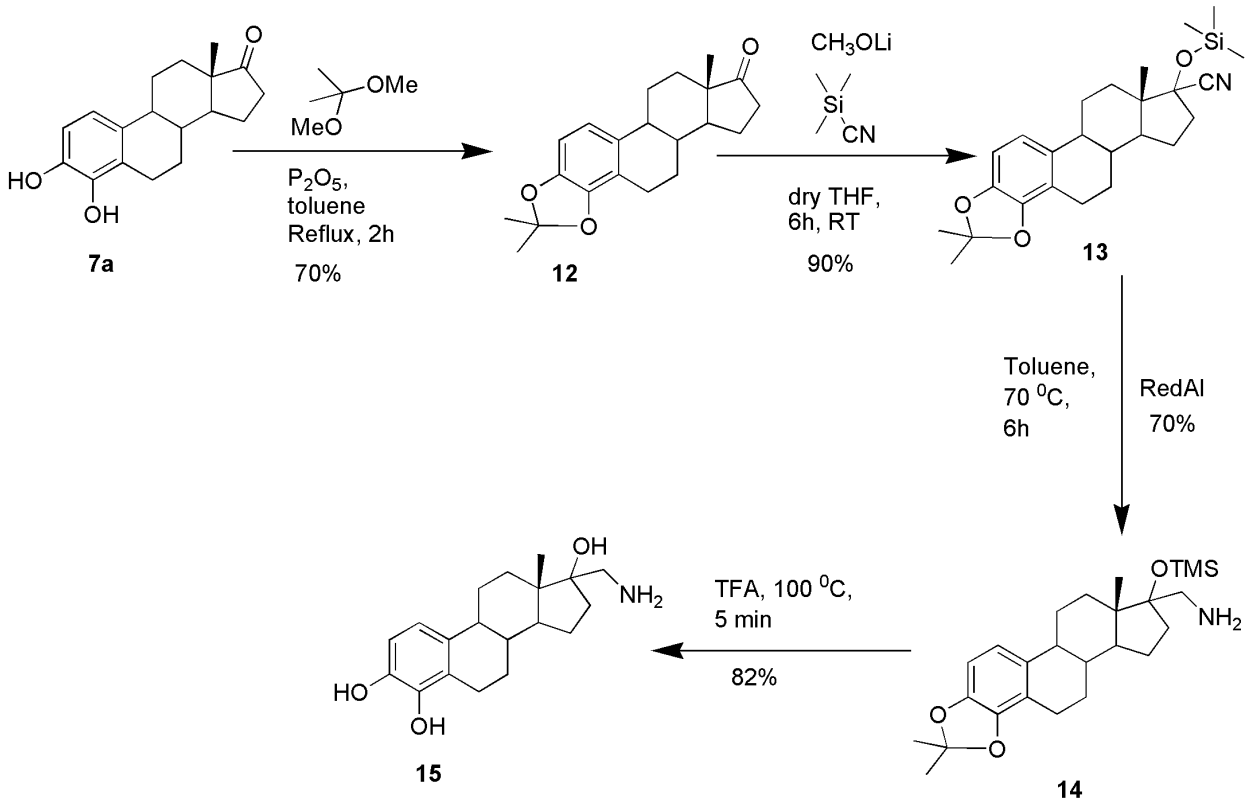

Once the aminomethyl (-CH_2NH_2) linker was established on C-17 of **15**, estrogen-derived DNA adducts were synthesized by 1. oxidizing compound **15** with MnO_2 to form 3,4-quinone derivative, which acted as an electrophile initiating a 1,4-Michael addition to adenine, a purine base resulting 4-OHE_2-17-AM-1-N3Adenine (**16**) and to 2'-deoxyguanosine (dG) to yield 4-OHE_2-17-AM-1-N7Guanine (**17**). (Scheme 2.6)

Scheme 2.6 Synthesis of estrogen-derived DNA adducts with the aminomethyl (-CH_2NH_2) linker

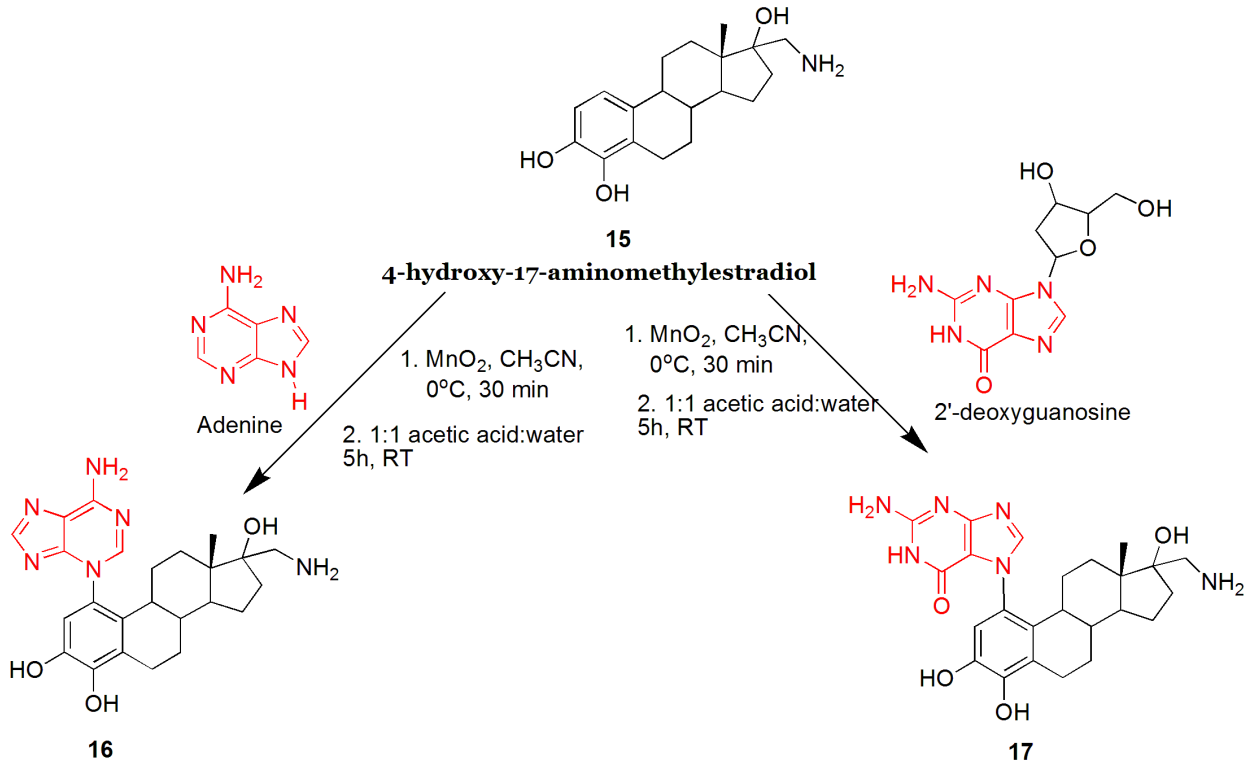

2.4. Experimental Section

All chemical reactions were carried out using Schlenk techniques under argon atmosphere unless otherwise noted. Anhydrous solvents were used in all the reactions unless stated.

HPLC. HPLC purification was carried out on a Waters 600E solvent delivery system equipped with a Waters 990 photodiod array (PDA) detector interfaced with an APC-IV Powermate computer. A preparatory reverse phase HPLC was conducted by using SunFire^{TM} PrepC 18 OBD^{TM} 10 µm, (30x500mm) column at a flow rate of 25 mL/min. The gradient was started with 30% MeOH and 70% (water + 0.1% trifluoro acetic acid (TFA)) with a linear gradient to 100% MeOH in 30 minutes.

Synthesis of compound **2** and **3**

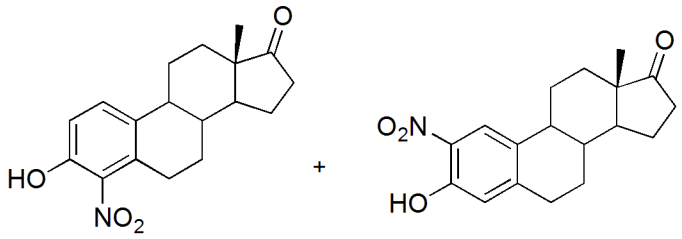

4-NO_2 -Estrone (E_1) **2**

2-NO_2 - Estrone (E_1) **3**

A two necked round bottom flask, fitted with a stir bar and a thermometer, was charged with estrone (E_1) (10g, 0.037 mol), followed by addition of glacial acetic acid (300 mL). The reaction mixture was allowed to heat up to 120 ^{0}C at which the white suspension dissolved. The reaction mixture was then allowed to cool down slowly until it reached 50 ^{0}C-55 ^{0}C. A warm (50 ^{0}C-55 ^{0}C) nitrating agent (100 mL water + 2.5 mL 70% HNO_3 + 0.1g $NaNO_2$) was added dropwise. The solution slowly turned dark brown. Once the addition of the nitrating agent was complete, the reaction mixture was allowed to cool to room temperature. After 1h at room temperature, it was placed overnight in refrigerator (4^{o}C). The brown colored solid was filtered in vacuum and washed with 3*100 mL cold water yielding 4.3g of 4-nitroestrone (**2**, 37%)

4-nitroestrone (**2**)

^{1}H- NMR ($CDCl_3$, 400MHz) δ (ppm): 9.5 (s, 1H), 7.5 (d, *J*= 9Hz, 1H), 7.0 (d, *J*= 8.8Hz, 1H), 3.23 (m, 1H), 3.0 (dd, *J* =5.4, 8.5Hz, 1H, H-6, 1H), 2.50 (dd, *J* = 8.7, 16.1 Hz, 1 H, H-16), 2.35 (m, 1 H), 2.36 (m, 1H), 2.23-2.0 (m, 4H), 1.98-1.90 (m, 1 H), 0.94 (s, 3H, CH_3), 1.70-1.35 (m, remaining H).

^{13}C-NMR (CD_3Cl_3, 400MHz) δ (ppm): 220.6, 152.4, 134.2, 133.5, 133.1, 116.9, 50.3, 48.0, 44.6, 37.3, 36.0, 31.7, 28.0, 26.4, 26.1, 21.6, 14.0

2-nitroestrone (**3**)

^{1}H- NMR ($CDCl_3$, 400MHz) δ (ppm): 10.4 (s, 1H), 7.9 (s, 1H), 6.8 (s, 1H), 2.9 (m, 1H), 2.5 (dd, 1H), 2.4 (dd, 1H), 2.2 (m, 1H), 2.0 (m, 1H), 1.64-1.46 (m, 4H), 0.92 (s, 3H, CH_3)

^{13}C-NMR ($CDCl_3$, 400MHz) δ (ppm): 220.5, 153.0, 149.0, 133.3, 132, 121.7, 119.1, 50.5, 48.0, 43.6, 37.8, 36, 31.4, 29.8, 26.0, 25.8, 21.7, 13.9

Synthesis of Compound **4**

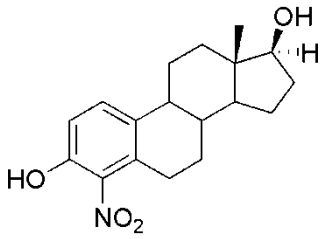

4-NO_2 -17-β–E_2

4

4-NO_2E_1 (2g, 6.34 mmol) was added to 120 mL methanol (4^oC) in a 500 mL beaker, followed by dropwise addition of 0.8 mL 20% NaOH solution. The solution was warmed in order to dissolve all 4-NO_2E_1. Once the reaction reached room temperature, a solution of $NaBH_4$ (0.8g, 0.021 mol) in 120 mL methanol was added to the reaction mixture. The reaction was stirred for half an hour and allowed to stand overnight in the dark. The red reaction mixture was diluted by adding it to 600 mL water. Quenching the excess of $NaBH_4$ and its reaction products by acidification by 4 mL conc. HCl led to a yellow precipitate. The mixture was kept in the refrigerator for 1h, filtered, dried over vacuo to obtain 1.75g (yield 87.5%) of 4-NO_2E_2.

^{1}H- NMR ($CDCl_3$, 400MHz) δ (ppm): 9.5 (s, 1H), 7.5 (d, *J*= 8.8Hz, 1H), 6.9 (d, *J*= 9.0Hz, 1H), 3.7 (t, *J*= 8Hz, 1H), 3.2 (m, 1H), 2.9 (dd, *J*= 5Hz, 1H), 2.31(m, 1H), 2.2 (m, 2H), 1.9(m, 2H), 1.7(t X qu, 1H), 1.4-1.1 (m, 8H), 0.80 (s, 3H)

^{13}C-NMR ($CDCl_3$, 400MHz) δ (ppm): 152.3, 134.5, 134.2, 133.2, 116.6, 81.9, 50, 44.6, 43.3, 37.7, 36.8, 30.8, 28.2, 26.8, 23.1, 11.3

Synthesis of Compound **5**

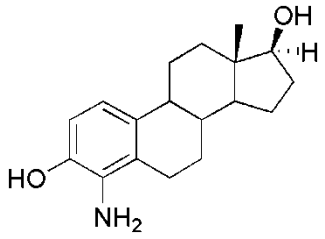

4-NH_2 -17-β–E_2

5

A two necked 1 L round bottom flask fitted with reflux condenser and stir bar was charged with compound **4** (2.25 g, 7.1 mmol), which was then dissolved in 300 mL acetone and 60 mL water. The reaction was treated with 60 mL 1M NaOH and allowed to reflux. At reflux temperature,

$Na_2S_2O_4$ was added in small portions to make sure no violent reaction took place. The color of the solution started to change from reddish brown to pale yellow. The reaction was further stirred at reflux for half an hour. Most of acetone was removed in a rotavap and the pH of the solution was decreased to 6 by adding HCl. The acidic solution was then kept in the refrigerator (4^oC) overnight. The yellow solid was filtered to obtain 2.0g (yield 98.5%) of compound **5**.

^{1}H- NMR (DMSO-d_6, 400MHz) δ (ppm): 8.8 (s, br, 1H), 6.47 (d, *J*= 8.2Hz, 1H), 6.39 (d, *J*= 8.2Hz, 1H), 4.5 (d, *J*= 5Hz, 1H), 4.0 (s, br, 2H), 3.5 (sext, *J*= 3.8Hz, 2H), 2.54 (d, 1H), 2.3 (m, 1H), 2.2 (m, 1H), 2.0 (m, 1H), 1.8 (m, 3H), 1.6 (m, 1H), 1.4-1.0 (m, rest of H), 0.64 (s, 3H)

^{13}C- NMR (DMSO-d_6, 400MHz) δ (ppm): 141.6, 133.1, 131.1, 121, 113.0, 111.4, 80.2, 55.0, 49.7, 43.9, 42.7, 38.0, 36.7, 30, 27, 26.3, 24.5, 22.9, and 11.3

Synthesis of Compound **7b**

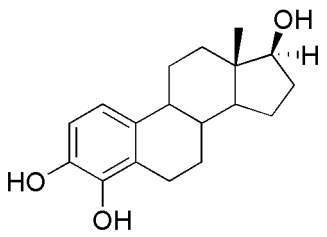

4-hydroxy-E_2

7b

Compound **5** (1g, 3.48 mmol) was dissolved in 300 mL glacial acetic acid. $NaIO_4$ (10g, 0.046 mol) was dissolved in 700 mL 0.1N HCl in a 2 L beaker. The solution of compound **5** was added dropwise to the solution of $NaIO_4$ within three minutes. The reaction was then stirred for half an hour at room temperature. The color changed from yellow to red. The quinine was extracted with 3 x 200 mL chloroform. KI (3g, 0.018 mol) was added to the combined organic layers and shaked well in separatory funnel. The organic layer was then washed with 3 x 100 mL 5% sodium bisulfate, 3 x 100 mL ultrapure water. The organic layer was evaporated in rotavap to yield 0.92g crude product **7b** which was purified by HPLC.

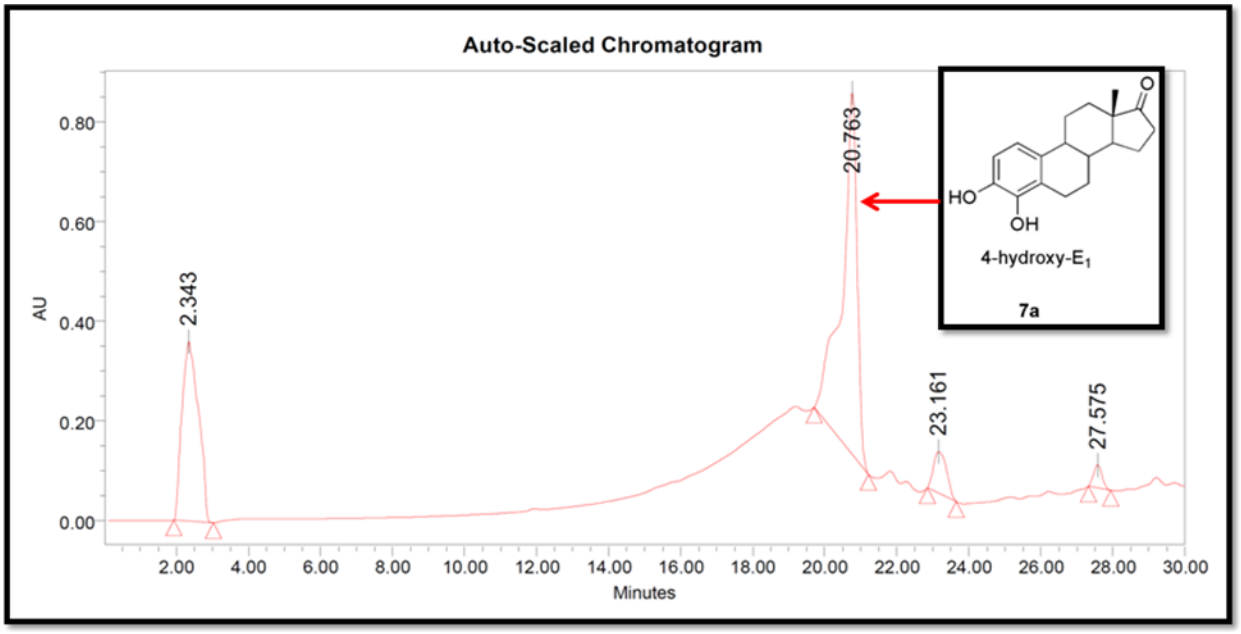

Fig 2.3 Prep-HPLC purification of 4-OHE$_1$ (20.76 min)

^{1}H- NMR (DMSO-d$_6$, 400MHz) δ (ppm): 8.9 (s, 1H), 8.0 (s, 1H), 6.55 (s, 2H), 2.8 (dd, *J*= 5.5Hz, 1H), 2.46 (dd, *J*= 8.3Hz, 1H), 2.3 (m, 1H), 2.15-1.9 (m, 4H), 1.75-1.2 (m, rest of H), 0.8 (s, 3H)

^{13}C- NMR (DMSO-d$_6$, 400MHz) δ (ppm): 220, 142.3, 131.0, 123.7, 115.3, 112.4, 55.0, 49.7, 47.3, 43.7, 37.5, 35.5, 31.4, 26, 25.7, 23.5, 21.2, 13.5

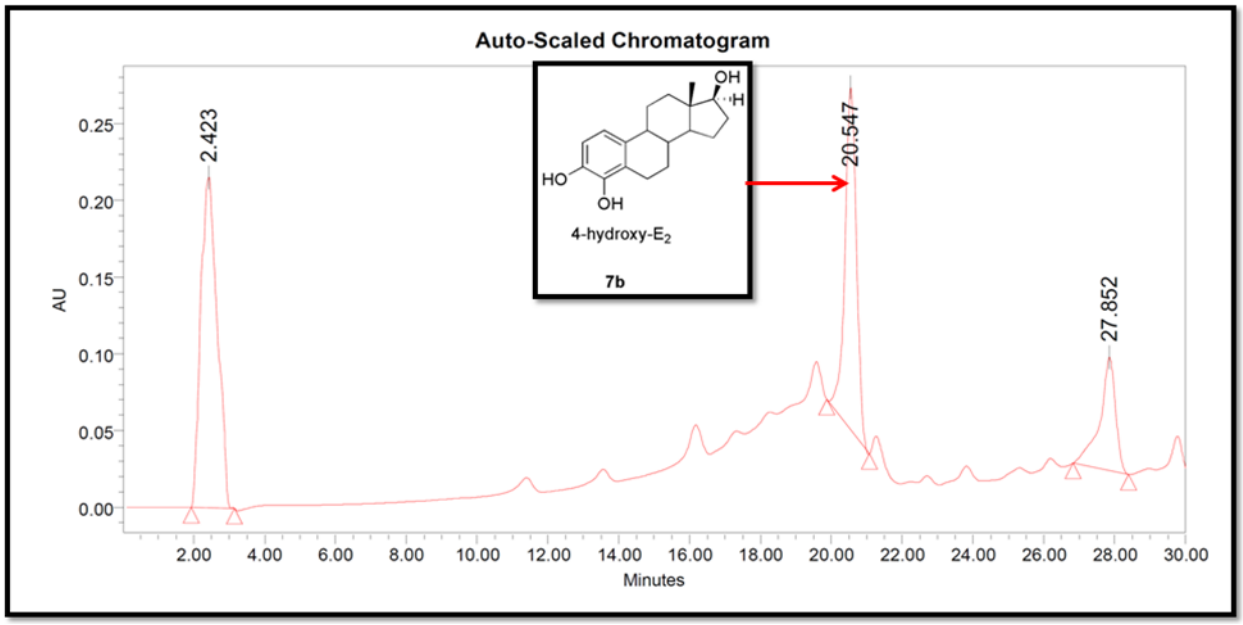

Fig 2.4 4-OHE$_2$ eluted at 20.54 min under prep-HPLC conditions

^{1}H- NMR (DMSO-d$_6$, 400MHz) δ (ppm): 8.9 (s, br, 1H), 8.0 (s, br, 1H), 6.5 (s, 2H), 3.2 (d, 1H), 2.46 (dd, *J*= 8.3Hz, 1H), 2.3 (m, 1H), 2.15-1.9 (m, 4H), 1.75-1.2 (m, rest of H), 0.8 (s, 3H)

^{13}C- NMR (DMSO-d_6, 400MHz) δ (ppm): 142.3, 141.5, 131.0, 123.7, 115.3, 112.4, 55.0, 49.7, 47.3, 43.7, 37.5, 35.5, 31.4, 26, 25.7, 23.5, 21.2, 13.5

Synthesis of Compound **10a** and **10b**

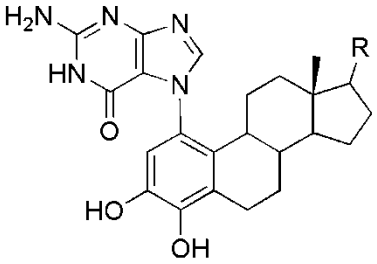

4-OH-E1/E_2-1-N_7Gua

R= O, Estrone; **10a**
OH, Estradiol; **10b**

Compound **7b** (0.1g, 0.346 mmol) was dissolved in dry acetonitrile (10 mL) in a 50 mL round bottom flask. The solution temperature was cooled down to 0 ^{0}C by using an ice bath within 15 minutes. The oxidizing agent MnO_2 (0.2g, 2.3 mmol) was added and the reaction was stirred for 30 min at 0 ^{0}C. The reaction was then filtered by means of a syringe and divided into two parts of 5 mL each.

2'-deoxyguanosine (2'-dG) (0.495g, was dissolved in 10 mL 1:1 acetic acid : water. 5 mL filtered solution of 3, 4-quinone estradiol was added to the above reaction and allowed to stir at room temperature for 5h. The reaction mixture was then subjected to prep HPLC to obtain pure **10b**.

A

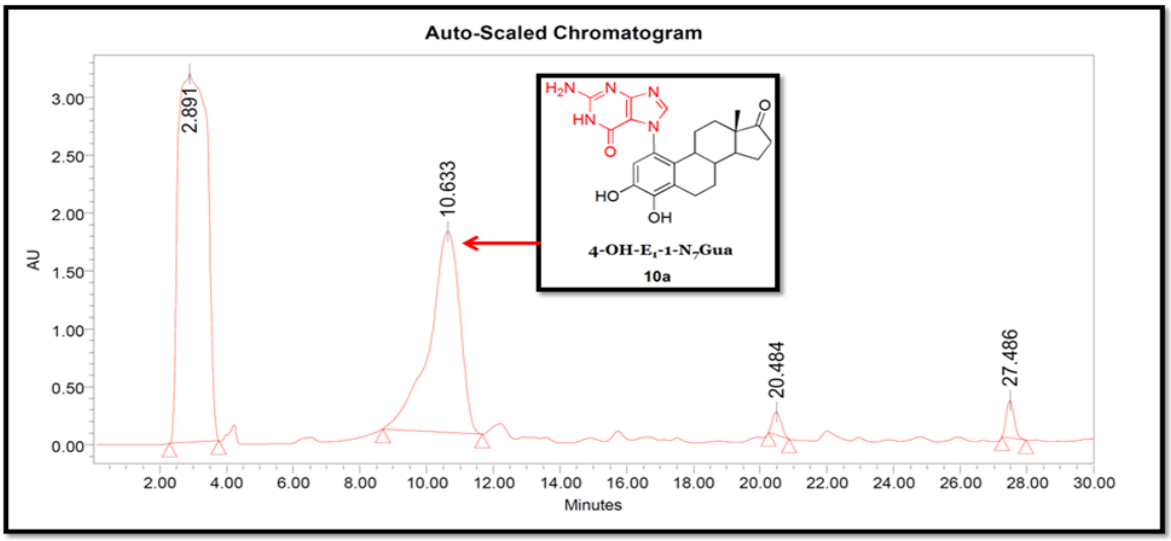

B

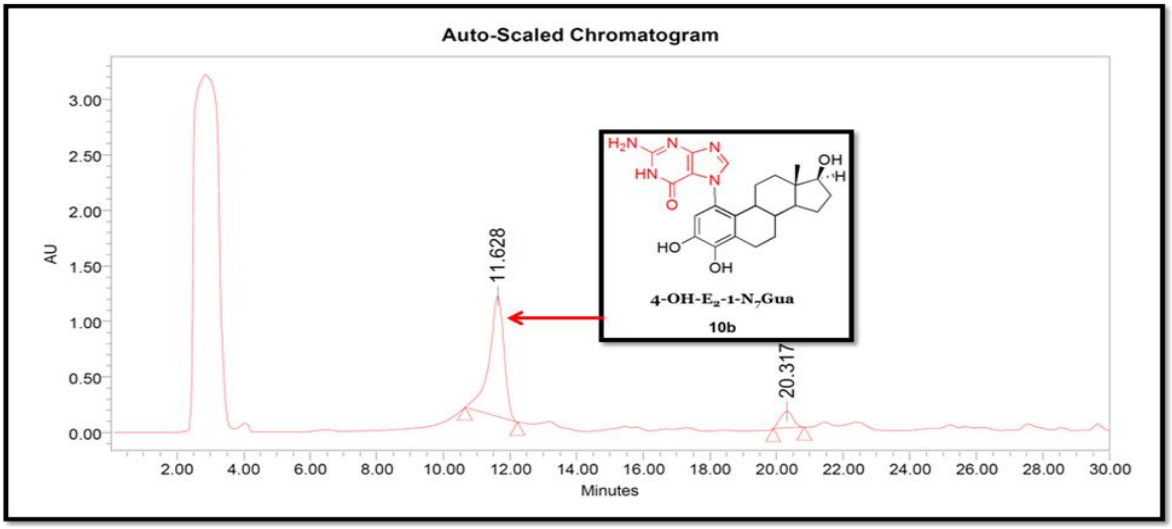

Fig 2.5 4-OHE$_1$-1-N$_7$Gua was eluted at 10.63 min (**A**) and 4-OHE$_2$-1-N$_7$Gua adduct peak showed at 11.62 min (**B**)

Synthesis of Compound **11a** and **11b**

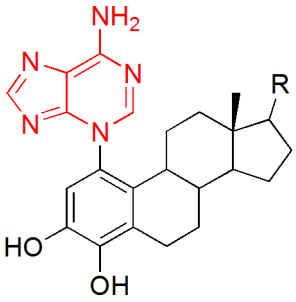

4-OH-E1/E$_2$-1-N$_3$Ade

R= O, Estrone; **11a**
OH, Estradiol; **11b**

Adenine (0.235g, 1.74 mmol) was dissolved in 10 mL 1:1 acetic acid: water. 5 mL solution of 3, 4-quinone estradiol was added. The mixture was allowed to stir at room temperature for 5h. The crude reaction mixture was then purified by preparative HPLC affording pure **11a**.

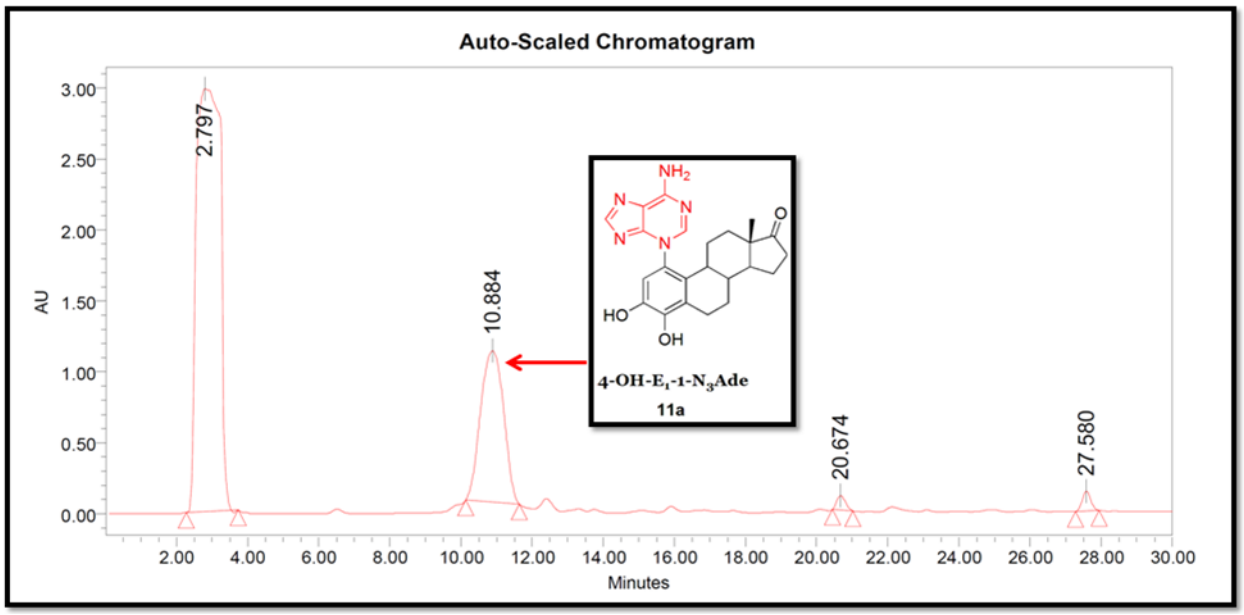

Fig 2.6 The peak at 10.88 min represented the 4-OHE$_1$-1-N$_3$Ade adduct

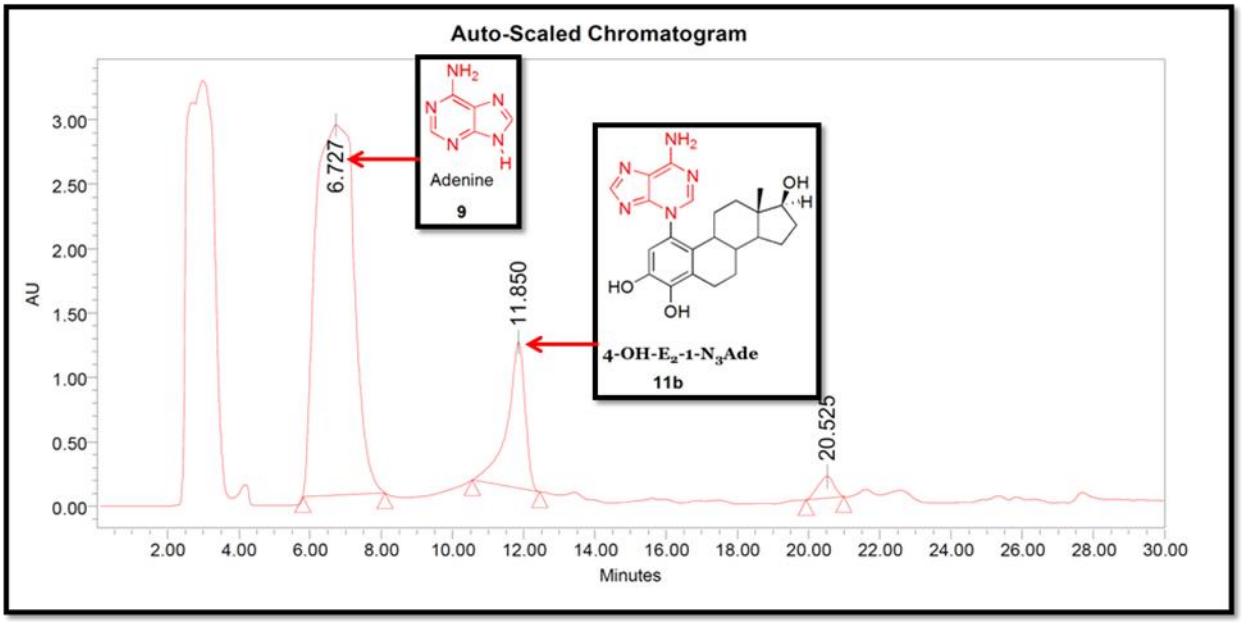

Fig 2.7 Estradiol derived adenine adduct (**11b**) was purified through prep HPLC (11.85 min). Excess adenine was also recovered (6.727 min)

Synthesis of acetonide (**12**)

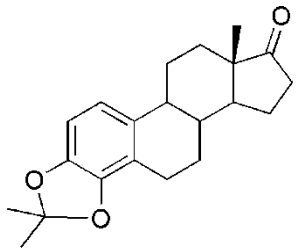

12

4-OHE$_1$ (100 mg, 0.35 mmol), 2,2-dimethoxypropane (200 µL) and a catalytic amount of P_2O_5 were suspended in dry toluene. The mixture was heated under reflux with a soxhlet extractor containing $CaCl_2$. The reaction mixture was refluxed for 2 h. Additional 2, 2-dimethoxypropane was added if required for the completion of reaction (TLC control). Refluxing was continued until TLC showed no starting material. The reaction mixture was treated with 1 M solution of Na_2CO_3 (10 mL) after cooling to room temperature. The organic layer separated and the aqueous layer was extracted with hot toluene (2 times). The combined toluene layers were washed with water and dried over sodium sulfate. After evaporation of solvent, a dark yellow colored oil was obtained, which was purified on silica gel column. Yield 70%.

^{1}H NMR ($CDCl_3$): 6.72 (d, *J* = 8.3 Hz, 1 H, H-1), 6.56 (d, *J* = 8.3 Hz, 1 H, H-2), 2.84 (dd, *J* =5.4, 8.5 Hz , 1H, H-6), 2.65 (m , 1 H, H-6), 2.50 (dd, J = 8.7, 16.1 Hz, 1 H, H-16), 2.35 (m, 1 H), 2.36 (m, 1H), 2.23-2.0 (m, 4H), 1.98-1.90 (m, 1 H), 1.67 (s,3 H, CH_3), 1.66(s,3 H, CH_3), 0.91 (s,3 H, CH_3), 1.70-1.35 (m, remaining H). FAB-MS: *m/z* 327.4312 [$(M+H)^+$] corresponding to $C_{21}H_{27}O_3$ calc. 327.4293.

Synthesis of protected cyanohydrine (**13**)

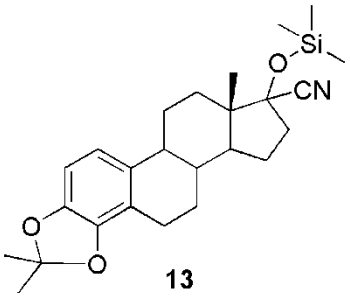

13

Under argon and at room temperature a 25 mL round bottom flask was charged with anhydrous THF (0.5 mL), lithium methoxide (1.2 mg) and trimethylsilyl cyanide (250 ul). The resulting yellow colored solution was stirred for 10 min and solid acetonide (**7**, 172 mg, 0.53 mmol) was added. The stirring was continued for 6h. After completion, the reaction was quenched with 10% Na_2CO_3 (3 mL) and extracted with tert-butyl methyl ether (3 times). Combined ether layers were evaporated to afford an oily product and used as such for the next step. Yield 225 mg (95%).

Synthesis of aminomethylestradiol (**14**)

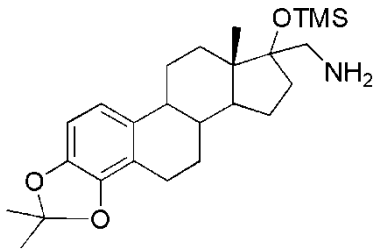

14

The crude **13** (225 mg) was dissolved in toluene (2 mL) and 300 ul of RedAl® was added. The reaction mixture was stirred at 70°C for 4h and then at room temperature for overnight. Completion of reaction was checked by TLC. The reaction was carefully quenched with 1 M NaOH (2 mL), resulting in two layers. The upper layer (organic) was removed; the aqueous layer (lower) was extracted with hot toluene (2 times) and combined. After evaporation, the gummy material was obtained and used as such for the next step. Yield 159 mg (~70%).

Synthesis of 4-hydroxy-17-aminomethylestradiol (**15**)

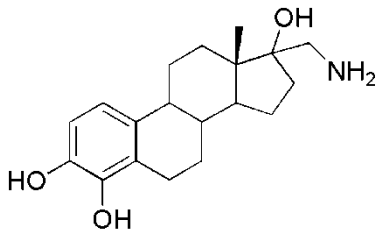

15

The crude **14** was treated with trifluoroactic acid at 100 °C for 5 min and then brought to room temperature. The mixture was left to stir at room temperature until HPLC analysis indicated the complete removal of protective acetonoid group. After completion, the reaction mixture was directly injected into preparative HPLC under reverse phase condition to purify the target catechol (**15**). Yield 85%. ^{1}H NMR (DMSO-d_6): 7.80 (br s, 3 H, exchangeable with D_2O shaking), 6.66 (d, J = 8.3 Hz, 1 H, H-1), 6.55 (d, J = 8.3 Hz. 1 H, H-2), 2.93 (m, 1 H, 17-CH_2NH$_2$), 2.88 (m, 1 H, 17-CH_2NH$_2$), 2.73 (m, 1 H), 2.66 (m, 1 H), 2.50 (m, 2 H), 0.82 (s, 3 H, CH_3), 2.20-0.9 (m, remaining H). FAB-MS: *m/z* 318.4356 [(M+H)$^+$] corresponding to $C_{19}H_{28}O_3$ calc. 318.4306.

HPLC Conditions. Preparative reverse phase HPLC was conducted at a flow rate of 25 mL/min. The gradient was started with 10% acetonitrile and 90% (water + 0.1% trifluoro acetic acid (TFA)) with a linear gradient to 100% acetonitrile in 30 minutes. (Fig 8)

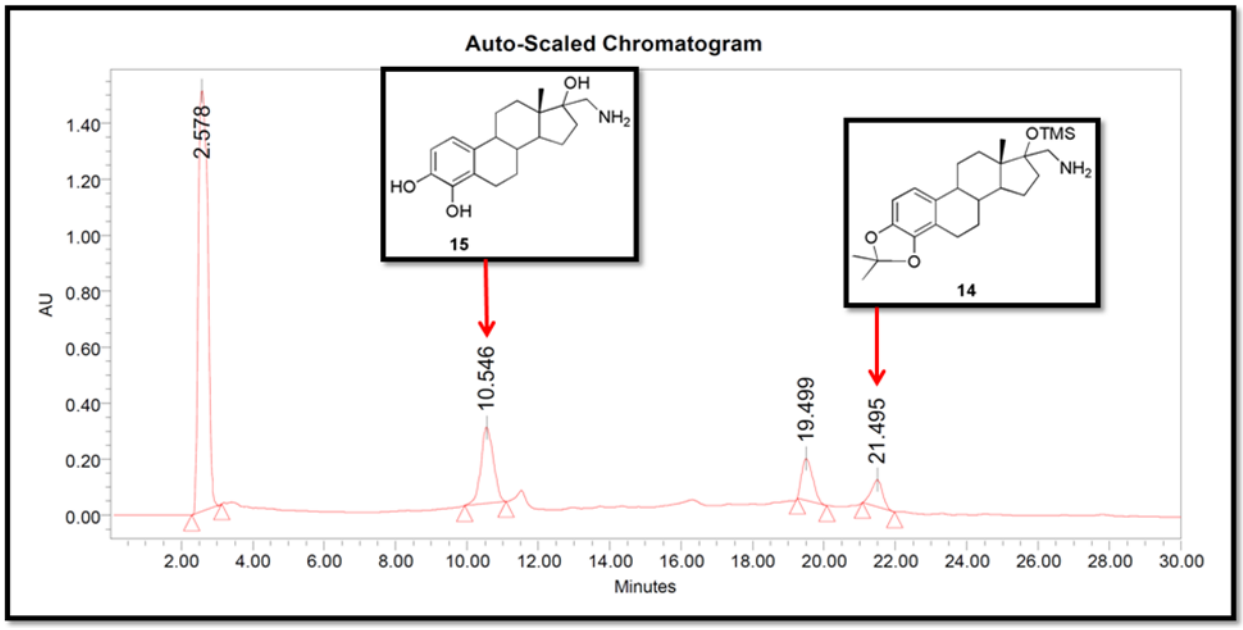

Fig 2.8 4-OHE$_2$-17-AM was purified through prep HPLC (10.54 min)

Synthesis of 4-hydroxy-17-aminomethylestradiol-1-N3Ade (**16**)

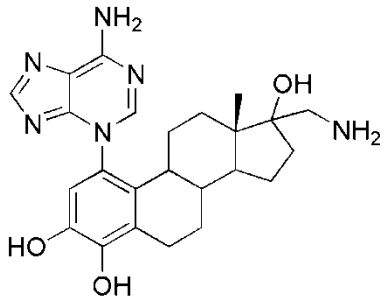

16

The catechol 10 (10 mg) was oxidized to quinone with MnO_2 (20 mg) in acetonitrile (2 mL) at 0 ^oC. After 30 min, the yellowish-green quinone solution was added to a stirred solution of adenine (10 eq) in a mixture (1:1) of acetic acid/water. The reaction was stirred for 10 h and then the adenine adduct was purified by preparative HPLC.

Analytical HPLC. Analytical HPLC was performed with column phenomenex (250x4.60 mm) with flow rate of 1mL/min and injection volume of 100 µL. The initial concentration used was 10% acetonitrile and 90% (water +0.1%TFA) with a linear gradient reaching 100% acetonitrile in 10 minutes.

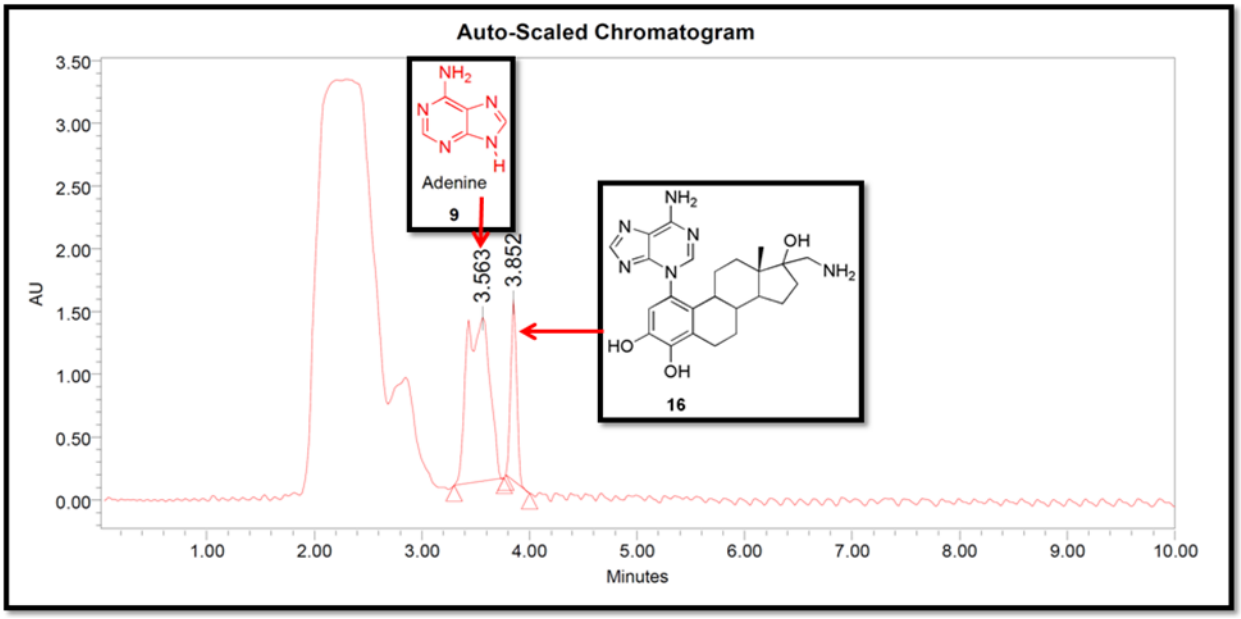

Fig 2.9 Analytical HPLC purification of 4-OHE$_2$-17-aminomethyl-1-N3Ade (3.85 min)

2.5. Discussion

Chemical synthesis of estrogen-derived DNA adducts: 4-OHE$_2$-1-N3Ade and 4-OHE$_2$-1-N7Gua are important for the indirect detection of these adducts in urine samples of women at high-risk of and with breast cancer. Structures of these compounds were elucidated with ^{1}H-, ^{13}C- NMR, supported by tandem mass spectrometry (MS/MS) on both an ion trap and a quadrupole time-of-flight (QTOF) mass spectrometer.

The linker synthesis is significant in executing the labeling strategies discussed in my thesis. Introduction of an aminomethyl (-CH$_2$NH$_2$) group in C17 of 4-OHE$_2$ was achieved with the intension to connect with a molecule with a carboxyl (-COOH) functional group. The primary NH$_2$ group initiates faster nucleophilic reaction than the aromatic NH$_2$ group present on purine DNA bases, thereby, selectively labeling through primary NH$_2$ group. (Fig 2.10)

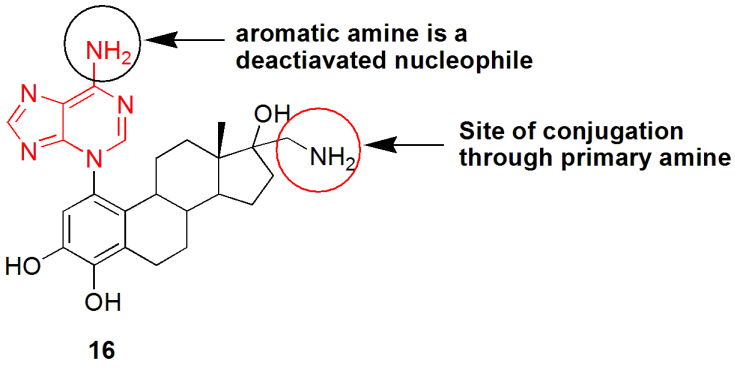

16

4-hydroxy-17-aminomethlyestradiol-1-Adenine

Fig 2.10 The logic behind preferential conjugation through primary amine linker is higher nucleophilicity of this group.

2.6. Conclusions

The synthesis of estrogen-derived DNA adducts has been orchestrated in order to use them in developing a diagnostic tool to detect these adducts in urine of subjects with breast or prostate cancer. An aminomethyl linker has also been introduced in C17 of these adducts to label them with molecules such as organic dyes, aqueous QDs containing carboxylic acid terminal. The labeling of these adducts with aqueous QDs have been discussed in chapter 4.

References

1. Martucci, C. P.; Fishman, *J. Pharmacol. Ther.* **1993**, *57*, 237-257.
2. Zhu, B. T.; Conney, A. H. Carcinogenesis, 1998, 19, 1-27
3. Cavalieri, E. L.; Kumar, S.; Todorovic, R.; Higginbotham, S.; Badawi, A. F. *Chem. Res. Toxicol.* **2001**, *14*, 1041-1050.
4. Cavalieri, E. L.; Stack, D. E.; Devanesan, P. D. *Proc. Natl. Acad. Sci. U.S.A.*, **1997**, *94*, 10937-10942.
5. Li, K. –M.; Devanesan, P. D.; Rogan, E. G.; Cavalieri, E. L. *Proc. Am. Assoc. Cancer Res.* **1998**, *39*, 636.
6. Todorovic, R.; Devanesan, P.; Higginbotham, S.; Zhao, J.; Gross, M. L.; Rogan, E. G.; Cavalieri, E. L. *Carcinogenesis*, **2001**, *22*, 905-911.
7. Li, J. J.; Li, S. A.; Klicka, J. K.; Parsons, J. A.; Lam, L. K. Cancer Res. 1983, 43, 5200-5204.
8. Liehr, J. G.; Fang, W. F.; Sirbasku, D. A.; Ari-Ulubelen, A. *J. Steroid Biochem.* **1986**, *24*, 353-356.
9. Li, J. J.; Li, S. A. *Fed. Proc.* **1987**, *46*, 1858-1863.
10. Rajah, T. T.; Pento, J. T. *Res. Comm. Molecul. Pathol. Pharmacol.* **1995**, *89*, 85-92.
11. Kong, L-Y.; Szaniszlo, P.; Albrecht, T.; Liehr, J. G. *Int. J. Oncol.*, **2000**, *17*, 1141-1149.
12. Chakravarti, D.; Mailander, P. C.; Li, K.-M.; Higginbotham, S.; Zhang, H.; Gross, M. L.; Cavalieri, E.; Rogan, E. *Oncogene*, **2001**, *20*, 7945-7953.
13. Tsutsui, T.; Tamura, Y.; Yagi, E.; Barrett, J. C. *Int. J. Cancer*, **2000**, *86*, 8-14.
14. Russo, J.; Lareef, M. H.; Tahin, Q.; Hu, Y. -F.; Slater, C.; Ao, X.; Russo, I. H. *J. Steroid Biochem. Mol. Biol.* **2002**, *80*, 149-162.
15. Russo, J.; Lareef, M. H.; Balogh, G.; Guo, S.; Russo, I. H. J. Steroid Biochem. Mol. Biol. **2003**.
16. Li, K. –M.; Todorovic, R.; Devanesan, P.; Higginbotham, S.; Köfeler, H.; Ramanathan, R.; Gross, M. L.; Rogan, E. G.; Cavalieri, E. L. *Carcinogenesis*, **2004**, *25(2)*, 289-297.
17. Chen, P. C.; Chen, S. C. *Int. J. of Quant. Chem.* **2001**, *83*, 332-337.

CHAPTER 3- Direct Synthesis of Aqueous Quantum Dots through a 4, 4'-bipyridine-Based Twin Ligand Strategy

ABSTRACT

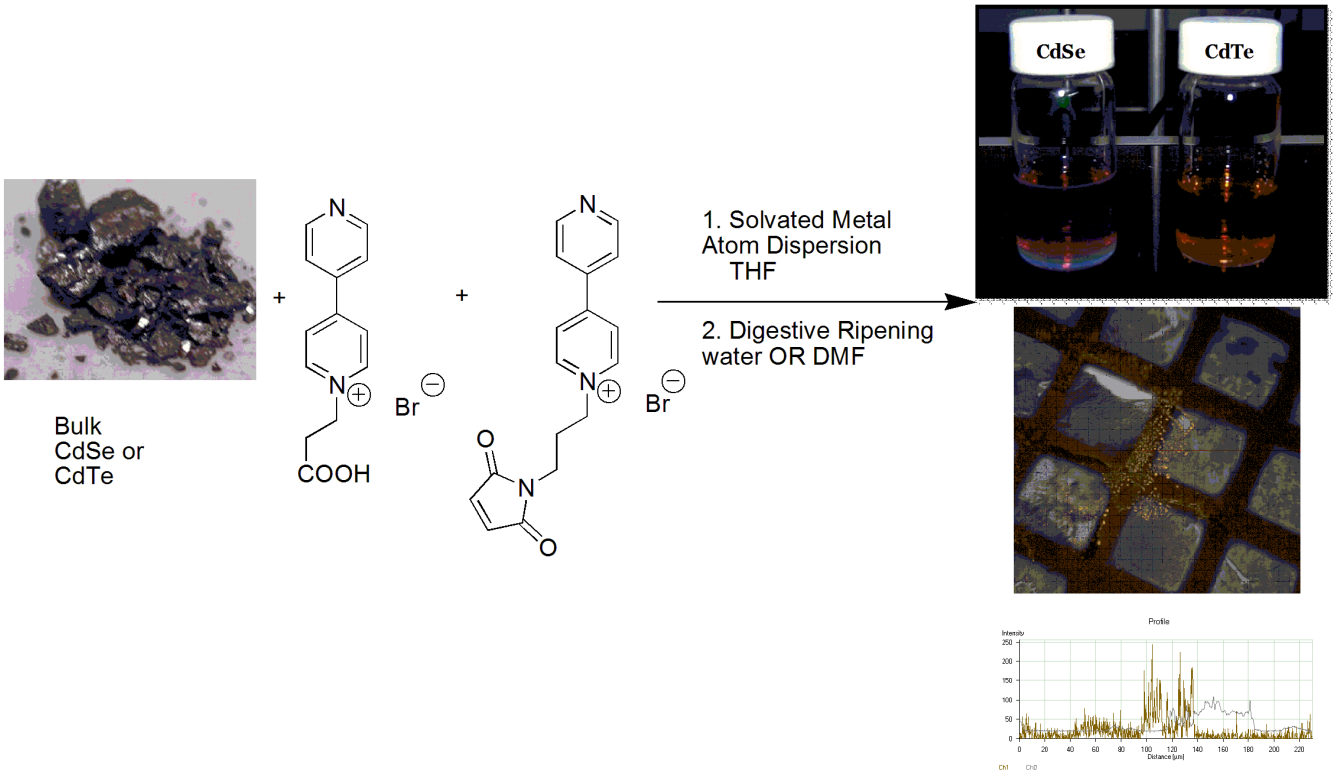

Fig 3.1 Direct synthesis of water soluble CdSe and CdTe quantum dots by evaporation-cocondensation-reflux technique

We report a new class of derivatized 4,4'-bipyridinium ligands for use in synthesizing highly fluorescent, extremely stable, water soluble CdSe and CdTe quantum dots (QDs) for bioconjugation. We employed an evaporation-condensation technique, also known as solvated metal atom dispersion (SMAD), followed by a digestive ripening procedure. This method has been used to synthesize both metal nanoparticles and semiconductors in the gram scale with several stabilizing ligands in various solvents. The SMAD technique comprised evaporation/ condensation and stabilization of CdSe or CdTe in tetrahydrofuran (THF). The as-prepared product was then digestively ripened both in water and dimethyl formamide (DMF), leading to narrowing of the particle size distributions. The ligands were synthesized by nucleophilic

substitution (S_N2) reactions using 4,4'-bipyridine as a nucleophile. Confocal microscopy images confirmed the orange color of the nanocrystalline QDs with diameters of ~5nm that have been also observed by using TEM (transmission electron microscopy). As a part of our strategy, 85% of the 4,4'-bipyridinium salt was synthesized as propionic acid derivative and used to both stabilize the QDs in water and label basic amino acids and different biomarkers utilizing the carboxylic acid functional group. 15% of the 4,4'-bipyridinium salt was synthesized as N-propyl maleimide and used as second ligand in order to label any protein containing the amino acid cysteine by means of a 1, 4- Michael addition.

3.1. Introduction

The discovery of quantum dots (QDs) and their bright luminescence has inspired scientists to explore their application as bioimaging agents in medical diagnostics,[1,2] as photosensitizing agents in the photodynamic therapy of cancer,[3,4] and as components if solar cells [5,6] and light emitting devices (LEDs).[7-8] Quantum dots feature size and composition tunable electronic and optical properties with sharp, Gaussian emission spectra in addition to large absorption coefficients across a wide spectral range.[9-11] These are definite advantages of QDs over traditional dyes as imaging agent *in vivo* and *in vitro*. Most reported syntheses of QDs are carried out by using hydrophobic ligand encapsulation.[12, 13] However, the importance of synthesizing biocompatible, aqueous QDs is immense, especially for the purpose of labeling of monoclonal antibody and biomarkers. Dubois et. al. reported a synthesis of aqueous QDs by exchanging the initial hydrophobic ligand trioctylphosphine oxide (TOPO) with the hydrophilic ligand dithiocarbamate. This ligand exchange method required the presence of a ZnS shell around the CdSe core to prevent the extinction of photoluminescence. [14] Other synthesis procedures involved QD surface modification through imidazole-based random copolymer ligands,[15] and surfactant/lipid micelles,[16] resulting in large (diameter>10nm) supramolecular assemblies. These aqueous QDs can be monoconjugated through either carboxylate terminal or amine terminal groups. Direct synthesis of aqueous QDs from bulk CdSe or CdTe by twin ligands for double bioconjugation was not known to date. Our synthesis comprises of the environment-friendly evaporation-condensation method known as Solvated Metal Atom Dispersion (SMAD) technique, followed by digestive ripening to obtain stable, monodisperse, orange colored QDs. The SMAD technique has already been used to synthesize hydrophobic QDs,[18] both aqueous and non-aqueous gold colloids,[19, 20] and silver nanoparticles with biocidal activity.[21] The biggest advantages of this synthesis are the independence of the solvent and ligand

choice, no metal salt byproduct formation, and the possibility to scale up the reaction to gram scale for industrial applications. The choice of 4,4'-bipyridinium salts as ligands for QD stabilization and bioconjugation was inspired by the success of ligand exchange experiments in our lab though the stability of QDs after ligand exchange was not enough for further application. We decided to use 4, 4'-bipyridinium salts for direct surface passivation of CdSe and CdTe QDs through SMAD. The synthesis of aqueous CdSe and CdTe QDs was achieved by the following twin ligands: 1. 4,4'-bipyridinium carboxylic acid (**3**) used for water solubility through H-bonding with water and 2. 4,4'-bipyridinium maleimide (**7**) used for coupling with cysteine-SH through 1, 4-conjugate addition or Michael addition reaction. (Fig 3.2)

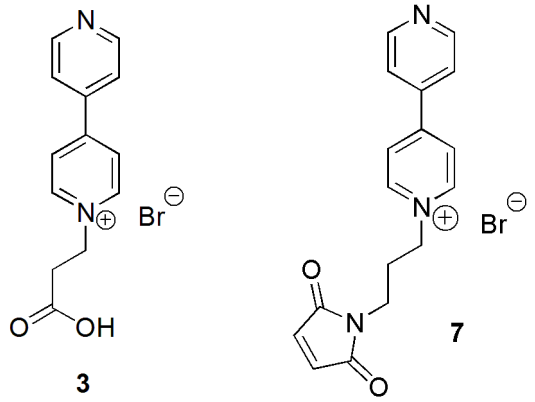

Fig 3.2 4,4'-bipyridinium salt based twin ligands used to synthesize aqueous QDs

QDs synthesized in gram quantities in a SMAD reactor in water had narrow size distributions from 4 nm to 4.5 nm. This was achieved by using the "digestive ripening" technique, which has been pioneered by Dr. Klabunde at Kansas State University.[22, 23, 24] This process involves refluxing of the as-prepared SMAD colloid in a solvent resulting in a remarkable narrowing of the size distribution observed in TEM experiments. The UV-/Vis, fluorescence microscopy and confocal microscopy images also confirm the synthesis of water soluble QDs.

3.2. Experimental Section

Scheme 3.1 Flow Diagram of Synthetic Steps of Water Soluble QDs through Evaporation-Condensation

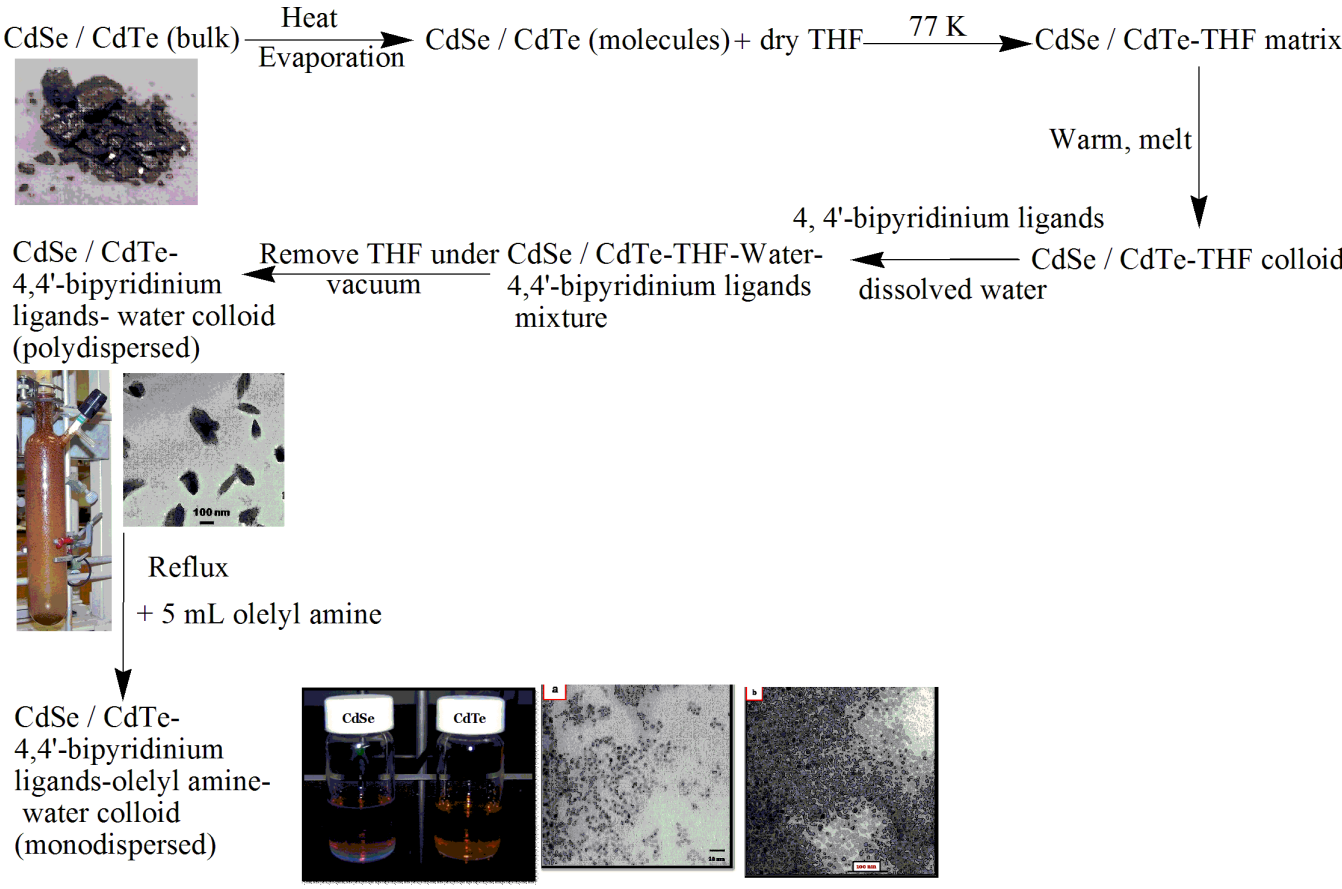

3.2.1. CdSe-Water- 4,4'-bipyridinium Ligands Colloid:

A 39-boron nitride crucible (from Mathis) was assembled in the SMAD reactor and 0.20g of CdSe (1.04 mmol) was added to the crucible. Ligand **3** (9.71g, 31.4 mmol) and ligand (2.2g, 5.2 mmol), dissolved in 40 mL degassed nanopure water was placed at the bottom of the reactor together with a stir bar. The reactor was attached to 100 mL degassed THF in a Schlenk tube. The reactor was then cooled down to 77 K by immersing it in a liquid nitrogen filled Dewar, followed by the complete evacuation of the reactor until a vacuum or 0.53 Pa was reached. 15 mL THF was evaporated in 30 min. forming a layer of solvent on the walls of the reactor. Bulk CdSe on the crucible was heated slowly and co-condensed with THF (60 mL) over a period of 3 h. The frozen matrix had a brownish red color at the end of the vapor deposition process. Once

the process was complete, the Dewar was removed and the reactor was filled with argon. The frozen matrix was melted by heating from outside with a heat gun. The melted matrix was allowed to stir for 30 min. The as-prepared brown red matrix was siphoned under argon into a Schlenk tube.

The Schlenk tube containing the freshly prepared CdSe-colloid, which was stabilized by the twin-4,4'-dipyridinium ligands in THF/water, was connected to a vacuum line and the THF was evaporated overnight. The total volume of the final colloid was 40 mL containing 0.20g of CdSe.

3.2.2. Digestive Ripening:

The CdSe-colloid, stabilized by the twin-4,4'-dipyridinium ligands in water, was divided into two parts. 20 mL of this suspension was filled in a 100 mL round bottom flask with a glass window for UV/Vis-detection. The round bottom flask was connected with a UV/Vis-spectrometer on-a-chip through an optical fiber for the recording of continuous UV/Vis spectra. The colloid was refluxed under argon for 8h.

Another 20 mL colloid was subjected to high vacuum to evaporate the water, thus forming the dry product. It was transferred to a 100 mL round bottom flask and dissolved in 20 mL dry DMF. 5 mL of oleyl amine was also added to increase the rate of monodisperse particle formation.[25] The reaction was refluxed for 3h under argon. QD in DMF was placed in an ultracentrifuge (8000 RPM) for 15 minutes and the precipitate was dissolved in water.

3.3. Characterization

UV/Vis Spectroscopy:
UV/Vis absorption spectra were measured by using a DH-2000 optical spectrophotometer (Ocean Optics Inc.)

Fluorescence Spectroscopy:
Fluorescence spectra were obtained by using Fluoro Max-2 instrument from HORIBA Jobin Yvon Company. These samples were excited at 400 nm with slit width of 5 nm.

Photoluminescence Spectroscopy

The photoluminescence (PL) quantum yield of CdSe and CdTe was calculated relative to Rhodamine 6G in methanol assuming its PL quantum yield as 95%.[25, 26]

$$\Phi_{em} = \Phi_S(I/I_S)(A_S/A)(n^2/n_s^2)$$

Where, I(QD) and I_S(standard) are the integrated emission peak areas and

A(QD) and A_S(standard) are absorption (<0.1) at 480 nm

n(QD) and n_S(standard) are the refractive indices of the solvents

Φ_{em} and Φ_S are the PL quantum yield for the QD and standard respectively.

Transmission Electron Microscopy

TEM images were taken on a Philips CM100 operating at 100 kV. The samples were prepared by a drop of 3 µL CdSe and CdTe solution in water on a carbon-coated Formvar copper grid. The grids were allowed to dry overnight in vacuum in a desiccator.

3.4. Results and Discussion

The SMAD technique was first reported in 1986. It has been successfully used to synthesize metal nanoparticles and semiconductor nanocrystals.[18,23,27] We have performed the facile synthesis of two 4, 4'-bipyridinium ligands with high yields affording grams of the products, which were required for stabilizing CdSe and CdTe semiconductor nanocryctals synthesized by SMAD .

Synthesis of the 4,4'-Bipyridine Based Twin Ligands

The choice of the ligand was inspired by our preliminary work in ligand exchange between 4,4'-bipyridine and trioctylphosphine oxide (TOPO) though the QDs resulted after the ligand exchange had broad size distribution making them less useful for bioconjugation.

The logic behind the use of 85% carboxylic acid terminal derivative of 4, 4'-bipyridine (**3**) was to solubilize the QDs in water. The one step synthesis of **3** consisted of a nucleophilic substitution reaction by a S_N2 mechanism in DMF affording 80.2% yield. (Scheme 3.2)

Scheme 3.2 Synthesis of carboxylic acid derivative of 4,4'-bipyridine

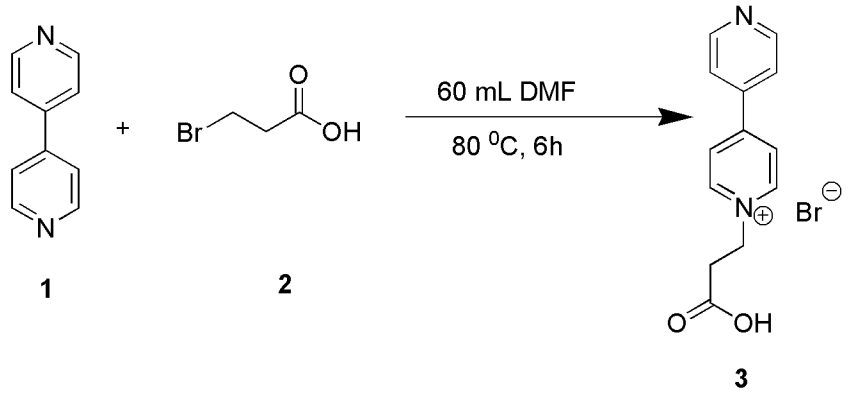

Our initial attempt to use a terminal maleimide derivative of 4, 4'-bipyridine (**7**) as ligand for QD stabilization was not successful, as the ligand was water soluble only before binding with the QDs, resulting in their rapid aggregation after QD synthesis. Compound **7** was prepared in a two-step chemical synthesis. The maleimide (**4**) served as a nucleophile in a Mitsunobu reaction, leading to compound **6** in 70% yield.[28] In the second step, 4,4'-bipyridine acted as nucleophile to displace the bromide in the C-Br bond of **6** . It is important to permit this reaction to run for three days at 35 ^{0}C in order to form the mono-substituted product. (Scheme 3.3)

Scheme 3.3 Synthesis of maleimide derivative of 4,4'-bipyridine

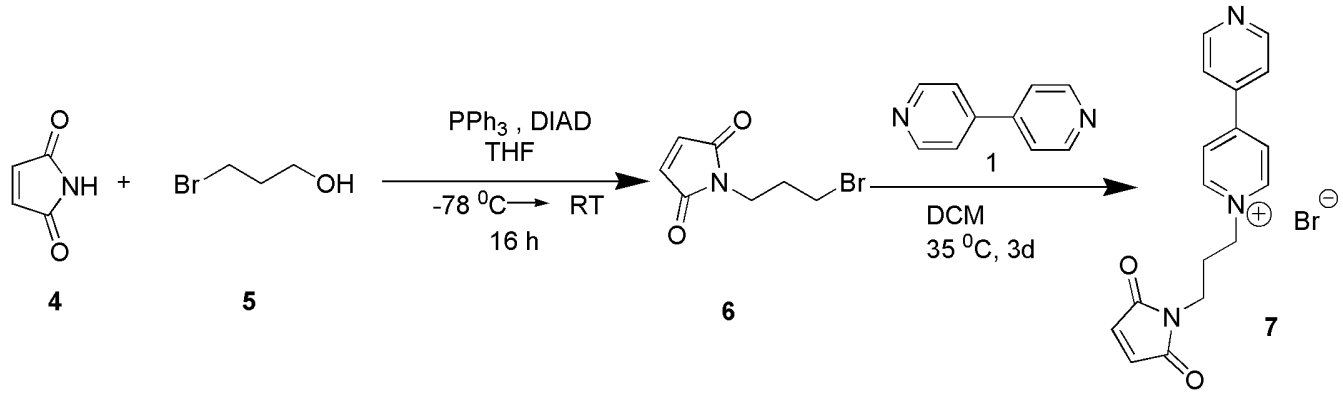

The 85:15/(**3**):(**7**) ligand ratio approach solved not only the water solubility problem, but also introduced two sites for potential double bioconjugation. The double bioconjugation schemes through –COOH and maleimide termini will be reported in chapter 4.

UV/Vis-Data Analysis

It is noteworthy that the positions of the UV/Vis-absorption maxima/shoulders of the CdTe quantum dots that have been prepared in DMF and in water differ by 50nm. In accordance with the literature, the observed red shift can be attributed to a larger particle size when ripened in

DMF, compared to in water. (Fig 3.3) The CdTe QDs growth was expedited by addition of 5 mL of oleylamine, which acted as a weak amine stabilizer, thereby, helping in growth kinetics.[25]

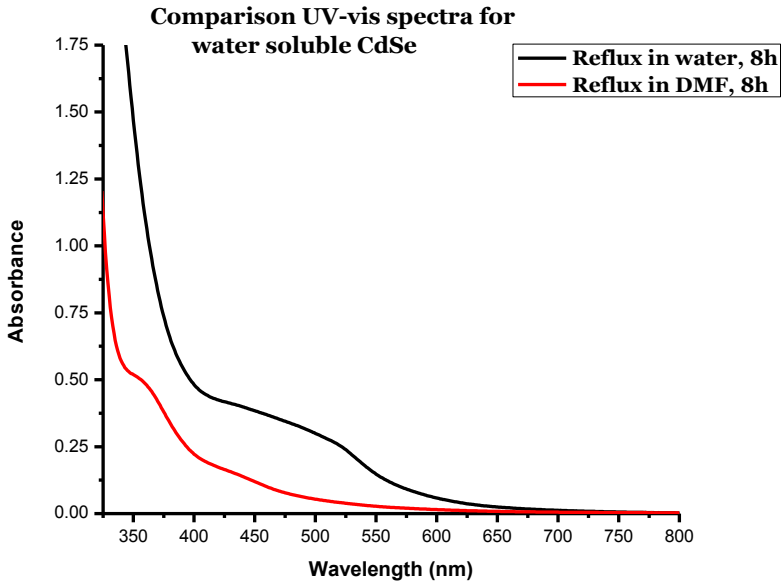

Fig 3.3 UV-vis spectra of CdSe ripened in water and in DMF

The evolution of particle size during digestive ripening of QDs was monitored through dynamic UV-vis spectra. It was observed that there was change in particle size distribution as well as enhanced absorbance as the particles were ripened for extended period of time. (Fig 3.4)

A

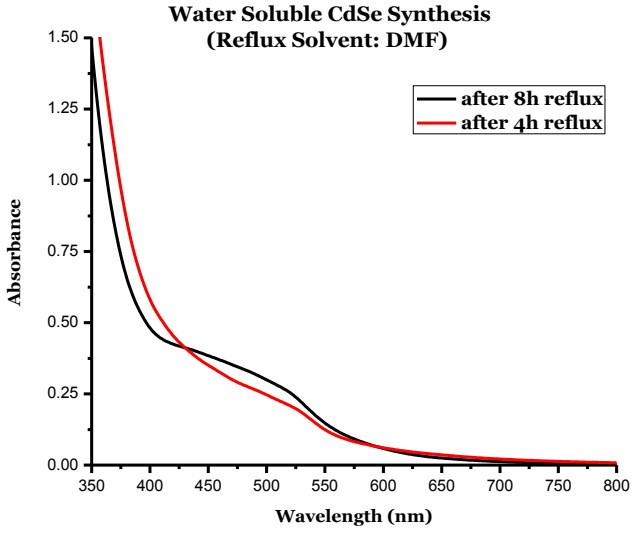

B

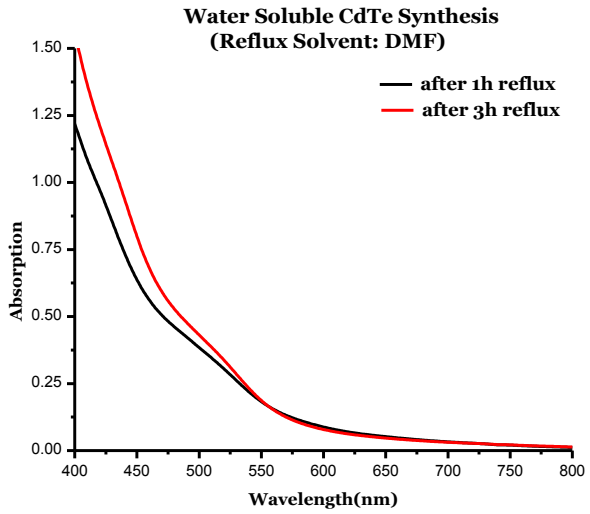

Fig 3.4 Evolution of absorbance spectra for CdSe (**A**) and CdTe (**B**) during digestive ripening

The fluorescence spectra of CdSe and CdTe QDs complimented the UV-Vis data as there was a red shift by about 50nm in CdTe spectrum emphasizing larger sized CdTe QDs. (Fig 3.5)

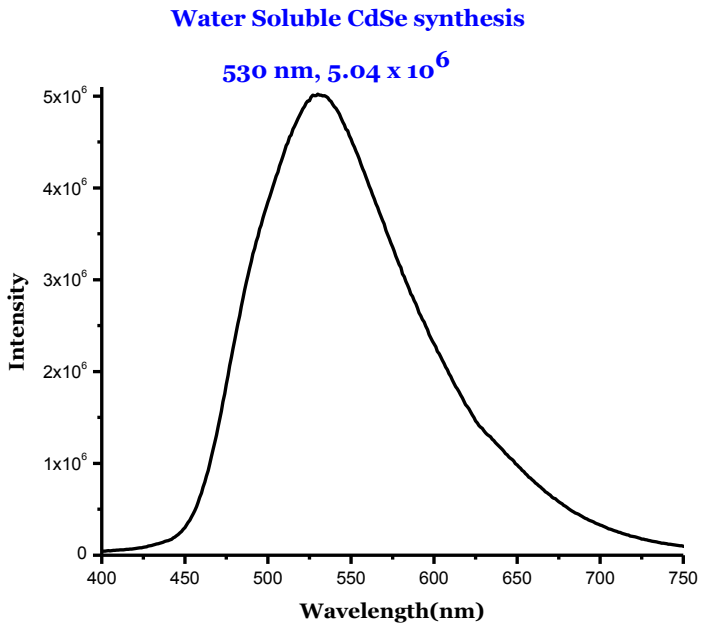

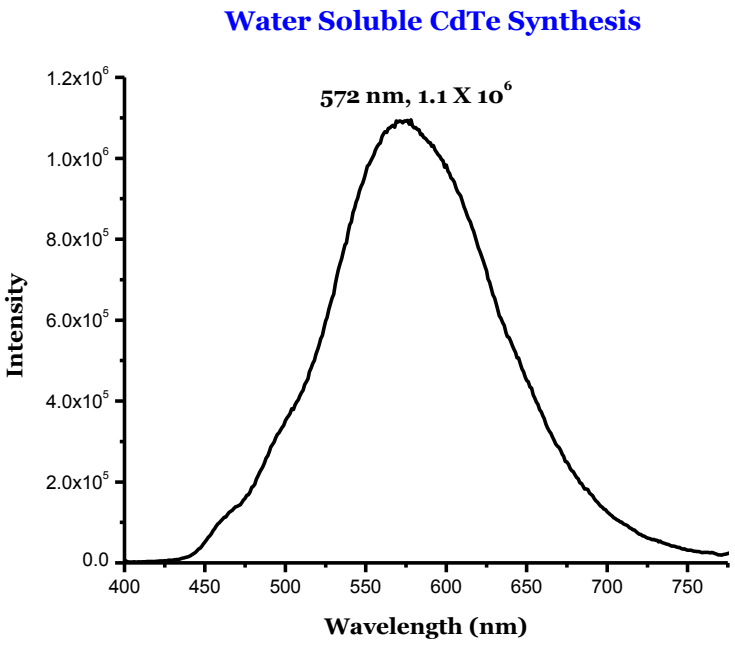

Fig 3.5 Fluorescence spectra of CdSe and CdTe QDs synthesized by twin ligand strategy

The QY (quantum yield) of the aqueous QDs found to be 12% which is comparable to QY of 16-28% for QDs in organic solvents when QDs are excited at 390nm with slit width of 5nm.[18, 25] (Table 3.1.)

Table 3.1. Quantum yield of water soluble QDs

QDs	Absorbances	$\lambda_{max,\ fluorescence}$	Intensity	QY (%)
CdTe	0.09	572 nm	$1.1*10^6$	12
CdSe	0.09	530 nm	$2.4*10^6$	25

The TEM images showed the average particle size of both CdSe and CdTe QDs to be 4.0 nm and 4.5 nm respectively. (Fig 3.6) The orange color of these QDs was confirmed with confocal microscopy. (Please refer to the following supporting information)

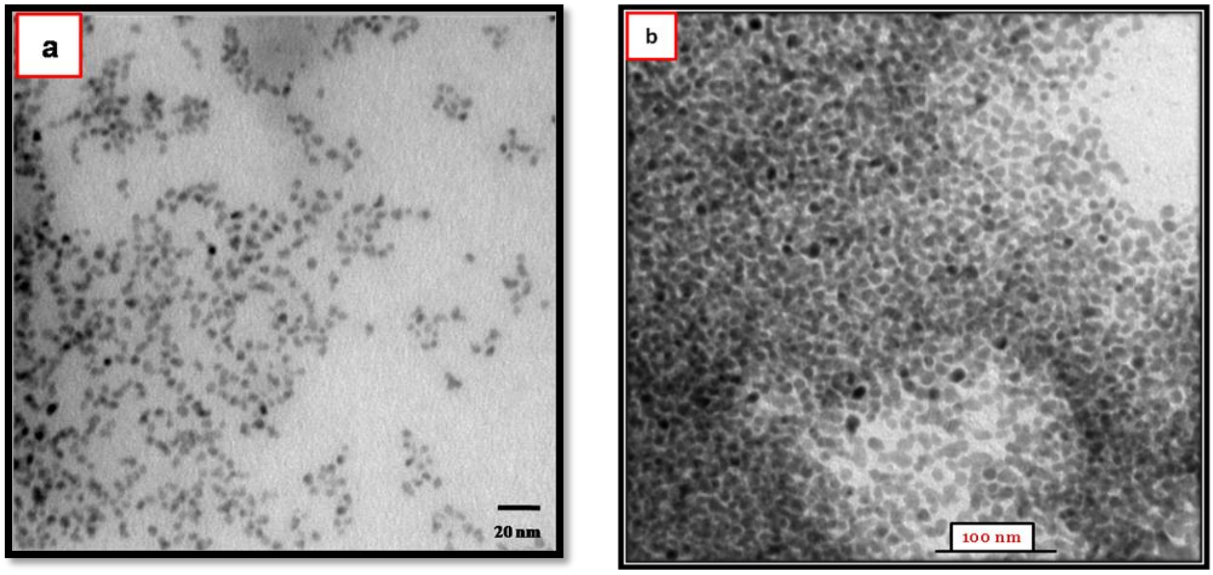

Fig 3.6 TEM images of (a) CdSe ripened in DMF for 8h and (b) CdTe QDs ripened in DMF for 3h

Photostability Experiments

The aqueous QDs were excited consecutively at 488 nm once in every second for 500 successive illuminations at laser powers of 1 mW, 1.5 mW and 1.9 mW. The photostability of these QDs was compared with QDs synthesized in organic solvents through SMAD technique-digestive ripening.[18] The mean life time ($1/\tau$) of both aqueous QDs and organic QDs stabilized by trioctylphosphine oxide (TOPO) ligand probably have similar lifetimes as there is a lot of variability in the numbers. (See Appendix B)

These results seem to suggest they are similar. The QDs can be "photoactivated" by illumination and that would lead to an increase in "on" times - and could erroneously be interpreted as an increase in lifetime, if the time transients aren't long enough (i.e., the particles aren't actually bleaching by the end of the 500 frames).

The comparison of images of both the CdTe types taken at zero second and four seconds after illumination with 1.9 mW, 488 nm wavelength laser shows fluorescence decay of the QDs. (Fig 3.7) This opens a window of opportunity for the use of aqueous QDs for biomedical application in future.

A. Aq. CdTe, 1.9mW, Time 0s Aq. CdTe, 1.9mW, Time 4s

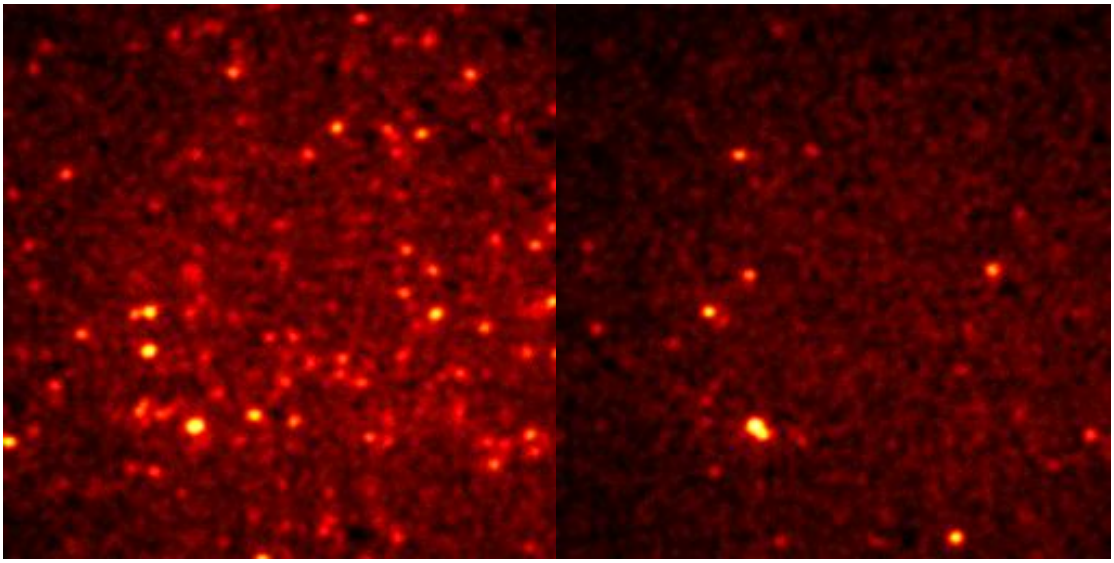

B. CdTe-TOPO, 1.9mW, Time 0s CdTe, 1.9mW, Time 4s

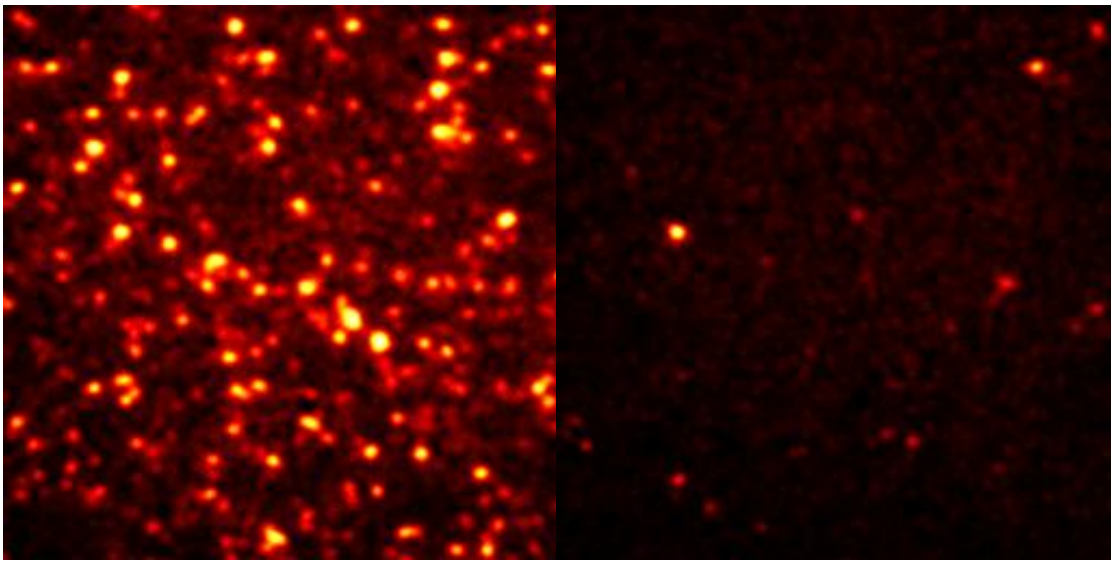

Fig 3.7 The real time images of aqueous CdTe stabilized by 4,4'-bipyridinium salt based ligands (**A**) and CdTe-TOPO in toluene (**B**) at the start of the experiment and after 4s of illumination with 1.9mW laser power.

3.5. Conclusions

We have achieved the direct synthesis of aqueous CdSe and CdTe QDs by SMAD, followed by digestive ripening. The result were highly fluorescent and photostable QDs. We will use the new QDs as imaging "tools" in detecting DNA-estrogen adducts, which are potential biomarkers for

breast and prostate cancer.[29, 30] It is noteworthy that QD synthesis from water resulted in lower quantum yields of luminescence, but significant photostability. Besides the water solubility, the biggest advantage of these QDs is the possibility of double bioconjugation through both –COOH and maleimide termini. A multitude of *in vitro* and possible *in vivo* application of these QDs can be envisioned in the field of biomedical research.

References

1. Bruchez, M., Jr.; Moronne, M.; Gin, P.; Weiss, S.; Alivisatos, A. P. *Science* **1998**, *281*, 2013-2105.

2. Dubertret, B; Skourides, P.; Norris, D. J.; Noireaux, V.; Brivanlou, A. H.; Libchaber, A. *Science* **2002**, *298*, 2759-1762.

3. Rakovich, A.; Savateeva, D.; Rakovich, T.; Donegan, J. F.; Rakovich, Y. P.; Kelly, V.; Lesnyak, V.; Eychmuller, A. *Nanoscale Res. Lett.* **2010**, *5(4)*, 753-760.

4. Chen, J. Y.; Lee, Y. M.; Zhao, D.; Mak, N. K.; Wong, R. N. S.; Chan, W. H.; Cheung, N. H. *Photochem. and Photobiol.* **2010**, *86(2)*, 431-437.

5. Huynh, W. U.; Peng, X. G.; Alivasatos, A. P. *Adv. Mater.* **1999**, *11*, 923-927.

6. Huynh, W. U.; Dittmer, J. J.; Alivasatos, A. P. *Science* **2002**, *295*, 2425-2427.

7. Caruge, J. –M.; Halpert, J. E.; Bawendi, M. G. *Nano Lett.* **2006**, *6*, 2991-2994.

8. Achermann, M.; Petruska, M. A.; Koleske, D. D.; Crawford, M. H.; Klimov, V. I. *Nano Lett.* **2006**, *6*, 1396-1400.

9. Dabbousi, B. O.; Rodriguez-Viejo, J.; Mikulec, F. V.; Heine, J. R.; Mattoussi, H.; Ober, R.; Jensen, K. F.; Bawendi, M. G. *J. Phys. Chem. B* **1997**, *101*, 9463-9475.

10. Zimmer, J. P.; Kim, S.-W.; Ohnishi, S.; Tanaka, E.; Frangioni, J. V.; Bawendi, M. G. *J. Am. Chem. Soc.* **2006**, *128*, 226-2527.

11. Peng, Z. A.; Peng, X. *J. Am. Chem. Soc.* **2001**, *123*, 183-184.

12. Murray, C. B.; Norris, D. J.; Bawendi, M. G. *J. Am. Chem. Soc.* **1993**, *115*, 8706-8715.

13. Talapin, D. V.; Rogach, A. L.; Kornowski, A.; Haase, M.; Weller, H. *Nano Lett.* **2001**, *1*, 207-211.

14. Dubois, F.; Mahler, B.; Dubertret, B.; Doris, R.; Mioskowski, C. *J. Am. Chem. Soc.* **2002**, *129*, 482-483.

15. Liu, W.; Greytak, A. B.; Lee, J.; Wong, C. R.; Park, J.; Marshall, L. F.; Jiang, W.; Curtin, P. N.; Ting, A. Y.; Nocera, D. G.; Fukumura, D.; Jain, R. K.; Bawendi, M. G. *J. Am. Chem. Soc.* **2010**, *132*, 472-483.

16. Fan, H.; Leve, E. W.; Scullin, C.; Gabaldon, J.; Tallant, D.; Bunge, S.; Boyle, T.; Wilson, M. C.; Brinker, C. J. *Nano Lett.* **2005**, *5*, 645-648.

17. Yan, C.; Tang, F.; Li, L.; Li, H.; Huang, X.; Chen, D.; Meng, X.; Ren, J. *Nanoscale Res. Lett.* **2010**, *5*, 189-194.

18. Cingarapu, S.; Yang, Z.; Sorensen, C. M.; Klabunde, K. J. *Chem. Mater.* **2009**, *21*, 1248-1252.

19. Stoeva, S.; Klabunde, K. J.; Sorensen, C. M.; Dragieva, I.; *J. Am. Chem. Soc.* **2002**, *124*, 2305-2311.

20. Lin, S.; Franklin, M. T.; Klabunde, K. J. *Langmuir*, **1986**, *2*, 259-260.

21. Smetana, A. B.; Klabunde, K. J.; Marchin, G. R.; Sorensen, C. M. *Langmuir*, **2008**, *24*, 7457-7464.

22. Franklin, M.; Klabunde, K. J.; *High-Energy Processes in Organometallic Chemistry*; Suslick, K. S.; Ed.; ACS Symposium Series; American Chemical Society: Washington, DC, 1987, 246-259

23. Lin, S.; Franklin, M. T.; Klabunde, K. J. *Langmuir* **1986**, *2*, 259-260

24. Klabunde, K. J. Method of Coating Substrates with Solvated Clusters of Metal Particles. U. S. Patent 4,877,647, 1989

25. Zhu, C. –Q.; Peng, W.; Xin, W.; Li, Y. *Nanoscale Res. Lett.* **2008**, *3*, 213-220.

26. Cumberhand, S. L.; Hanif, K. M.; Javier, A.; Khitrov, G. A.; Strouse, G. F.; Woessner, S. M.; Yun, C. S. *Chem. Mater.* **2002**, *14*, 1576-1584.

27. Trivino, G.; Klabunde, K. J.; Dale, E. *Langmuir*, **1987**, *3(6)*, 986-992

28. Walker, M. A. *J. Org. Chem.* **1995**, *60*, 5352-5355

29. Cavalieri, E.; Stack, D. E.; Devanesan, P. D.; Todorovic, R.; Dwivendy, I.; Higginbotham, S.; Johansson, S. L.; Patil, K. D.; Gross, M. L.; Gooden, J. K.; Ramanathan, R.; Cerny, R. L. Proc. Natl. Acad. Sci. U. S. A. 1997, 94, 10937-10942

30. Li, K. M.; Todorovic, R.; Devanesan, P. D.; Higginbotham, S.; Kofeler, H.; Ramanathan, R.; Gross, M. L.; Rogan , E. G.; Cavalieri, E. L. *Carcinogenesis*, **2004**, *25*, 289-297

CHAPTER 3- Direct Synthesis of Aqueous Quantum Dots through a 4, 4'-bipyridine-Based Twin Ligand Strategy

Supporting Information

Chemical Synthesis of 4,4'-bipyridinium salt based ligands

1. Synthesis of 4,4'-bipyridinium carboxylic acid (**3**)

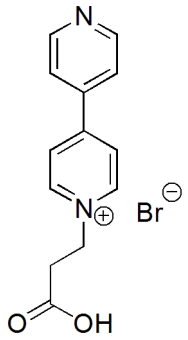

3

4, 4'-bipyridine (**1**) (4g, 0.025mol) and 3-bromo-propanoic acid (**2**) (3.85g, 0.025mol) were charged into a 250 mL round bottom flask and dissolved in 60 mL DMF. The reaction was then heated to 80 ^{0}C for 6 h. Greenish yellow precipitate started to form in half an hour of heating. Once the reaction mixture was cooled down to room temperature, it was kept in refrigerator (4 ^{0}C) for half an hour.

The greenish yellow solid was filtered and washed with cold ethanol (3* 10 mL) and dried under vacuo. DMF of the filtrate was removed further under high vacuo while heating leading to more product formation. (Yield 80.2%)

0.5g of the compound was crystallized from hot ethanol and allowed to return to room temperature. The compound was kept in refrigerator overnight.

^{1}H- NMR (d_6-DMSO, 400MHz) δ (ppm): δ 12.75 (br, s, 1H), 9.26 (d, J = 5.1 Hz, 2H), 8.88 (d, J = 5.4 Hz, 2H), 8.64 (d, J = 6.6 Hz, 2H), 8.05 (d, J = 6.6 Hz, 2H), 4.84 (t, J = , 2H), 3.14 (t, J = , 2H)

^{13}C NMR (d_6-DMSO, 400MHz) δ (ppm):

δ 171.7, 152.5, 151.0, 145.9, 141, 125.1, 122.0, 56.1, 34.4

2. Synthesis of N-propylbromomaleimide (**6**)

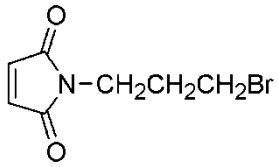

PPh_3 (1.35g, 5.15 mmol) was charged in a 100 mL round bottom flask and dissolved in 20 mL dry THF. The temperature of the reaction was brought down to -78 ^{0}C by using dry ice/acetone. Diisopropyl azo dicarboxylate (1.01 mL, 5.15 mmol) was added dropwise to the reaction mixture over 2 minutes resulting yellow solution. The reaction was stirred for 10 minutes followed by addition of 3-bromo propanol (0.77 mL, 8.5 mmol) for over 2 min. After 5 minutes of stirring, maleimide (0.5g, 5.15 mmol) was added in solid form at – 78 ^{0}C which dissolved in another 10 min. The reaction was then, brought to room temperature and allowed to stir at room temperature for 10 hours. A dark grey solution was resulted and TLC at 2:1 hexane: EtOAc showed formation of product. The reaction mixture was concentrated under raotavap and applied to silica gel. Column with an eluant of 2:1 hexane: EtOAc. After removing solvent, 0.78 g (69.64 %) pale yellow crystal of N-propyl bromo maleimide was obtained.

Melting Point: 45 ^{0}C.

^{1}H- NMR ($CDCl_3$, 400MHz) δ (ppm): 6.72 (singlet, 2H), 3.68 (triplet, J= 6.8Hz, 2H), 3.37 (triplet, J=6.6, 2H), 2.18 (quintet, J=6.6 Hz, 2H).

^{13}C-NMR ($CDCl_3$, 400 MHz) δ (ppm): 170.82, 134.43, 36.82, 31.69, and 29.82.

IR data (cm $^{-1}$, dropcast on KBr):

3088.48, 2960.46, 2924.61, 1700.71, 1408.82, 1234.71,

3. Synthesis of N-propylmaleimide 4,4'-dipyridinium salt (**7**)

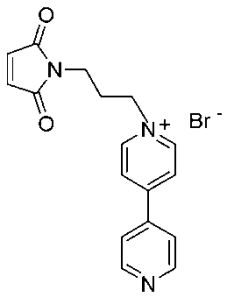

0.1 g (0.641 mmol) of 4, 4'-bipyridine and 0.14g (0.641 mmol) of N-propylbromo maleimide (**6**) was heated in 8 mL anhydrous dichloromethane40 ^{0}C for 24 hours. This resulted in mono quaternization of 4,4'-bipyridine. The light brown salt was filtered and dried under vacuum to obtain 0.15g (62.5%).

Melting Point: 312 ^{0}C.

^{1}H- NMR (d_6-DMSO, 400MHz) δ (ppm): 9.19 (doublet, *J* = 6.8 Hz, 2H), 8.84 (doublet, *J* = 6.24 Hz, 2H), 8.62(doublet, *J* = 6.8 Hz), 8.0 (doublet, *J* = 6.24 Hz, 2H), 7.05 (singlet, 2H), 4.6 (triplet, J = 8 Hz, 2H), 3.5(triplet, *J* = 6.4Hz, 2H), 2.16(quintet, *J* = 6.8Hz, 2H).

^{13}C-NMR (d_6-DMSO, 400 MHz) δ (ppm): 171.1, 152.3, 151.0, 145.4, 140.8, 134.7, 125.3, 121.8, 58.0, 34.0, 30.0

IR Data (cm^{-1}, dropcast on KBr)

2950.21, 2919.5, 2847.8, 1700.71, 1639.26, 1465.15, 1408.82, 1362.79, 1178.38, 814.8, 697.0

Confocal Microscopy Images. Confocal images of the QDs were based on Zeiss LSM 5 PASCAL (Laser Scanning Confocal Microscope) at exciting wavelength of 488 nm

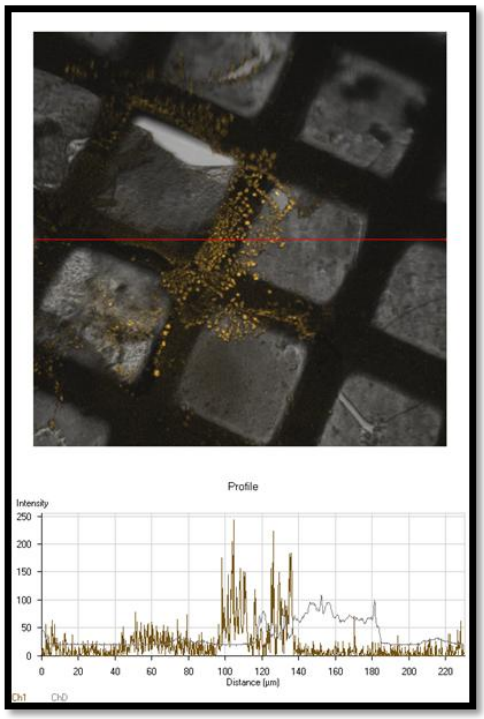

Fig 3.S1 Confocal image of CdTe QDs on TEM grids showed orange color

CHAPTER 4-Double Conjugation Schemes with Aqueous Quantum Dots Synthesized by Twin Ligand Strategy

ABSTRACT

Double conjugation schemes have been developed by using a new class of aqueous CdSe and CeTe quantum dots (QDs), synthesized by an evaporation/co-condensation method, followed by digestive ripening. These QDs were synthesized by applying a 4,4'-bipyridine based twin ligand strategy for achieving both water solubility and covalent conjugation. We will use these novel quantum dots to label (a) potential breast and prostate cancer biomarkers: 4-hydroxy-estradiol-2-N_3-Adenine (4-OH-E_2-N_3-Ade) and 4-hydroxy-estradiol-2-N_7-Guanine (4-OH-E_2-N_7-Gua) adducts through an EDC/NHS coupling reaction of the 4,4'-bipyridinium carboxylic acid ligand, and (b) the known carcinogen thio-pyrene through a 1,4- Michael addition reaction of the 4,4'-bipyridinium maleimide terminal ligand. The labeling of QDs with DNA-estrogen adducts and thio-pyrene was established by using ion exchange high pressure liquid chromatography (HPLC) and capillary electrophoresis. Imaging of the interactions of QD-labeled adducts and antibodies by applying ELISA substantiated the *in vitro* application of the novel QDs.

4.1 Introduction

Employing quantum dots (QDs) in bioimaging and sensing has become an "explosive" field of research during the last decade. Size tunable fluorescence,[1] resistance to photobleaching, opportunities for chemical QD surface modifications[2, 3, 4], and superior signal brightness[5, 6] have made QDs a more appealing imaging tools than traditional organic dyes. Several QD bioconjugation schemes have been developed for the quantitative determination of cancer in serum and saliva.[7] Immunofluorescent cell imaging,[8] redox coupled assemblies for *in vitro* and intracellular pH sensing,[9] and background free biomolecule detection[10] have been developed as well.

One of the paradigms of my thesis is that estrogen can act as an epigenetic carcinogen inducing point mutation in DNA double helix initiating breast cancer in women.[11, 12] This mutation results possibly in depurinating DNA-estrogen adducts: 4-hydroxyestrone (estradiol)-1-N3Adenine [4-OHE_1(E_2)-1-N3Ade] and 4-hydroxyestrone(estradiol)-1-N7Guanine [4-OHE_1(E_2)-1-N7Gua] are significantly enhanced in the urine of high risk women and women with breast cancer.[13] DNA-

estrogen adducts are possible biomarkers for breast and prostate cancer risk. Therefore, the development of a diagnostic biosensor based on a fluorescently labeled monoclonal IgG antibody is highly desired for early breast and prostate cancer diagnosis. The limit of detection (LOD) of the estrogen metabolites is in the range of $3x10^{-8}$ M.[14, 15] In an attempt to enhance the imaging sensitivity of the biosensor, water soluble CdSe and CdTe QDs have been synthesized. (Fig 4.1) The emission maximum of the CdTe QD that has been used for bio-labeling is ~570nm and we will term it as QD-570.

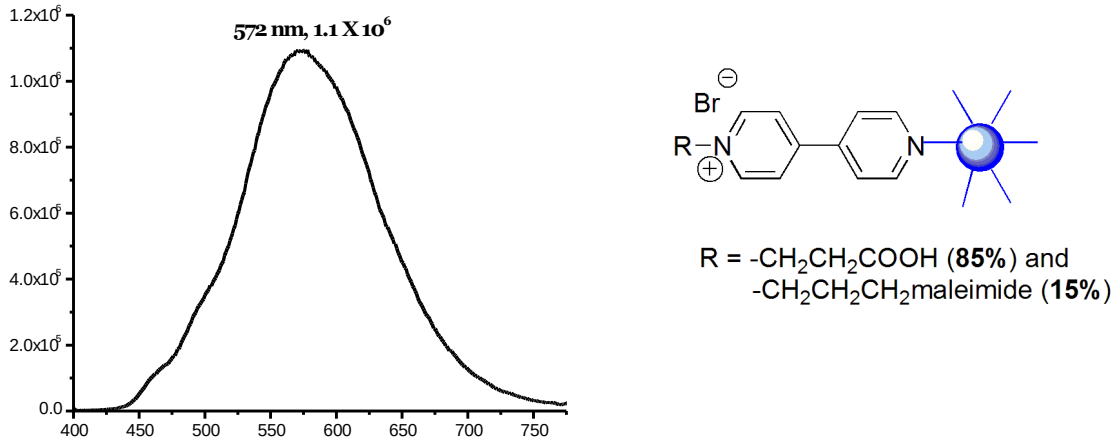

Fig 4.1 Fluorescence spectrum of CdTe QDs (QD-570) synthesized by 4, 4'-bipyridinium ligands for double conjugation

Superlative photostability and large molar extinction coefficients of QDs are the motivation behind their use as bioimaging tools. A new class of derivatized 4, 4'-bipyridinium ligands has been synthesized for QD surface stabilization in water.[16] One of the surface ligands of the QDs was exploited to label DNA-estrogen adducts through its –COOH functional group, yielding the labeled adducts **4** and **5**. (Scheme 4.1)

Scheme 4.1 Conjugation of DNA-estrogen adducts with CdTe QDs

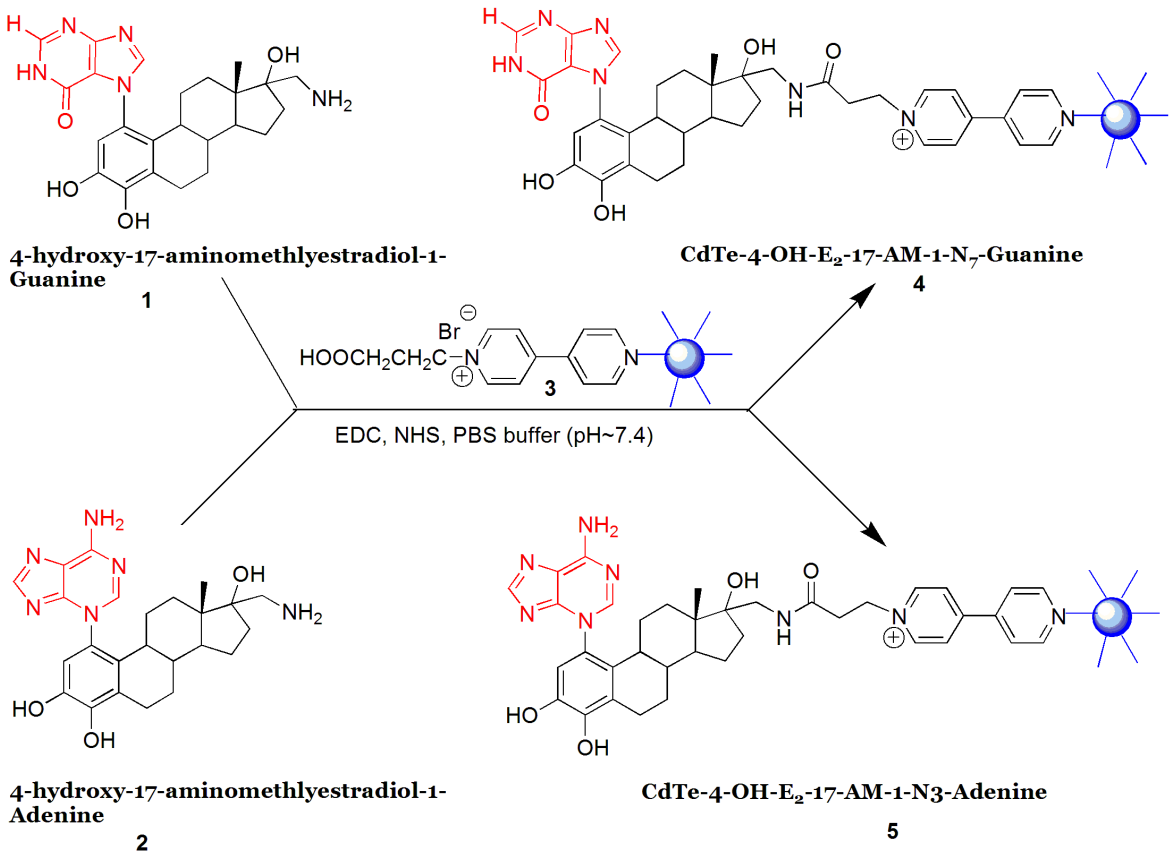

Pyrene is a polycyclic aromatic hydrocarbon (PAH) and a structural part of benzo[a]pyrene (BaP), a potent carcinogen believed to be the major cause of lung cancer. Benzo[a]pyrene is the most widely studied PAH. It undergoes metabolic activation through the "bay region diol epoxide".[17, 18] Analysis of human urinary metabolites of BaP showed the structural similarity with pyrene. Fluorescent labeling of these analytes with QDs is an important step in developing biosensor to detect metabolically activated BaP derivatives. We report a second conjugation scheme between aqueous QD synthesized by using the maleimide group and thio-pyrene. (Scheme 4.2)

Scheme 4.2 Conjugation of thiopyrene with CdTe QDs

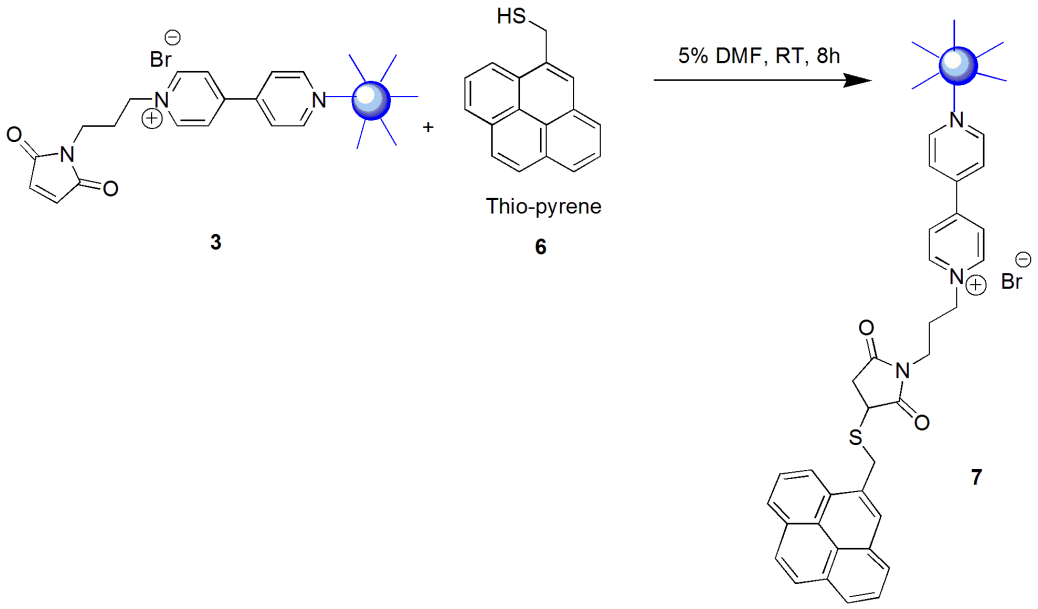

4.2 Experimental Section

General procedure for bioconjugation of DNA-17-aminomethyl-estradiol adducts with QDs through –COOH terminal ligand

CdTe QDs (10mg) was dissolved in phosphate buffered saline solution (PBS, pH~7.4, 10mM) to obtain a solution of 10mg/mL. This solution was incubated with 1-(3-dimethylaminopropyl)-3-ethylcarbodiimide hydrochloride (EDC, 5mg) and N-hydroxysuccinimide (NHS, 3mg) for 2h with continuous gentle mixing to activate QDs. The QD solution was divided into two parts of 0.5mL each for two labeling procedures.

2.2 mM solution of 4-OH-E_2-17-AM-1-N_7-guanine (15 mg in 5 mL) and 1.1 mM solution of 4-OH-E_2-17-AM-1-N_3-adenine (5 mg in 1 mL) was prepared in PBS buffer (pH~7.4, 10mM). DNA-estrogen adduct solution (1.0 mL) was added to activated QD solution (0.5mL) for two labeling experiments. Each resulting mixture was incubated for 3h at room temperature under gentle shaking. This mixture was stored at 4 ^{0}C overnight to allow unreacted EDC to hydrolyze and lose its activity. The solution was then dialyzed in a MW 3500 cut-off tube for 8h resulting in only QD labeled DNA-estrogen adducts.

General procedure for bioconjugation of thiopyrene with QDs through the ligand featuring the terminal maleimide functionality

A 25 mL round bottom flask was charged with thiopyrene (10mg, 0.04mmol) and 10mL CdTe QD solution, which resulted in a suspension. 0.5mL of DMF was added to dissolve thiopyrene and the resulting mixture was stirred overnight at room temperature. The excess of thiopyrene was removed by dialysis in a MW 3500 cut-off tube for 8h resulting only QD labeled thiopyrene. Thiopyrene and QD labeled thiopyrene were analyzed by HPLC using an ion exchange column (POROS HQ/20; 10mmDx100mmL)

4.3 Estimation of IgM antibody

I. BCA protein estimation kit (from pierce) to estimate concentration of IgM antibody

Dilute this antibody to a final concentration of 50 ng/100 ul (= 0.5 ug/ml) in 50 mM carbonate buffer (pH~9.6)

Note: For one plate, 96 x 100 µl = ~10 mL IgM solution in carbonate buffer. This means there is at least 5 µg IgM antibodies for one plate.

II. Direct ELISA Procedure:

1. Deliver 100 µl of IgM antibody solution in each well. Use a 8-chanel pipette to reduce the timing error.
2. Incubate overnight at 4 oC under static conditions.
3. Throw away the content and then, wash the well with washing buffer (0.5% tween 20 in PBS buffer pH~7.4, this will be called PBST now on) *3 times. During washing use multichanel pipette and make sure the attached antibody or any liquid from one well should never go into any other wells, otherwise there will be cross-well contamination.
4. Fill all ELISA well with 5% nonfat milk in PBS buffer (weigh 5g non fat dry milk and dissolve in 100 mL of PBST buffer)
5. Incubate for 2h at RT
6. Throw away everything and wash the wells with washing buffer *3 as in step 3
7. 12 column * 8 rows
8. Each column *8 for one concentration
9. Keep column 2 empty, fill column 1,3-12 with 100 µL of PBS buffer
10. Column 2: 1 µM of adduct labeled with QD

11. Column 3: 100 µL of 1 µM of adduct labeled with QD
12. Use a multi-channel pipette to mix the column 3 and then transfer 100 microL of solution from column 3 in to column 4, and so on until you reach column 12.
13. Discard 100 microL from column 12 making 100 microL in each well
14. Incubate for 2 h at RT and throw away with the content
15. Wash with washing buffer*3
16. Measure the intensity under plate reader

4.4 Results and Discussion

4.4.1 High Pressure Liquid Chromatography (HPLC): In order to determine the binding between the QDs and DNA-estrogen adducts and thiopyrene, a HPLC procedure was developed. HPLC chromatograms of QD-570, 4-OH-17-aminomethylestradiol-1-N_7-Guanine and their assembly are shown in Figure 4.2. The QD conjugated adduct eluted at 21 min, which is the average of only QD-570 (33min) and only the adduct (12min).

A

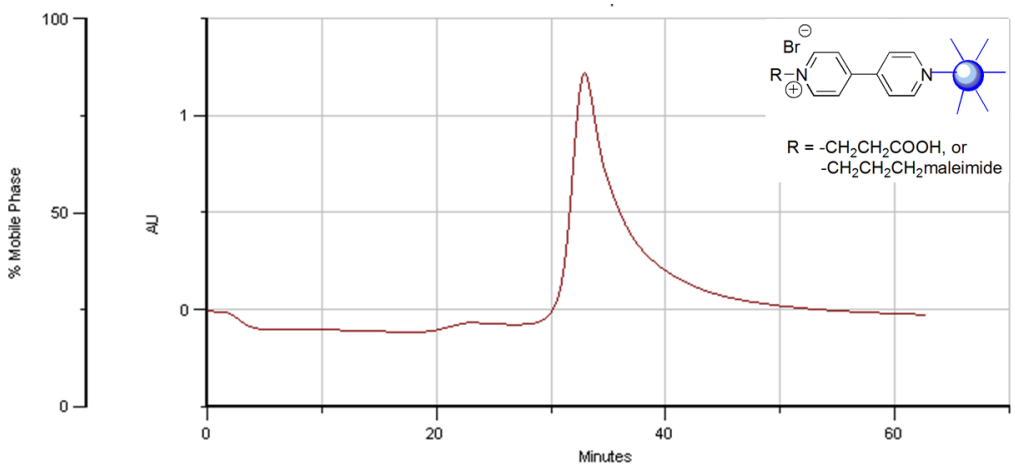

B

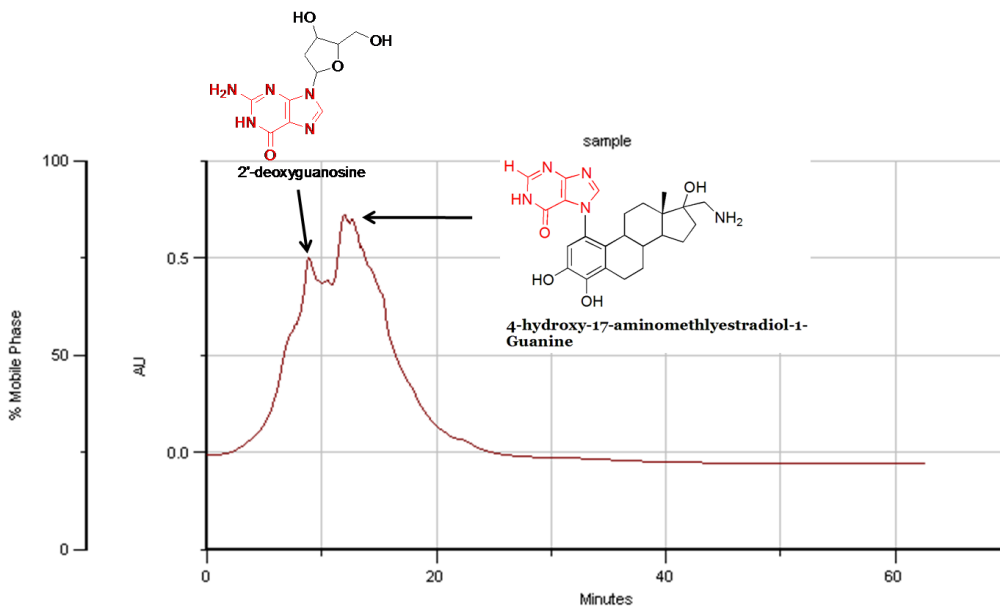

C.

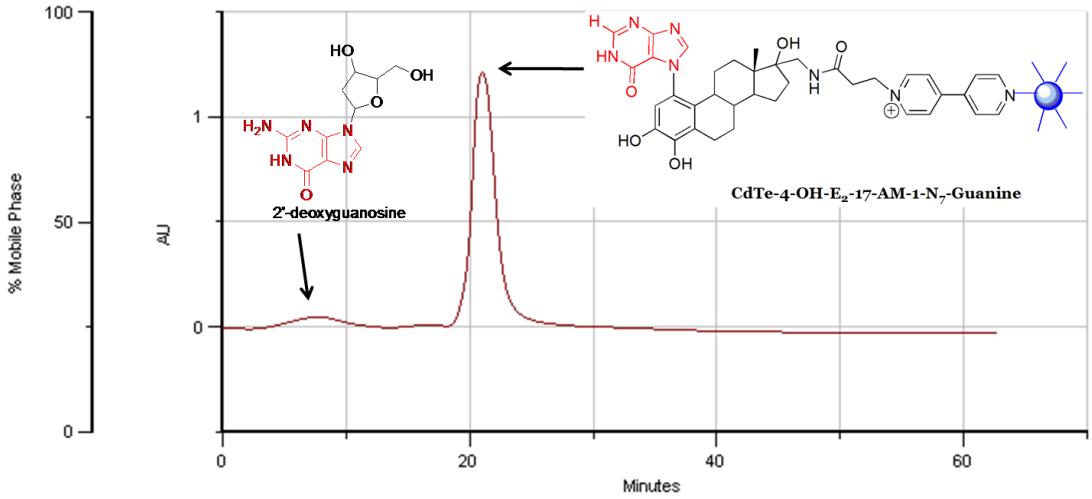

Fig 4.2 HPLC chromatograms of QD-570 (10^{-7}mg/mL) (**A**) 4-OH-E_2-17-AM-1-N_7-guanine (**B**) and QD-4-OH-E_2-17-AM-1-N_7-guanine (**C**) Upon binding of QD-570, the adduct peak shifts from 12 min to 21 min confirming QD-adduct assembly

The HPLC chromatograms for QD-570, 4-OH-17-aminomethylestradiol-1-N_3-Adenine and their conjugation showed three distinct peaks confirming QD-570 labeling. (Fig 4.3) The larger elution time for CdTe-4-OH-E_2-17-AM-1-N_3-adenine (26 min) is possibly due to aggregation of QD-adduct assemblies as seen under transmission electron microscopy (TEM). The aggregation

may be the result of QD-adduct assemblies through both aromatic and aliphatic amines present in 4-OH-E_2-17-AM-1-N_3-adenine. The broad peak signifies polydisperse particles after bioconjugation. (**B** in Fig 4.3)

A

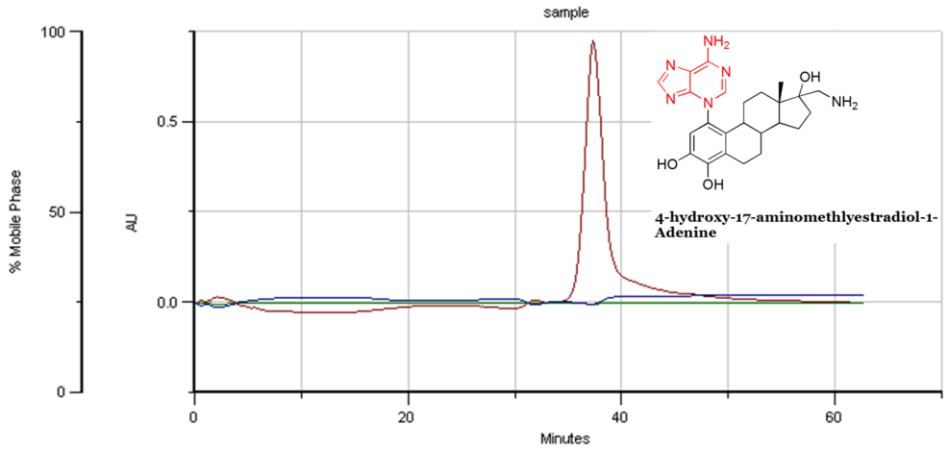

B

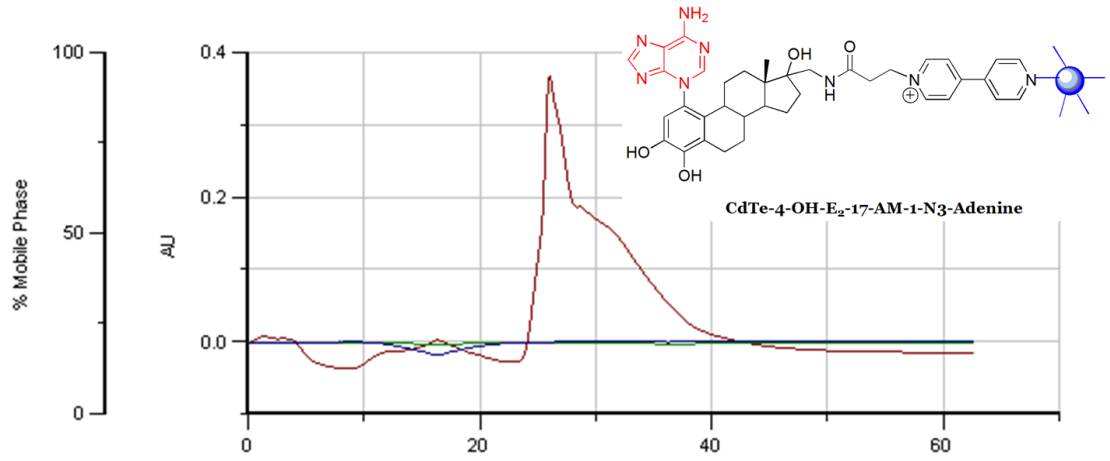

Fig 4.3 HPLC chromatograms of 4-OH-E_2-17-AM-1-N_3-adenine (**A**) and CdTe-4-OH-E_2-17-AM-1-N_3-adenine (**B**)

Thio-pyrene and its conjugate with QD-570 have shown similar elution peaks in HPLC (21min, 21.5min respectively). The bioconjugation is confirmed as no QD-570 peak is observed in the HPLC chromatogram of the CdTe-S-pyrene. (Fig 4.4)

A

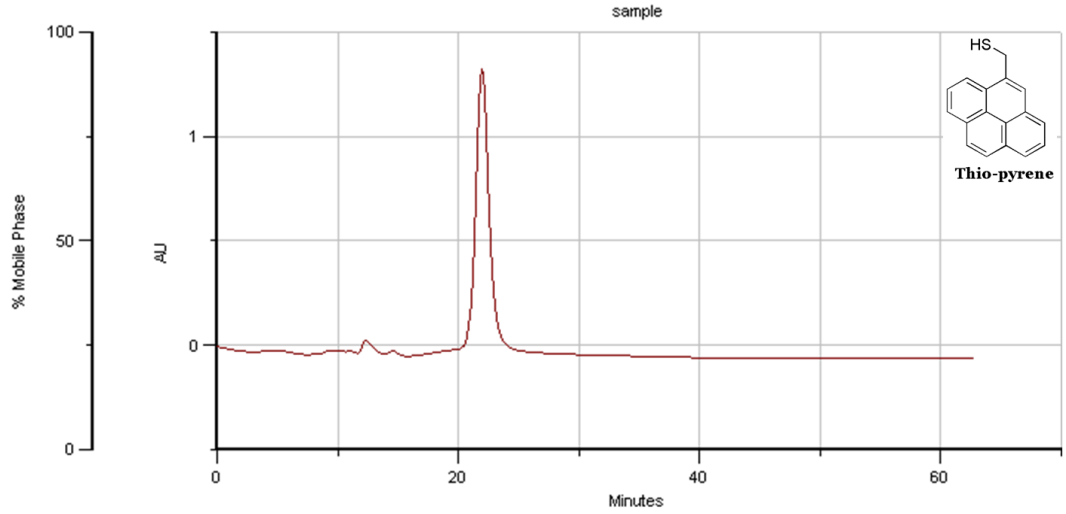

B

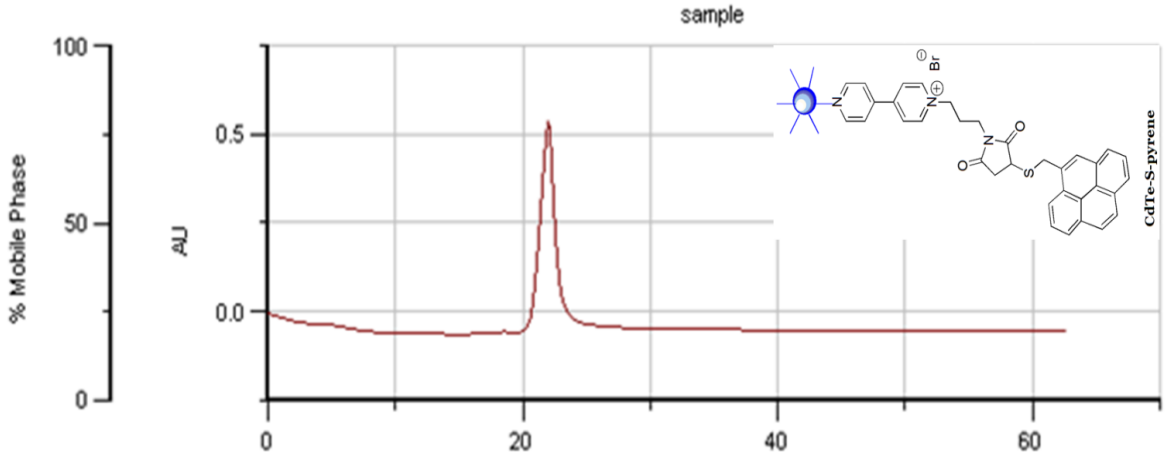

Fig 4.4 HPLC chromatogram of thio-pyrene (**A**) and CdTe-S-pyrene conjuagate (**B**). The QD-570 peak at 33 min is not observed after bioconjugation making sure successful labeling.

The HPLC peaks of the QD-570, DNA-estrogen adducts, thiopyrene and their conjugates with QD-570 are summarized in the table 4.1.

Table 4.1 Elution time for DNA-estrogen adducts, CdTe QD and DNA-estrogen-QD conjugates

QD, adducts and conjugates	Elution Time (min)
CdTe QD	33
4-OH-17-aminomethlyestradiol-2-Guanine	12
4-OH-17-aminomethlyestradiol-2-Guanine-QD	21

4-OH-17-aminomethlyestradiol-2-Adenine	37
4-OH-17-aminomethlyestradiol-2-Adenine-QD	26
Thiopyrene	21
Pyrene-S-QD	21.5

4.4.2 ELISA

In order to confirm the labeling of DNA-derived estrogen adducts through carboxylic acid (-COOH) functional group or thiopyrene through maleimide functionality present on CdTe QDs, a direct enzyme linked immunosorbent assay (ELISA) was performed. IgM antibody raised against DNA-estrogen adducts was used to recognize the labeled adducts on an ELISA plate (from where is the antibody). No fluorescent signal could be recorded with IVIS Lumina II equipped with a charge-coupled device (CCD) camera. However, ELISA test with 8E11 monoclonal antibody (mAb),[19] used to recognize the pyrene moiety of CdTe labeled thiopyrene showed fluorescent signal from CdTe. The wells on ELISA plate was excited at 470nm and images were captured by CCD camera confirming the bioconjugation. (Fig 4.5)

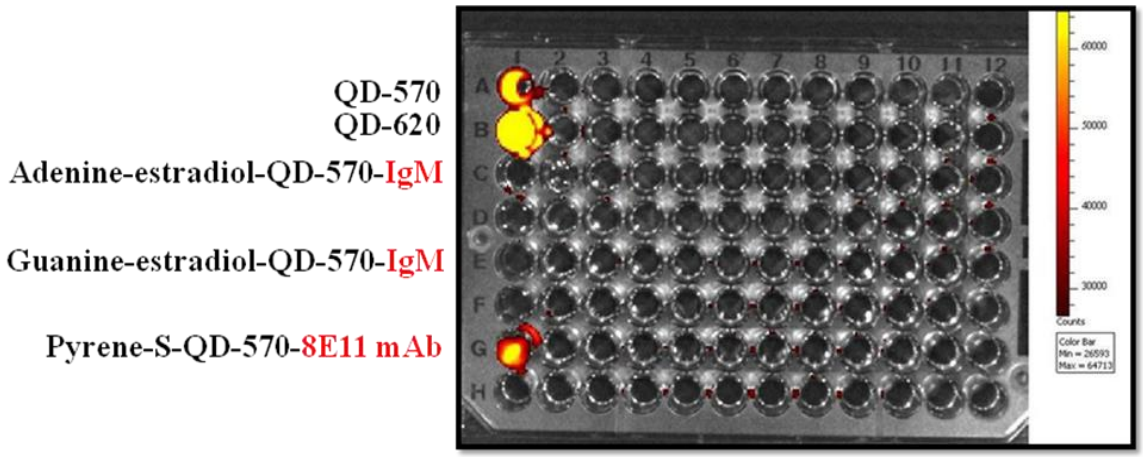

Fig 4.5 CdTe labeled thiopyrene excited at 470 nm for 10 s captured in CCD camera; commercial QD-620 was used to compare intensity with our QD-570

The lack of fluorescent signal from the adduct-QD-570 conjugates was most likely due to low concentration of QDs as there was statistically large number of adduct per QD-570 through about 85% carboxylic acid terminal ligand present on the surface of QD. (Fig 4.6) On the other hand, there was statistically much less number of thiopyrene per QD-570 since thiopyrene bound covalently only through 15% maleimide terminal ligand used to stabilize the QDs thereby

increasing population of pyrene-S-QD-570 being recognized by 8E11 mAb, an IgG type of antibody.

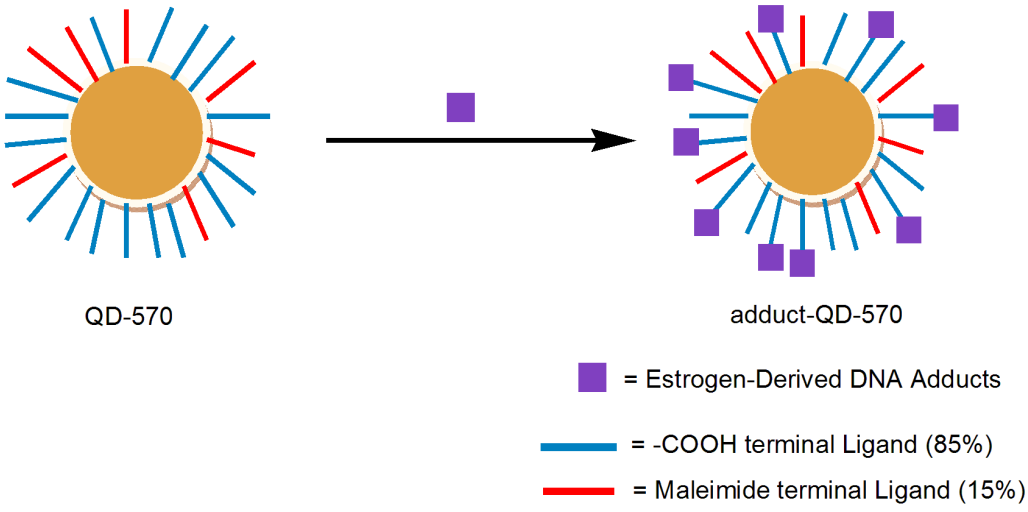

Fig 4.6 Crowding of DNA-Estrogen adducts around CdTe QDs through –COOH group

In addition, the IgM antibodies used to recognize DNA-estrogen-QD-570 conjugates are transmembrane proteins present in B-cell membranes. IgM antibodies are pentamers produced in a primary response to an antigen.[20] The large size of IgM make it difficult to diffuse well in the intercellular tissue fluids and hence, found in low concentration. It undergoes maturation through heavy chain class switching (from μ chain to γ chain) into serum-soluble IgG. (Fig 4.7) The steric hindrance offered by the IgM molecule is the probable reason for weak antibody-antigen interaction. It is important to develop IgG type antibody for better recognition. An effort is ongoing in the Iowa State University, Ames, Iowa in the direction of generating IgG type antibody against DNA-derived estrogen adducts, which has the potential to resolve the low binding constant of first generation IgM antibodies.

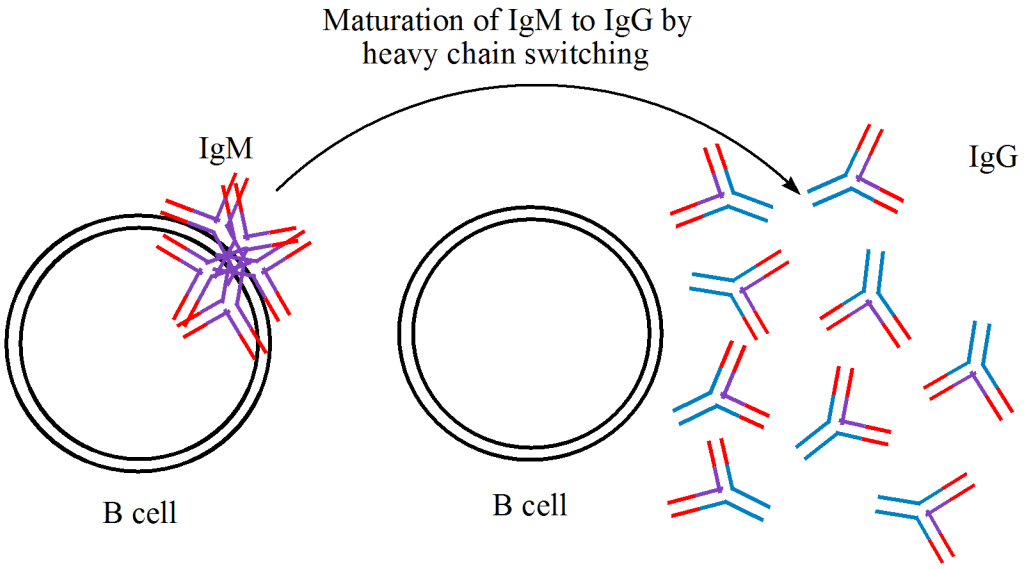

Fig 4.7 Maturation of IgM molecules into IgG requires heavy chain class switching

In summary, the lack of fluorescence signal from estrogen-derived DNA adduct labeled with QD-570 in ELISA experiment may be due to (1) low concentration of QD-570 which has statistically very high number of adducts, (2) steric hindrance to non-covalent antibody-antigen interaction due to crowding of adducts around the QD-570 and (3) large size of IgM molecule (molecular weight 180,000) offers steric resistance to antibody-antigen interaction. (Fig 4.8)

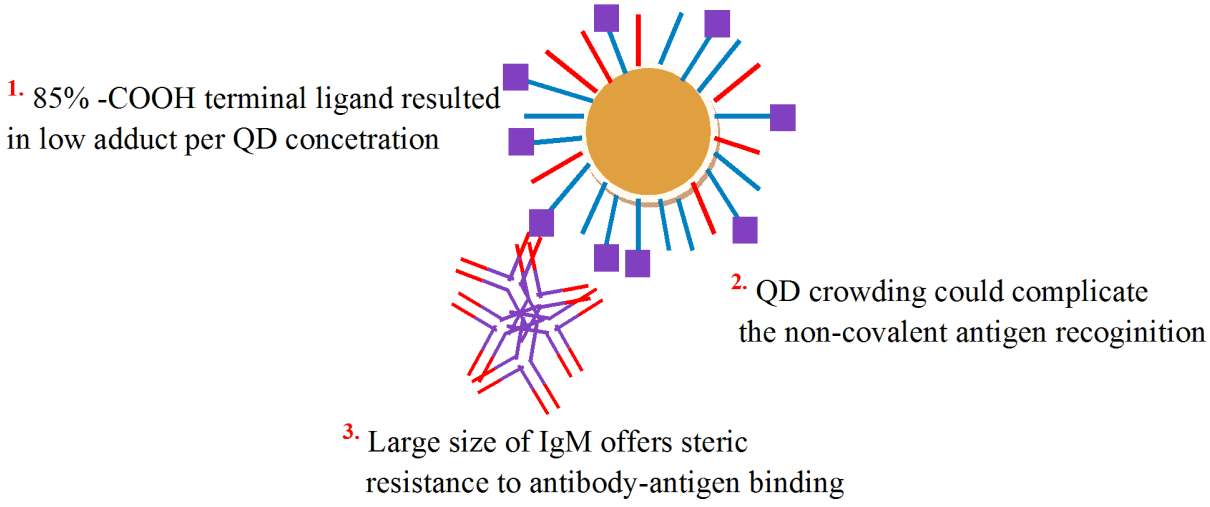

Fig 4.8 Summary of possible reasons for lack of fluorescence in ELISA experiment

4.5 Conclusions

The synthesis of water-soluble CdTe nanoparticles by using twin 4,4’-bipyridinium salt based ligands featuring either a terminal carboxylic acid group or a maleimide unit, has been reported. Two bioconjugation schemes using these water soluble CdTe QDs are principally possible. This demonstrates the importance of this new class of QD stabilizing ligands. We envision not only bioconjugation of molecules with primary amine or thiol functional group through this strategy, but also photochemistry, such as Förster resonance energy transfer (FRET) on the QD surface.

REFERENCES

1. Chan, W.; Maxwell, D. J.; Gao, X.; Bailey, R. E.; Han, M.; Nie, S. *Anal. Biotechnol.* **2002**, *13*, 40-46.
2. Gao, X.; Cui, Y.; Levenson, R. M. ; Chung, L. W. K. ; Nie, S. *Nat. Biotechnol.* **2004**, *22*, 969.
3. Dubertret, B. ; Skourides, P. ; Norris, D. J. ; Noireaux, V. ; Brivanlou, A. H. ; Libchaber, A. *Sience*, **2002**, *298*, 1259-1762.
4. For review, see Michaler, X.; Pinaud, F. F.; Bentolia, L.A.; Tsay, J. M.; Doose, S.; Li, J. J.; Sundaresan, G.; Wu, A. M.; Gambhir, S. S.; Weiss, S. *Science*, **2005**, *307*, 538-544.
5. Murray C. B.; Norris, D. J.; Bawendi, M. G. *J. Am. Chem. Soc.* **1993**, *115*, 8706-8715.
6. Dabbousi, B. O.; Rodriguez-Viejo, J.; Mikulec, F. V.; Heine J. R.; Mattoussi, H.; Ober, R.; Jensen, K. F.; Bawendi, M. G. *J. Phys. Chem. B.* **1997**, *101*, 9463-9475.
7. Jokerst, J. V.; Raamanathan, A.; Christodoulides, N.; Floriano, P. N.; Pllard, A. A.; Simmons, G. W.; Wong, J.; Gage, C.; Furmaga, W. B.; Redding, S. W.; McDevitt, J. T. *Biosensors and Bioelectronics*, **2009**, *24(12)*, 3622-3629.
8. He, Y.; Su, Y.; Yang, X.; Kang, Z.; Xu, T.; Z.; Ruiqin, F.; C.; Lee, S. -T. *J. Am. Chem. Soc.* **2009**, *131(12)*, 4434-4438.
9. Medintz, I. L.; Stewart, M. H.; Trammell, S. A.; Susumu, K.; Delehanty, J. B.; Mei, B. C.; Melinger, J. S.; Blanco-Canosa, J. B.; Dawson, P. E.; Mattoussi, H. *Nat. Materials*, **2010**, *9(8)*, 676-684.
10. Kim, Y.; Kim, W.; Yoon, H. –J.; Shin, S. K. *Bioconjugate Chemistry*, **2010**, *21(7)*, 1305-1311.
11. Chakravarti, D.; Mailander, P. C.; Li, K. –M.; Higginbotham, S.; Zhang, H. L.; Gross, M. L.; Meza, J. L.; Cavalieri, E. L.; Rogan, E. G. *Oncogene*, **2001**, *25*, 289-297.
12. Chakravarti, D.; Mailander, P. C.; Higginbotham, S.; Cavalieri, E. L.; Rogan, E. G. *Proc. Am. Assoc. Cancer Res.* **2003**, *44*, 180.
13. Zhao, Z.; Kosinska, W.; Khmelnitsky, M.; Cavalieri, E. L.; Rogan, E. G.; Chakravarti, D.; Sacks, P.; Guttenplan, J. B. *Chem. Res. Toxicol.* **2006**, *19*, 475-479
14. Jankowiak, R.; Markushin, Y.; Cavalieri, E. L.; Small, G. J. *Chem. Res. Toxicol*. **2003**, *16*, 304-311

15. Markushin, Y.; Kapke, P.; Saeed, M. Zhang, H.; Dawoud, A.; Rogan, E. G.; Cavalieri, E. L.; Jankowiak, R. *Chem. Res. Toxicol*. **2005**, *18*, 1520-1527
16. Kalita, M.; Cingarapu, S.; Jankowiak, R.; Klabunde, K. J.; Bossmann, S. H. *to be published*.
17. Hecht, S. S.; Carmella, S. G.; Villalta, P. W.; Hochalter, J. B. *Chem. Res. Toxicol*. **2010**, *23*, 900-908.
18. Hecht, S. S.; Yuan, J. –M.; Hatsukami, D. *Chem. Res. Toxicol*. **2010**, *23*, 1001-1008.
19. Lee, N. M.; Santella, R. M. *Carcinogenesis*, **1988**, *9(10)*, 1773-1777.
20. Kalita, M.; Lin, C.; Saeed, M.; Markushin, Y.; Cavalieri, E. L.; Rogan, E. G.; Jankowiak, R. *to be unpublished.*

CHAPTER 5- Concluding Remarks

Several challenging hurdles had to be overcome in our continuous effort to meet the goal of developing a commercial biosensor for indirect detection of the estrogen-derived DNA adducts in urine samples of women at high-risk and with breast cancer. It started with the chemical synthesis of DNA-estrogen adducts, 4-OH-E_1(E_2)-1-N3Ade and 4-OH-E_1(E_2)-1-N7Gua, potential biomarkers for breast and prostate cancer. In order to enhance the sensitivity of detection i.e. identifying these adducts at low concentration such as femtomolar (10^{-15} M) level, a labeling strategy with highly fluorescent quantum dots (QDs) had to be devised. An aminomethyl (-CH_2NH_2) linker was introduced at C-17 of these biomarkers for labeling strategy.

The challenge of synthesizing water soluble QDs was met by using a new class of 4,4'-bipyridinium salt based twin ligands. These ligands were used both to stabilize the QD nanocrystal surface and to label estrogen-derived DNA adducts. Direct synthesis of the aqueous QDs by metal evaporation-co condensation-reflux technique was able to subvert the problem of nanoparticle aggregation in water and broad emission spectrum. These QDs were found to be more photostable than traditional organic solvent soluble QDs synthesized by the same technique, thereby, opening a window for biomedical applications.

A ***double labeling strategy*** was developed with QDs being stabilized by two ligand systems. HPLC and ELISA studies showed labeling of thiopyrene through the maleimide functionality present on aqueous QDs. The success of ELISA test proved that the 8E11, an IgG antibody-QD labeled thiopyrene binding was strong and this methodology can be used to capture fluorescent signals through antibody-QD labeled antigen. The second labeling strategy of estrogen-DNA adducts through carboxylic acid (-COOH) terminal ligand of QDs was demonstrated by using anion exchange HPLC, though the ELISA experiment indicated that the concentration of QDs per adducts was too low to capture a fluorescent signal. Part of the problem may be the inability of the IgM immunoglobulin used on ELISA plate to recognize these adducts at the low concentrations required for detection. IgM is a transmembrane protein formed as a result of primary immune response on a B-cell membrane. Maturation of IgM takes place through heavy chain class switching from μ to γ heavy chain resulting in an IgG antibody, a water soluble protein with high binding constant to the antigen present in blood serum.

The problem of very low concentration of QDs labeling the estrogen-derived DNA adducts was construed as statistically large number of adducts per QD due to 85% carboxylic acid (-COOH) terminal ligand on QDs. This interpretation was supported by detectable fluorescent signal from QDs labeling thiopyrene as it was labeled through only 15% maleimide terminal ligand present on QDs. In order to enhance the concentration of QDs per adduct, the labeling strategy has to be modified to a dilutly adduct labeled QD solution to decrease the probability of reaction between aminomethyl group ($-CH_2NH_2$) on the estrogen-DNA adduct and the carboxyl (-COOH) group on the QDs. This will probably result in labeling these adducts with QDs in 1:1 ratio permitting positive ELISA results.

It is our intention to develop monoclonal IgG antibodies against the potential breast cancer biomarkers; 4-OH-E_1(E_2)-N3Ade and 4-OH-E_1(E_2)-N7Gua. One strategy would be to direct these adducts towards a special phagocyte known as dendritic cells (DCs) in a host animal. It would require labeling these adducts with an IgG antibody, N418, which is known to recognize the DC cell surface. Thus labeled adducts would, hopefully, be taken up by DCs and undergo proteolytic cleavage inside the cell finally exhibiting the estrogen-derived DNA adducts embedded in the histocompatibility complex II (MHC II) on the cell surface. Antigens exhibited on the DC surface have to activate T-helper (T_H) cells through MHC II-T-cell receptor (TCR) interaction inducing T_H cell to undergo a clonal expansion. Thus, proliferated T_H cells come across rare B-cells presenting exactly same estrogen-derived DNA adducts through MHC II activating B-cells to undergo clonal expansion. This, in turn, leads to production of IgG antibody from IgM antibody present on B-cell membrane by heavy chain class switching. This rather complicated mechanism makes IgG antibody generation challenging.

In summary, the central theme of my research was organic synthesis of standard estrogen-derived DNA adducts and an aminomethyl (CH_2NH_2) linker at C-17 position, synthesis of a new class of 4,4'-bipyridinium salt based twin ligands, synthesis of water soluble QDs and finally, conjugating these QDs through CH_2NH_2 linker. Evaporation-co-condensation-reflux technique introduced by Prof. Kenneth J. Klabunde research group at Kansas State University was used to synthesize the QDs. Water soluble QDs were found to be more photostable than QDs synthesized in toluene and superlative photostability of these QDs has made them an appealing bioimaging tool in biomedical research.

Appendix A - ^{1}H and ^{13}C NMR and Mass Spectra

A 1. ^{1}H and ^{13}C NMR Spectra

A 1.1 CHAPTER 2

Synthesis of Estrogen-Derived DNA Adducts and Their Structural Modifications for Conjugation

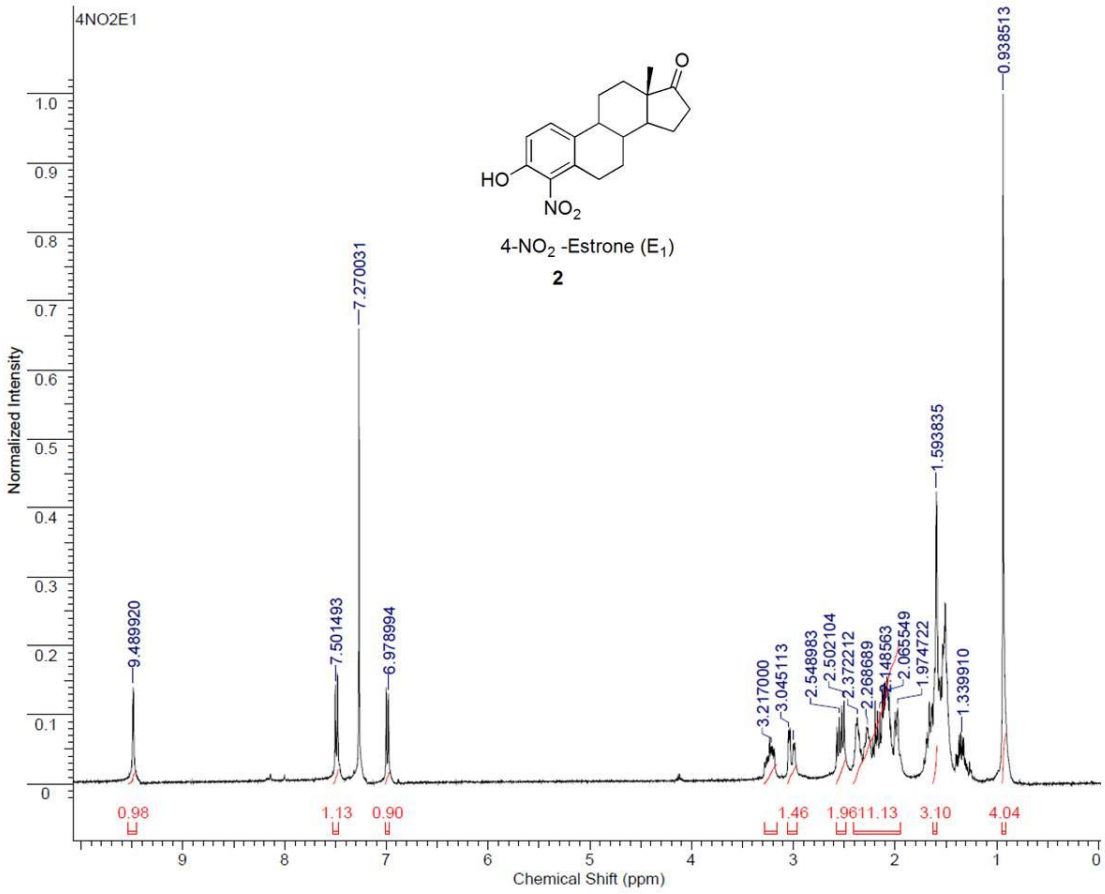

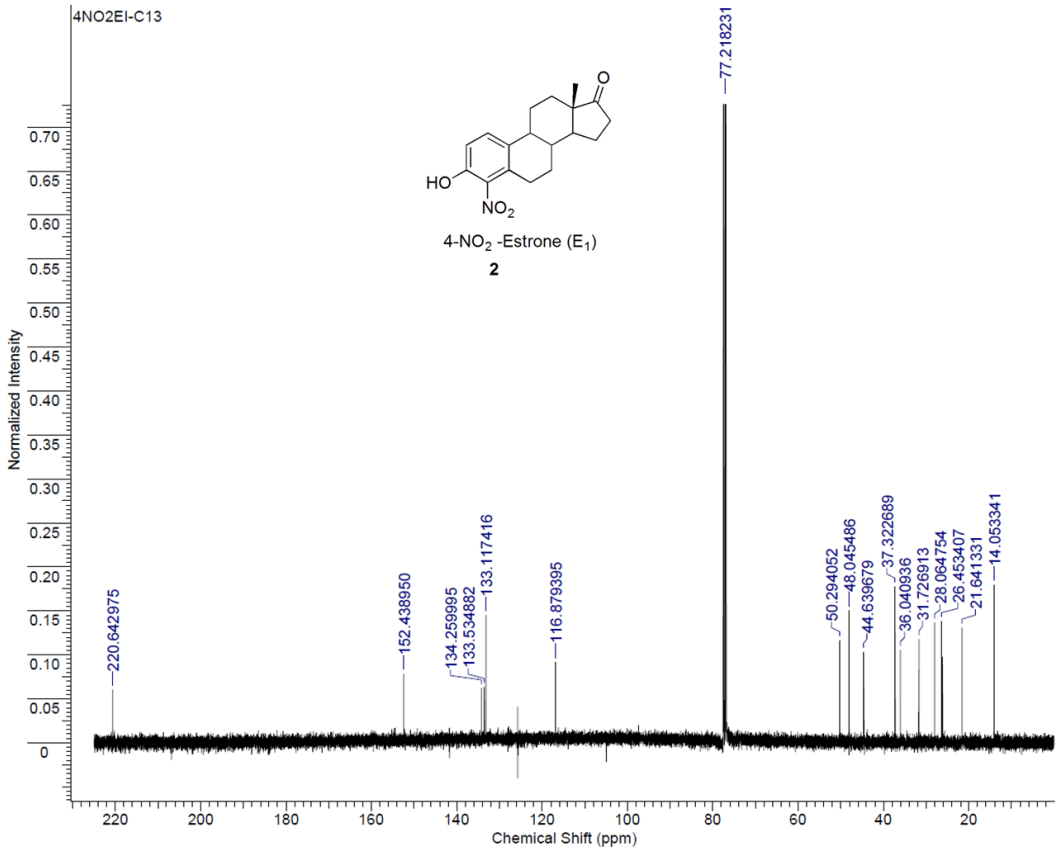
4NO2EI-C13
77.218231
220.642975
152.438950
134.259995
133.534882
133.117416
116.879395
50.294052
48.045486
44.639679
37.322689
36.040936
31.726913
28.064754
26.453407
21.641331
14.053341
Normalized Intensity
Chemical Shift (ppm)
4-NO2 -Estrone (E1)
2

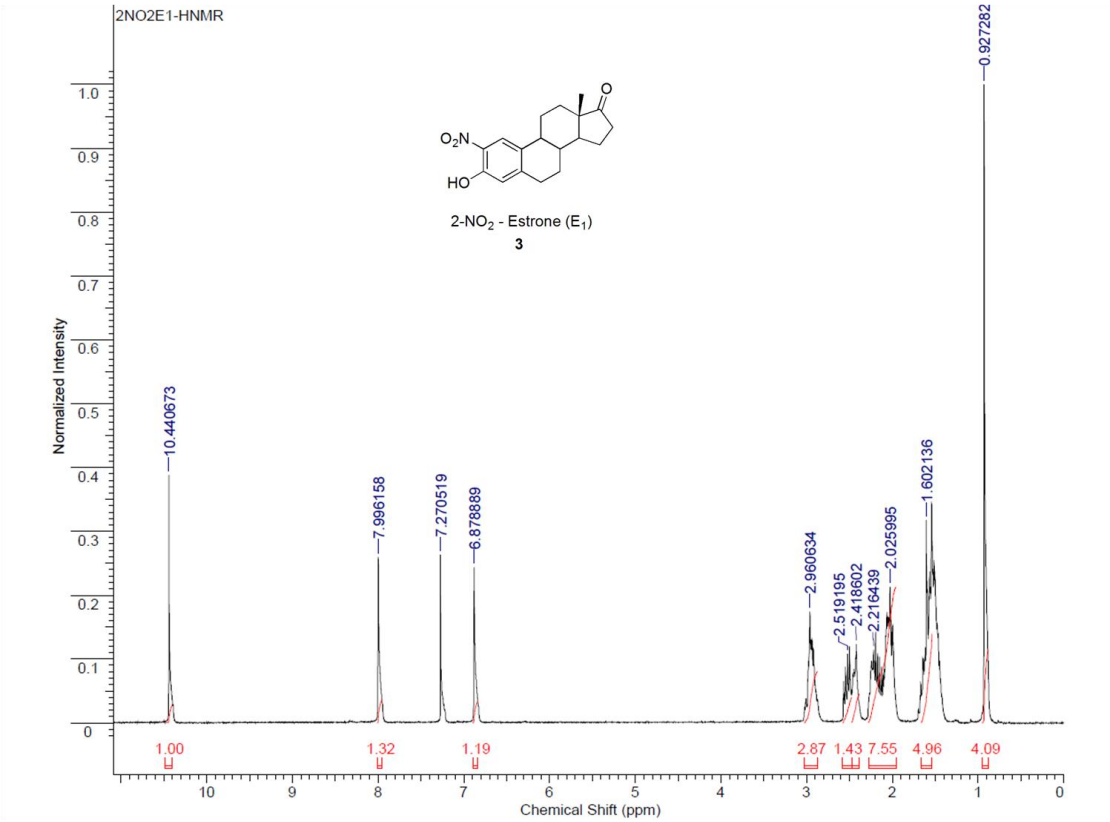
2NO2E1-HNMR
0.927282
10.440673
7.996158
7.270519
6.878889
2.960634
2.519195
2.418602
2.216439
2.025995
1.602136
1.00
1.32
1.19
2.87
1.43
7.55
4.96
4.09
Normalized Intensity
Chemical Shift (ppm)
2-NO2 - Estrone (E1)
3

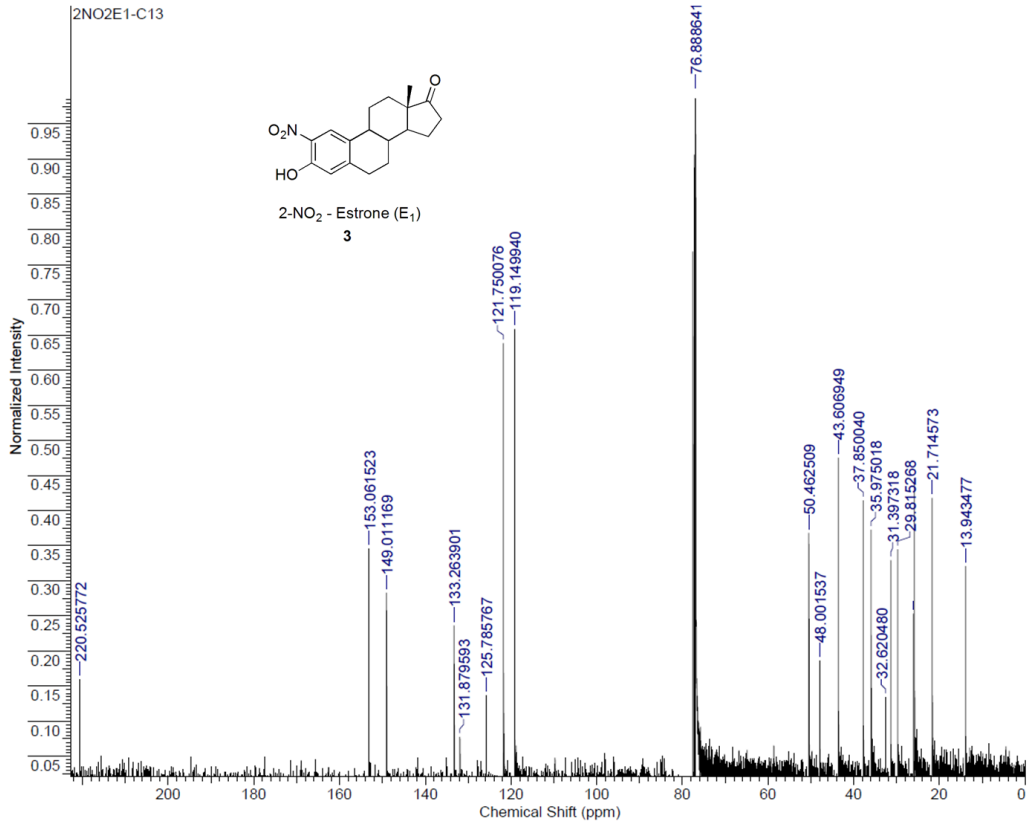
2NO2E1-C13
Normalized Intensity
Chemical Shift (ppm)
2-NO2 - Estrone (E1)
3
220.525772
153.061523
149.011169
133.263901
131.879593
125.785767
121.750076
119.149940
76.888641
50.462509
48.001537
43.606949
37.850040
35.975018
32.620480
31.397318
29.815268
21.714573
13.943477

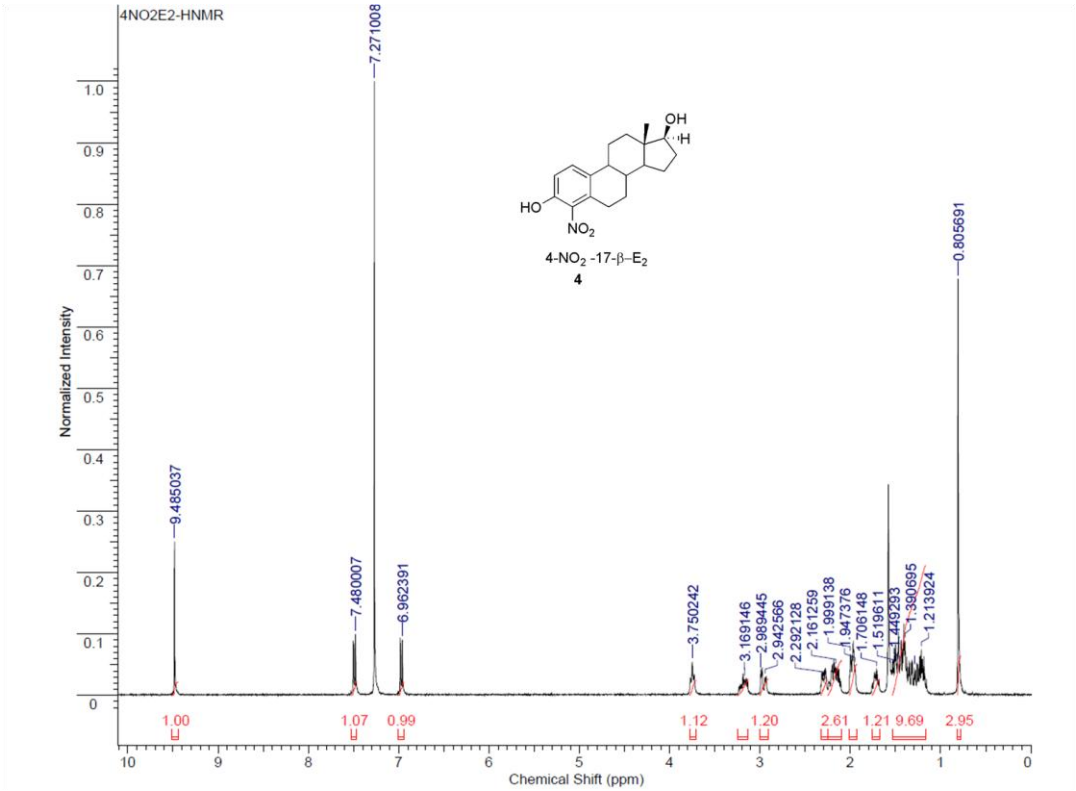
4NO2E2-HNMR
Normalized Intensity
Chemical Shift (ppm)
4-NO2 -17-β-E2
4
9.485037
7.480007
7.271008
6.962391
3.750242
3.169146
2.989445
2.942566
2.292128
2.161259
1.999138
1.947376
1.706148
1.519611
1.449293
1.390695
1.213924
0.805691
1.00
1.07
0.99
1.12
1.20
2.61
1.21
9.69
2.95

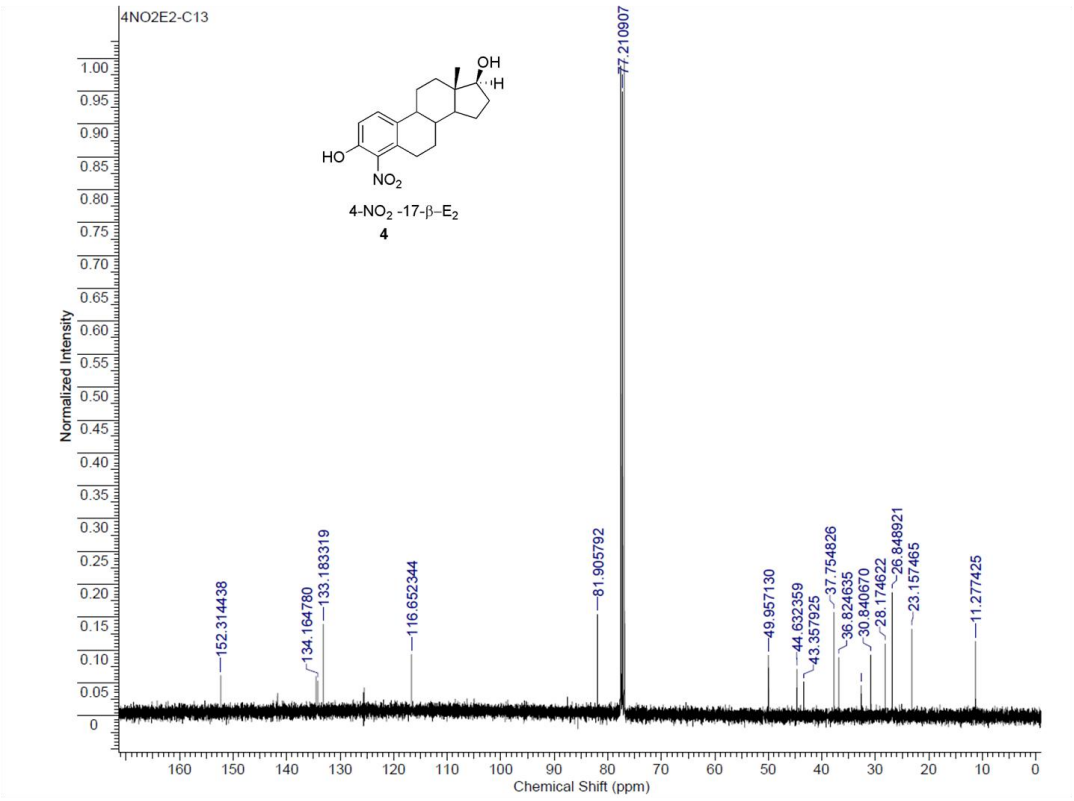
4NO2E2-C13
OH
H
HO
NO2
4-NO2 -17-β-E2
4
Normalized Intensity
Chemical Shift (ppm)
77.210907
152.314438
134.164780
133.183319
116.652344
81.905792
49.957130
44.632359
43.357925
37.754826
36.824635
30.840670
28.174622
26.848921
23.157465
11.277425

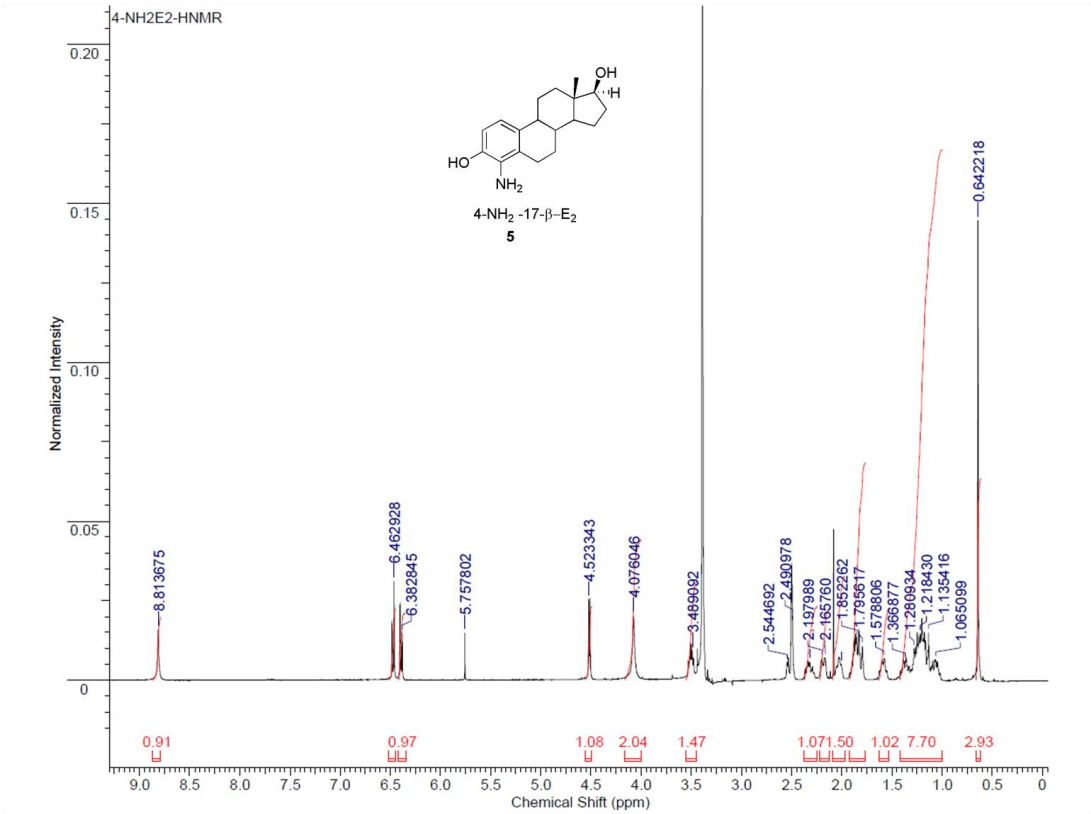
4-NH2E2-HNMR
OH
H
HO
NH2
4-NH2 -17-β-E2
5
Normalized Intensity
Chemical Shift (ppm)
8.813675
6.462928
6.382845
5.757802
4.523343
4.076046
3.489092
2.544692
2.490978
2.197989
2.165760
1.852262
1.795617
1.578806
1.366877
1.280934
1.218430
1.135416
1.065099
0.642218
0.91
0.97
1.08
2.04
1.47
1.07
1.50
1.02
7.70
2.93

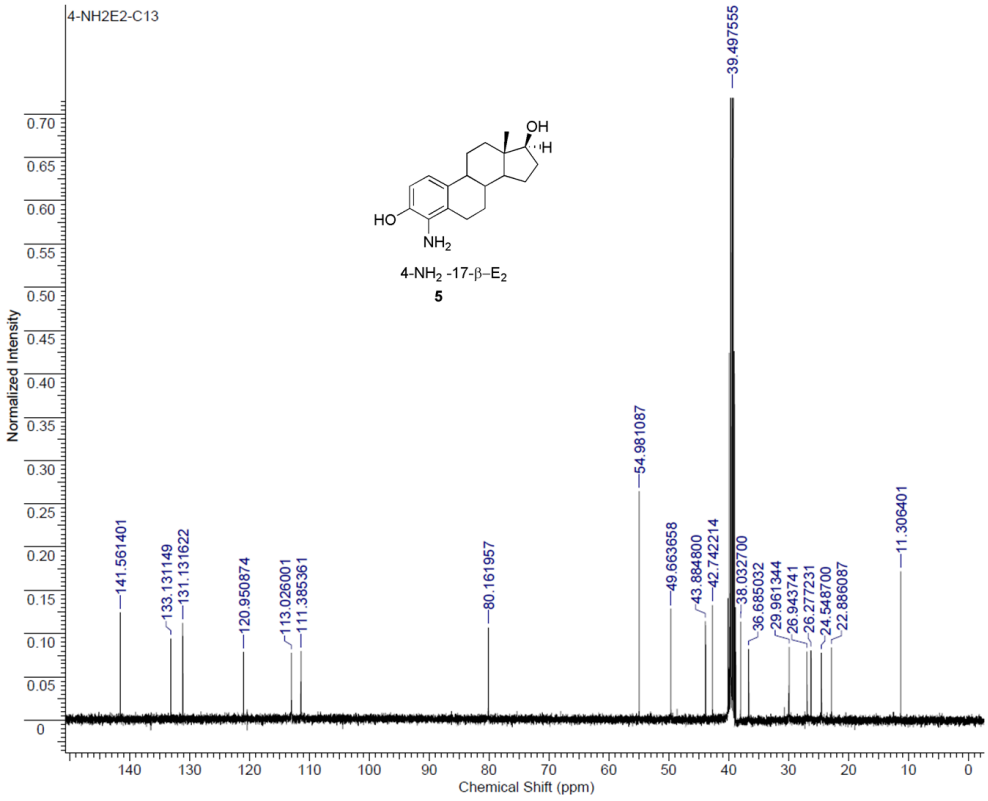

4-NH_2 -17-β-E_2

5

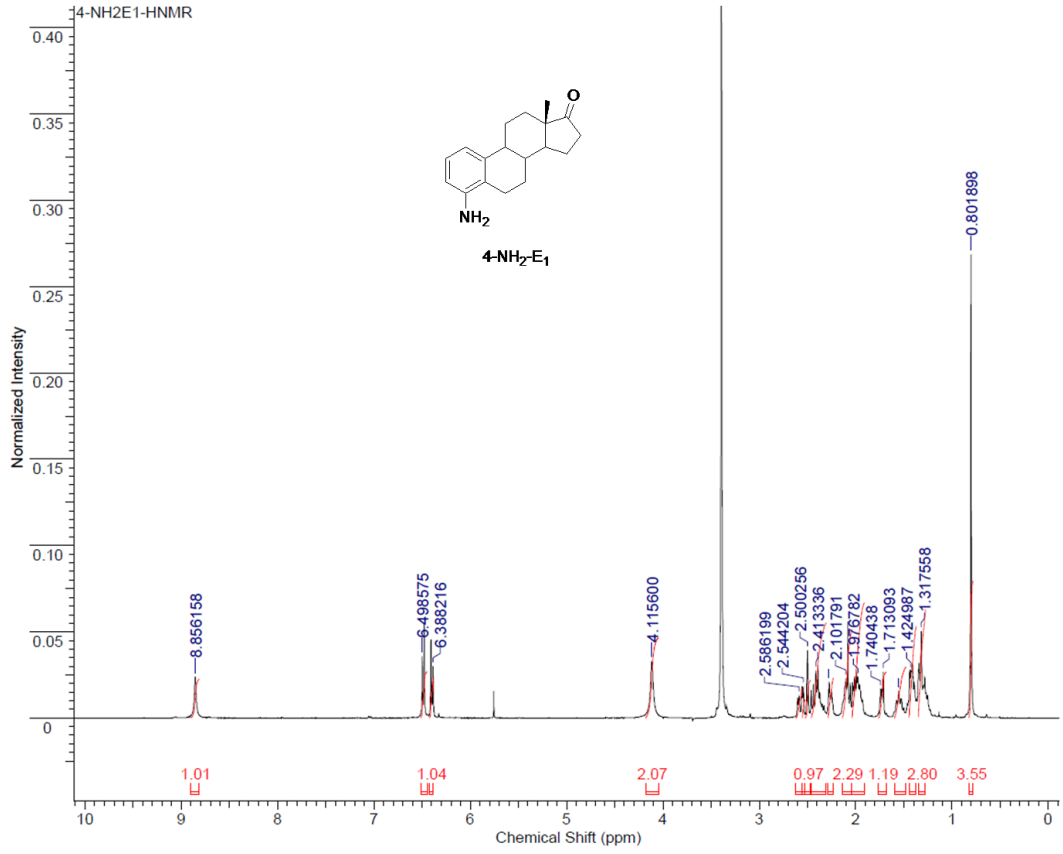

4-NH_2-E_1

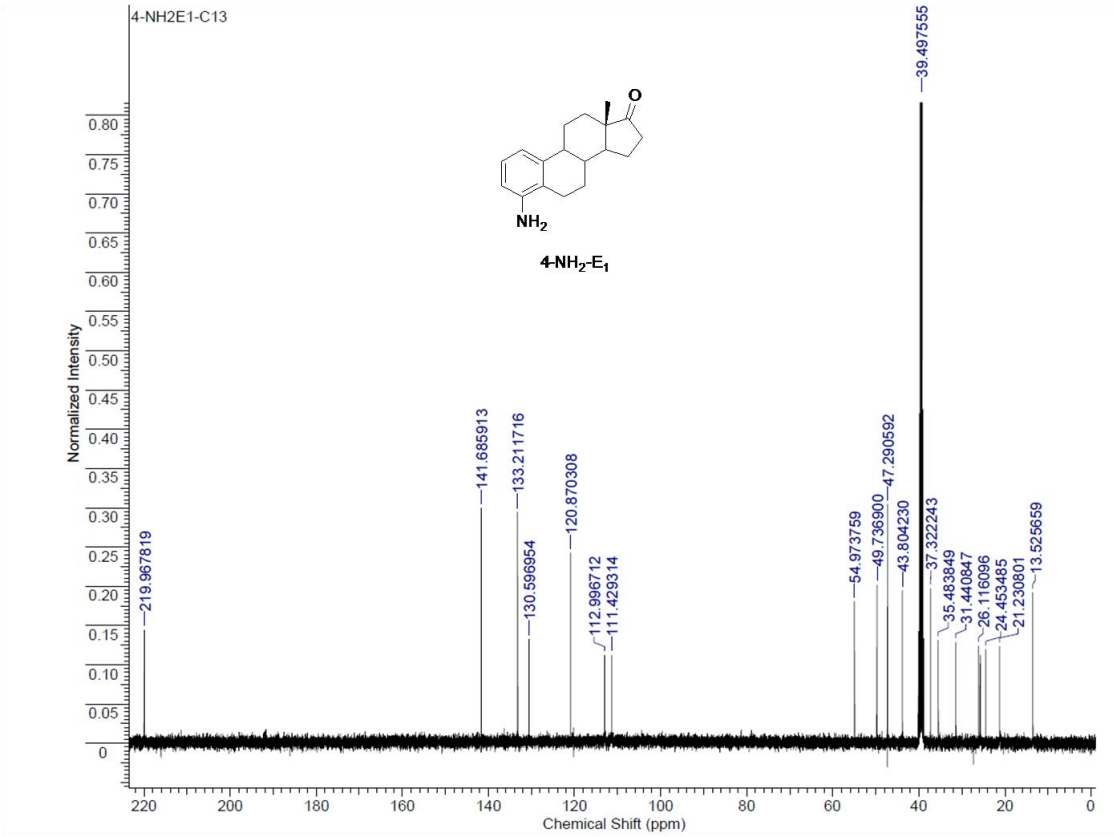
4-NH2E1-C13
O
NH2
4-NH2-E1
Normalized Intensity
Chemical Shift (ppm)
219.967819
141.685913
133.211716
130.596954
120.870308
112.996712
111.429314
54.973759
49.736900
47.290592
43.804230
39.497555
37.322243
35.483849
31.440847
26.116096
24.453485
21.230801
13.525659

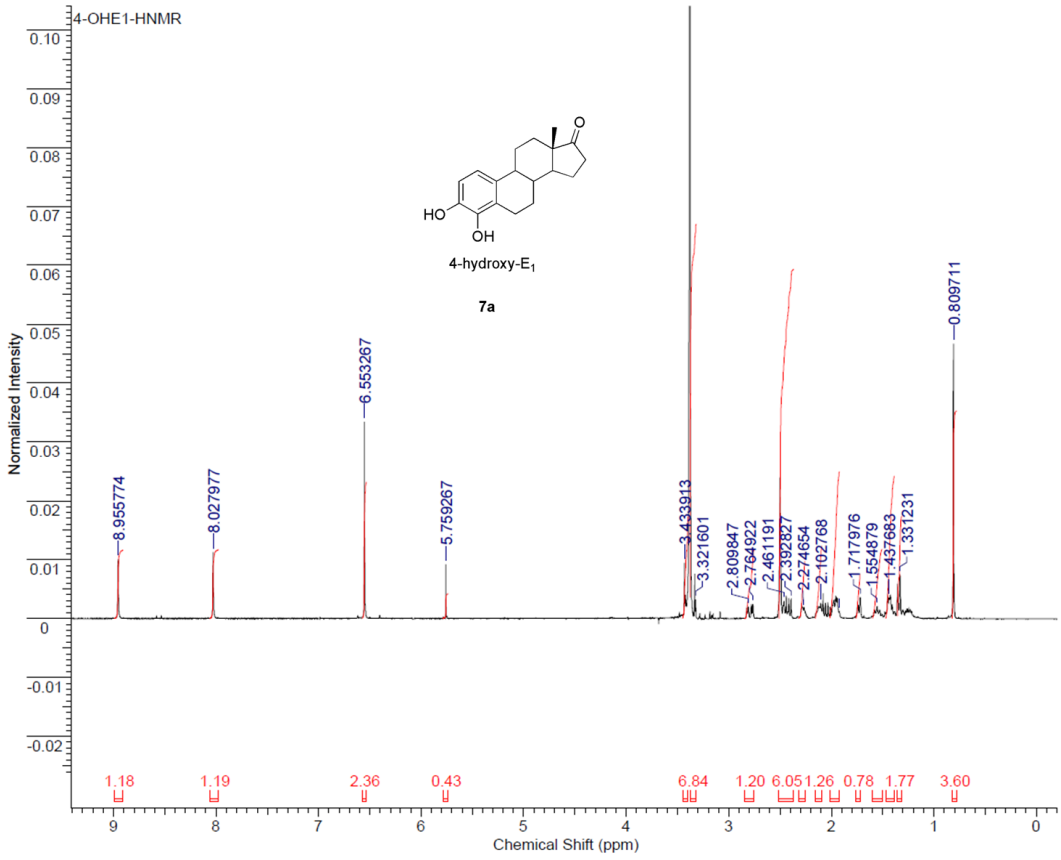
4-OHE1-HNMR
HO
OH
4-hydroxy-E1
7a
Normalized Intensity
Chemical Shift (ppm)
8.955774
8.027977
6.553267
5.759267
3.433913
3.321601
2.809847
2.764922
2.461191
2.392827
2.274654
2.102768
1.717976
1.554879
1.437683
1.331231
0.809711
1.18
1.19
2.36
0.43
6.84
1.20
6.05
1.26
0.78
1.77
3.60

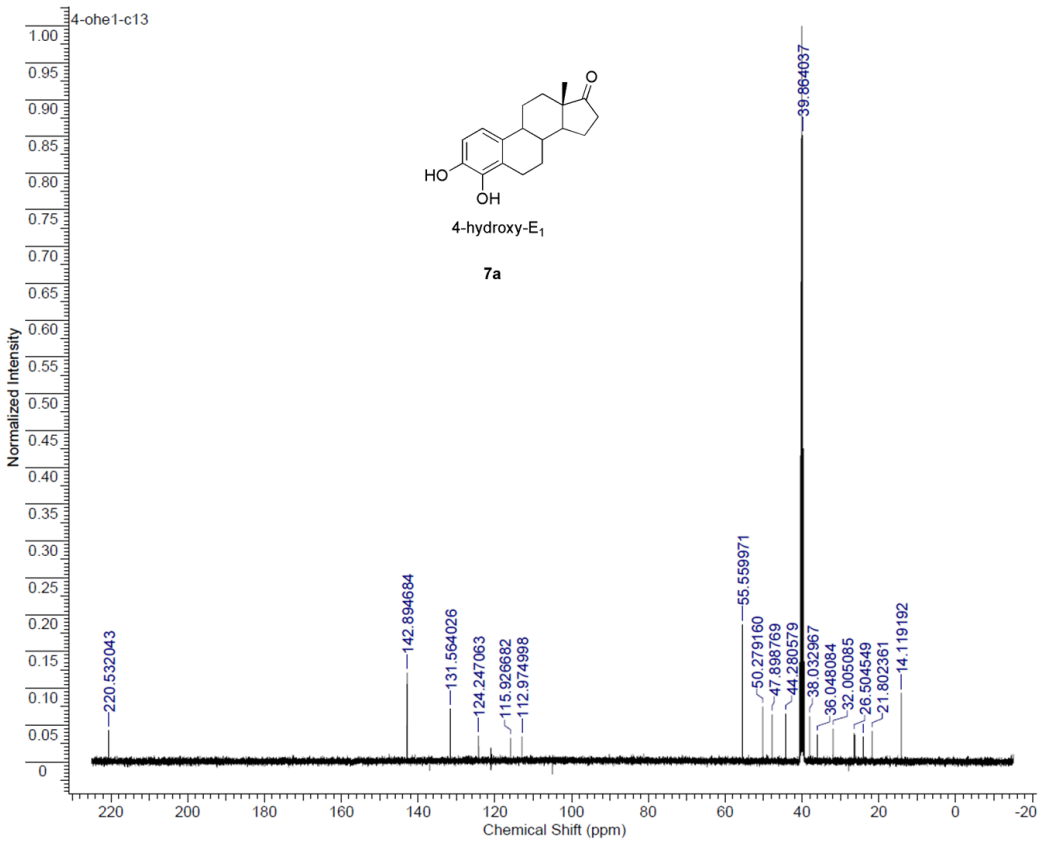
4-ohe1-c13
Normalized Intensity
Chemical Shift (ppm)
220.532043
142.894684
131.564026
124.247063
115.926682
112.974998
55.559971
50.279160
47.898769
44.280579
39.864037
38.032967
36.048084
32.005085
26.504549
21.802361
14.119192
HO
OH
O
4-hydroxy-E1
7a

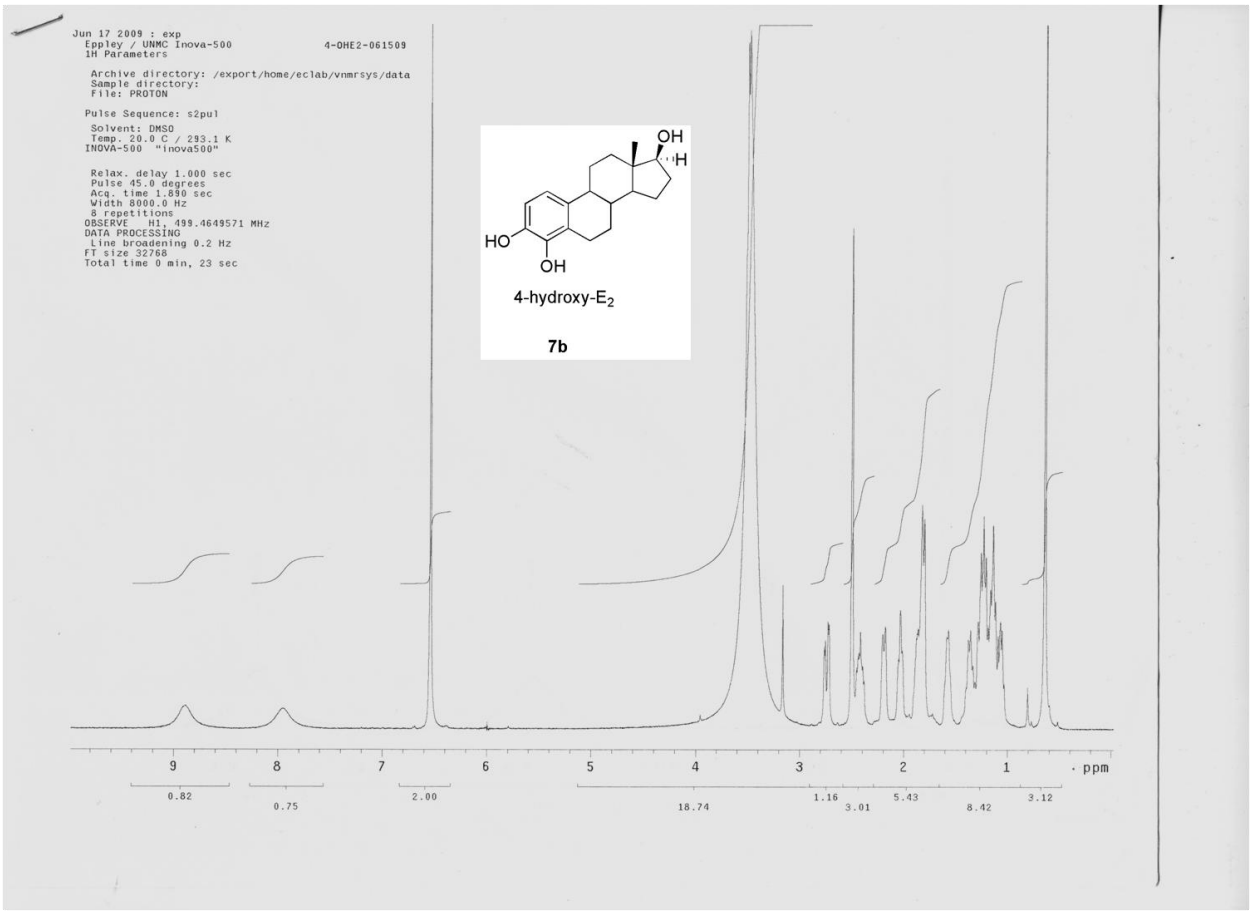
Jun 17 2009 : exp
Eppley / UNMC Inova-500
4-OHE2-061509
1H Parameters
Archive directory: /export/home/eclab/vnmrsys/data
Sample directory:
File: PROTON
Pulse Sequence: s2pul
Solvent: DMSO
Temp. 20.0 C / 293.1 K
INOVA-500 "inova500"
Relax. delay 1.000 sec
Pulse 45.0 degrees
Acq. time 1.890 sec
Width 8000.0 Hz
8 repetitions
OBSERVE H1, 499.4649571 MHz
DATA PROCESSING
Line broadening 0.2 Hz
FT size 32768
Total time 0 min, 23 sec
HO
OH
OH
H
4-hydroxy-E2
7b
ppm
0.82
0.75
2.00
18.74
1.16
3.01
5.43
8.42
3.12

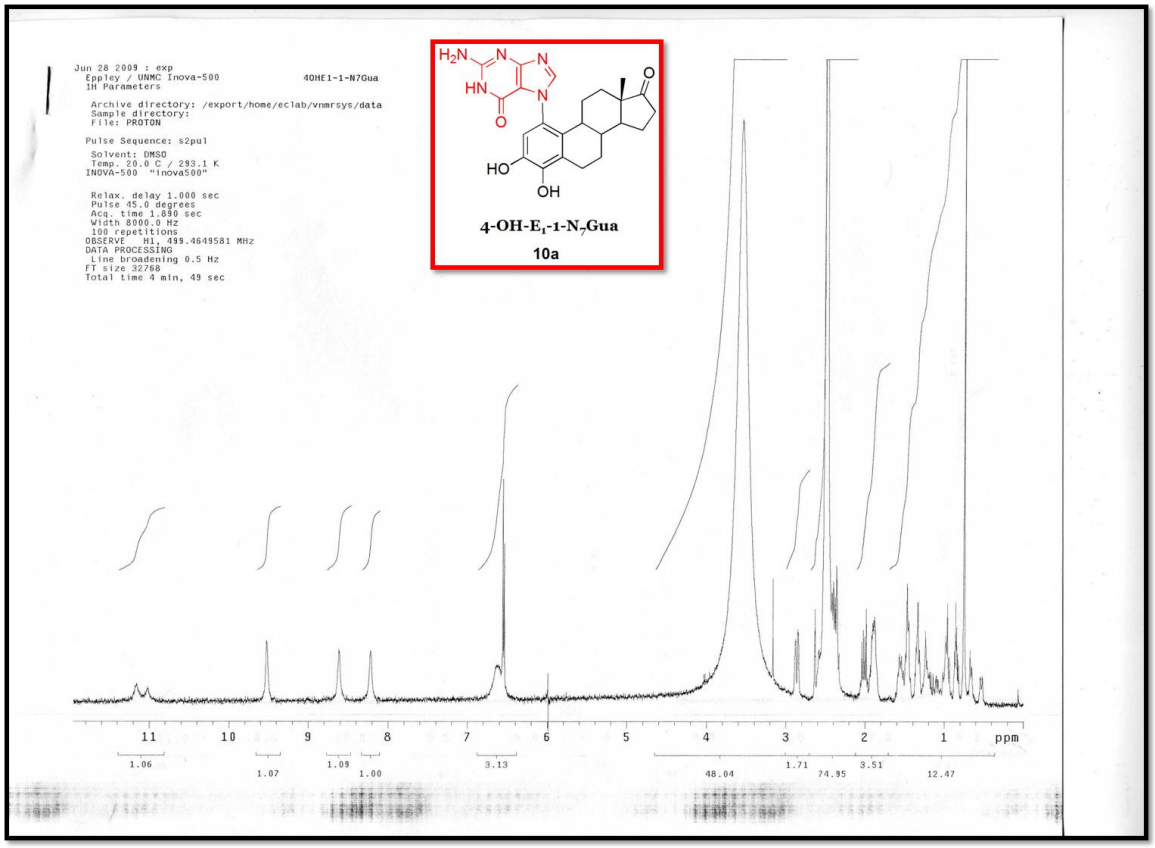
Jun 28 2009 : exp
Eppley / UNMC Inova-500
4OHE1-1-N7Gua
1H Parameters
Archive directory: /export/home/eclab/vnmrsys/data
Sample directory:
File: PROTON
Pulse Sequence: s2pul
Solvent: DMSO
Temp. 20.0 C / 293.1 K
INOVA-500 "inova500"
Relax. delay 1.000 sec
Pulse 45.0 degrees
Acq. time 1.890 sec
Width 8000.0 Hz
100 repetitions
OBSERVE H1, 499.4649581 MHz
DATA PROCESSING
Line broadening 0.5 Hz
FT size 32768
Total time 4 min, 49 sec
4-OH-E1-1-N7Gua
10a
ppm
1.06
1.07
1.09
1.00
3.13
48.04
1.71
74.95
3.51
12.47

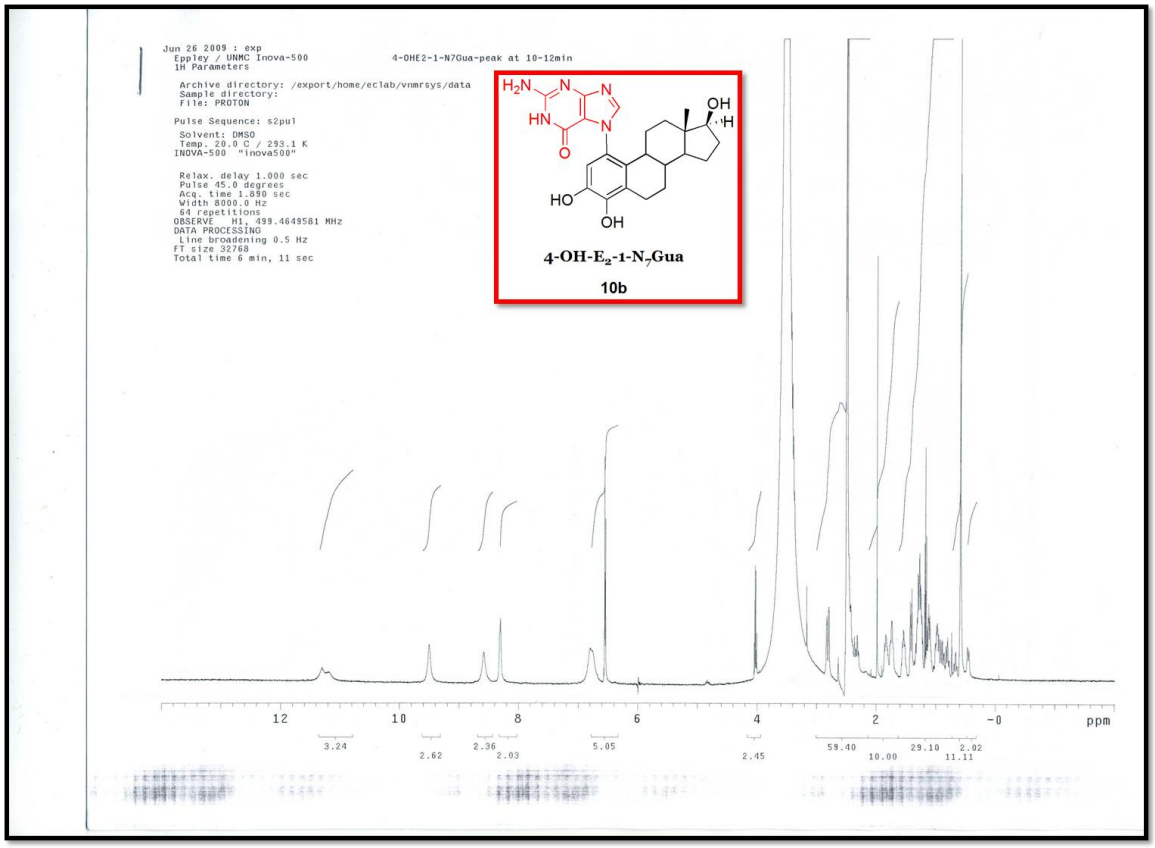
Jun 26 2009 : exp
Eppley / UNMC Inova-500
4-OHE2-1-N7Gua-peak at 10-12min
1H Parameters
Archive directory: /export/home/eclab/vnmrsys/data
Sample directory:
File: PROTON
Pulse Sequence: s2pul
Solvent: DMSO
Temp. 20.0 C / 293.1 K
INOVA-500 "inova500"
Relax. delay 1.000 sec
Pulse 45.0 degrees
Acq. time 1.890 sec
Width 8000.0 Hz
64 repetitions
OBSERVE H1, 499.4649581 MHz
DATA PROCESSING
Line broadening 0.5 Hz
FT size 32768
Total time 6 min, 11 sec
4-OH-E2-1-N7Gua
10b
ppm
3.24
2.62
2.36
2.03
5.05
2.45
59.40
10.00
29.10
2.02
11.11

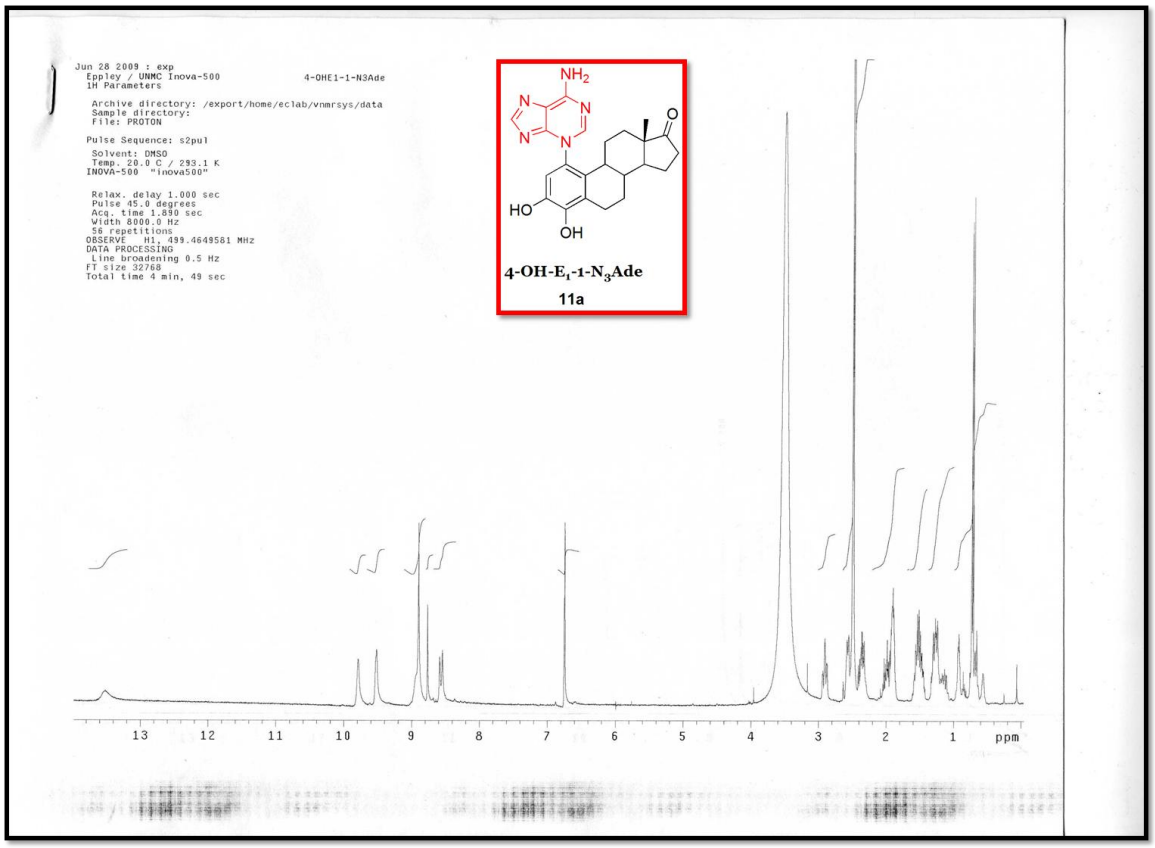
Jun 28 2009 : exp
Eppley / UNMC Inova-500
4-OHE1-1-N3Ade
1H Parameters
Archive directory: /export/home/eclab/vnmrsys/data
Sample directory:
File: PROTON
Pulse Sequence: s2pul
Solvent: DMSO
Temp. 20.0 C / 293.1 K
INOVA-500 "inova500"
Relax. delay 1.000 sec
Pulse 45.0 degrees
Acq. time 1.890 sec
Width 8000.0 Hz
56 repetitions
OBSERVE H1, 499.4649581 MHz
DATA PROCESSING
Line broadening 0.5 Hz
FT size 32768
Total time 4 min, 49 sec
4-OH-E1-1-N3Ade
11a
13 12 11 10 9 8 7 6 5 4 3 2 1 ppm

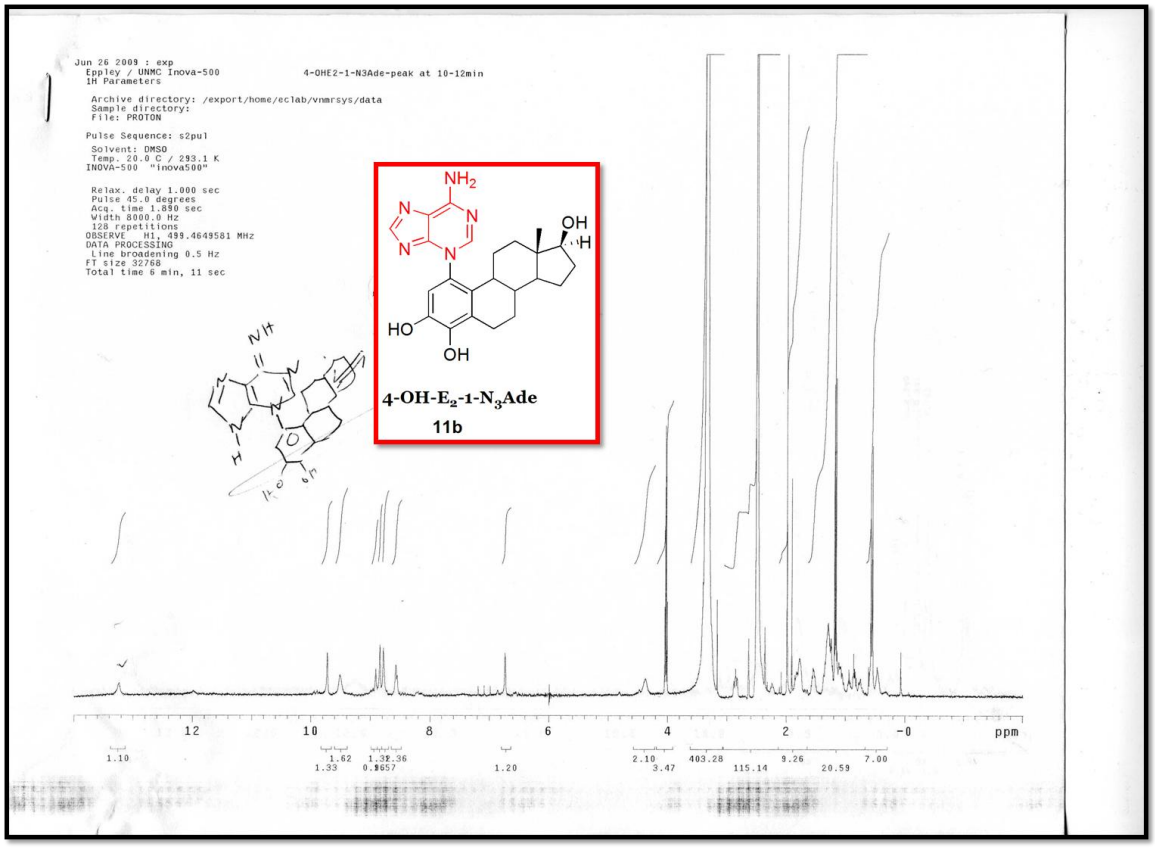
Jun 26 2009 : exp
Eppley / UNMC Inova-500
4-OHE2-1-N3Ade-peak at 10-12min
1H Parameters
Archive directory: /export/home/eclab/vnmrsys/data
Sample directory:
File: PROTON
Pulse Sequence: s2pul
Solvent: DMSO
Temp. 20.0 C / 293.1 K
INOVA-500 "inova500"
Relax. delay 1.000 sec
Pulse 45.0 degrees
Acq. time 1.890 sec
Width 8000.0 Hz
128 repetitions
OBSERVE H1, 499.4649581 MHz
DATA PROCESSING
Line broadening 0.5 Hz
FT size 32768
Total time 6 min, 11 sec
4-OH-E2-1-N3Ade
11b
12 10 8 6 4 2 -0 ppm
1.10
1.62
1.33
1.32
0.9657
1.20
2.10
3.47
403.28
115.14
9.26
20.59
7.00

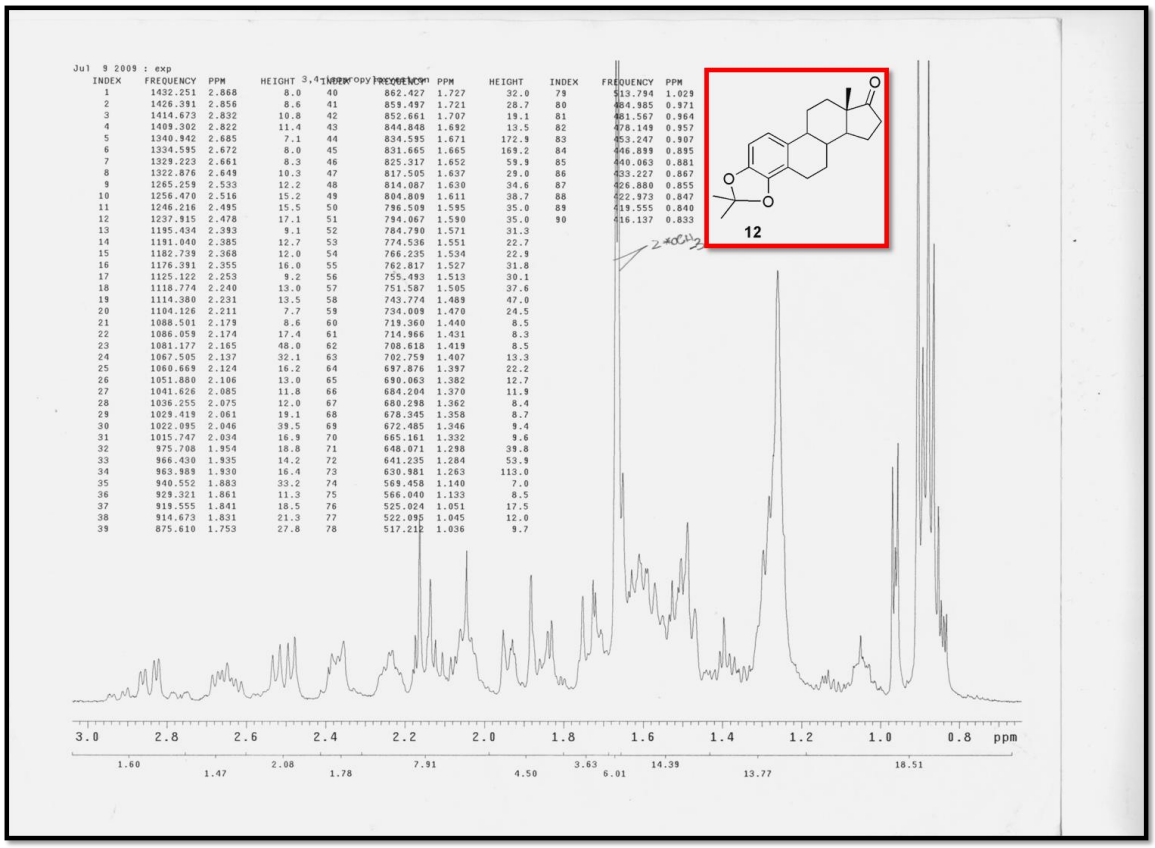
Jul 9 2009 : exp
12
3.0
2.8
2.6
2.4
2.2
2.0
1.8
1.6
1.4
1.2
1.0
0.8
ppm

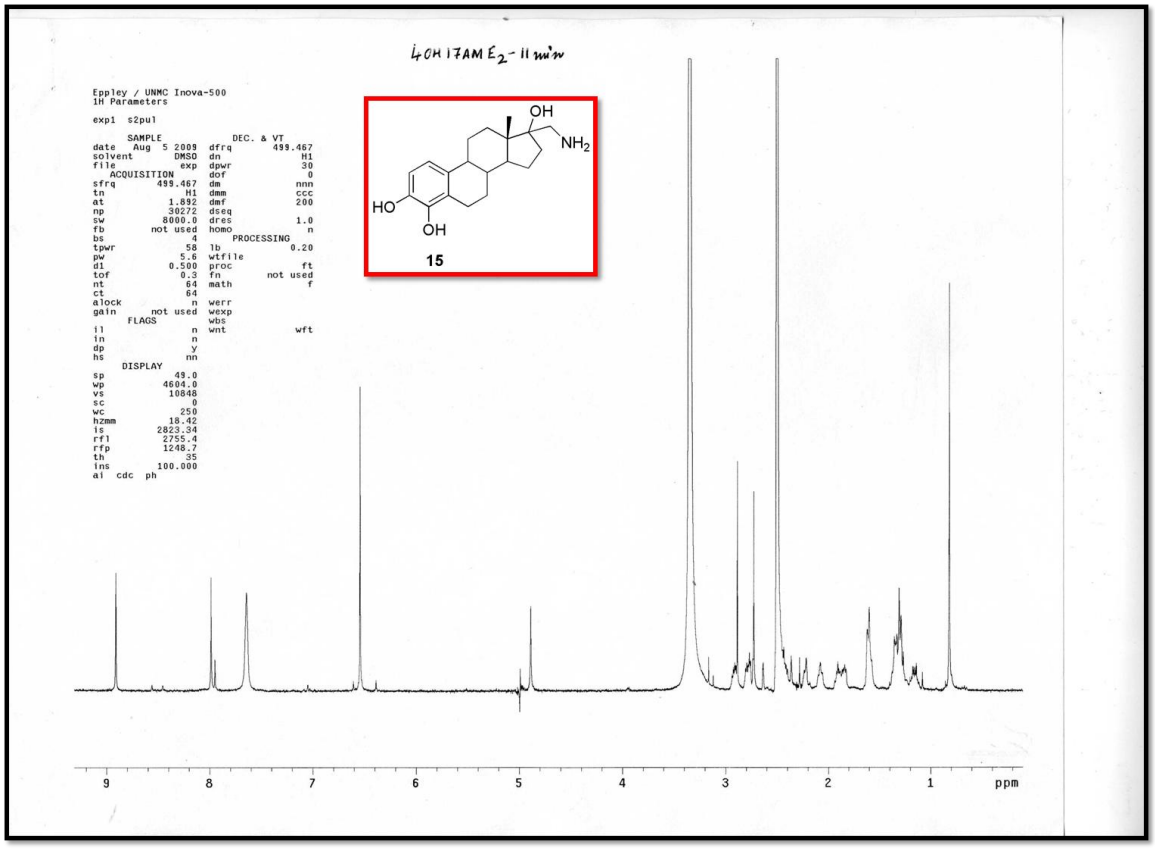
Eppley / UNMC Inova-500
1H Parameters
exp1 s2pul
15
9
8
7
6
5
4
3
2
1
ppm

A1.2 CHAPTER 3

Direct Synthesis of Aqueous Quantum Dots through a 4,4'-bipyridine-Based Twin Ligand Strategy

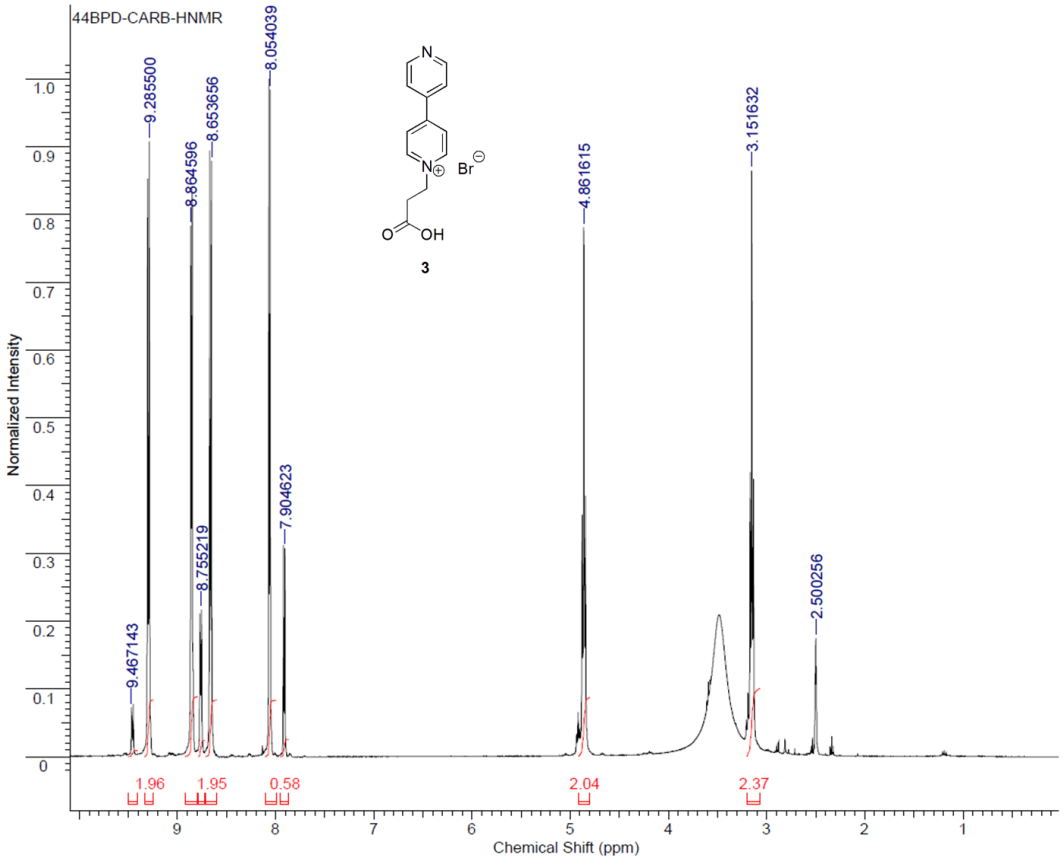

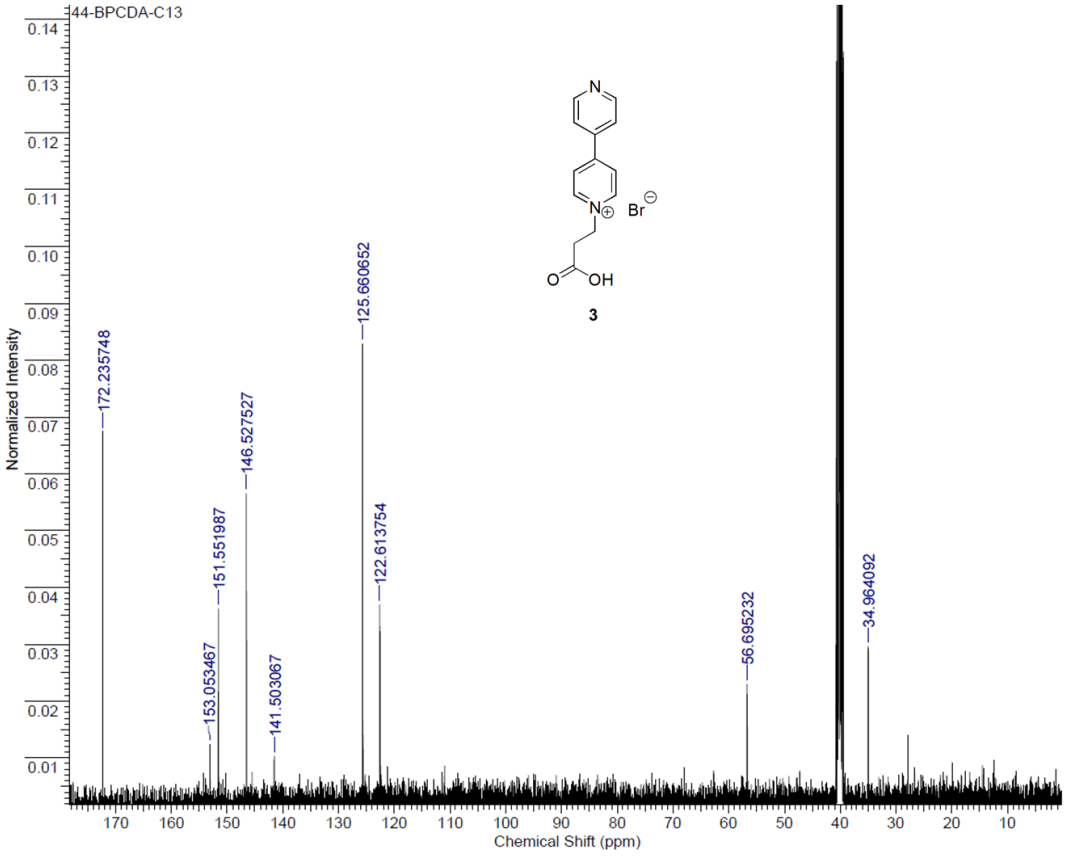
44-BPCDA-C13
Normalized Intensity
Chemical Shift (ppm)
172.235748
153.053467
151.551987
146.527527
141.503067
125.660652
122.613754
56.695232
34.964092
Br
OH
3

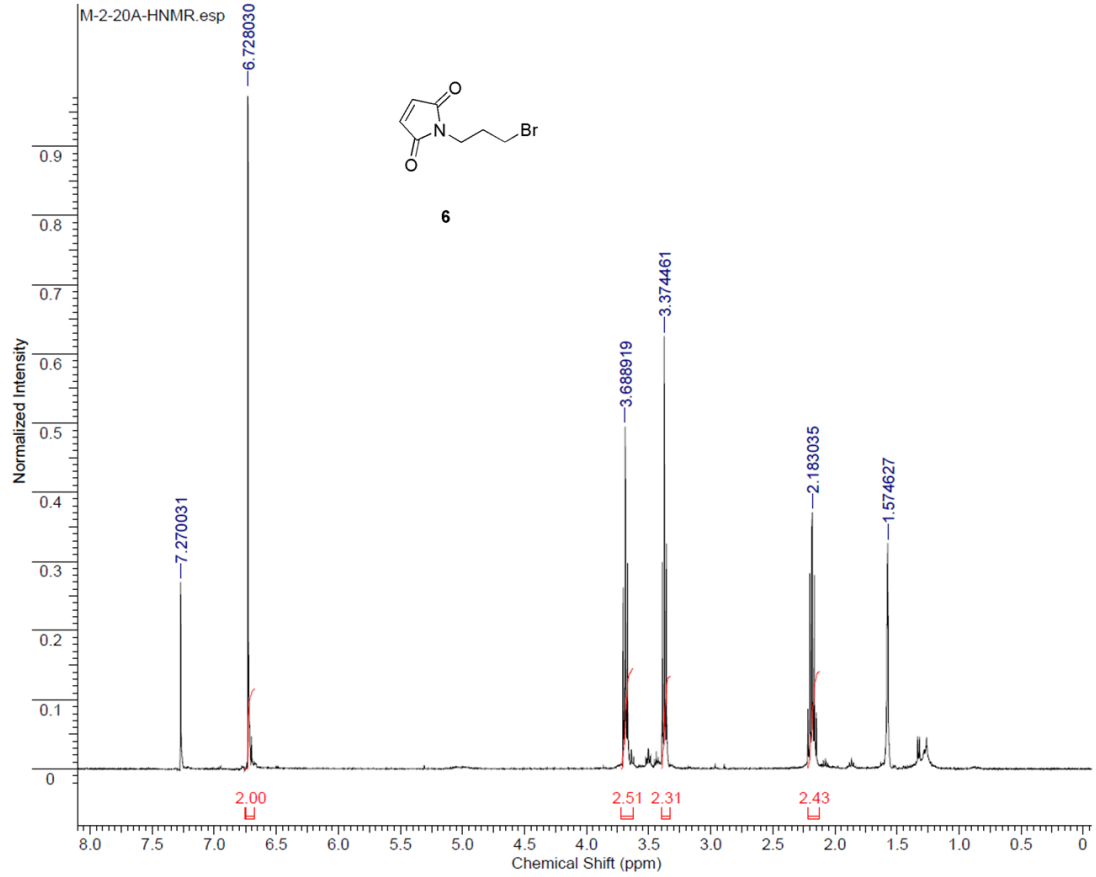
M-2-20A-HNMR.esp
Normalized Intensity
Chemical Shift (ppm)
6.728030
7.270031
3.688919
3.374461
2.183035
1.574627
2.00
2.51
2.31
2.43
Br
6

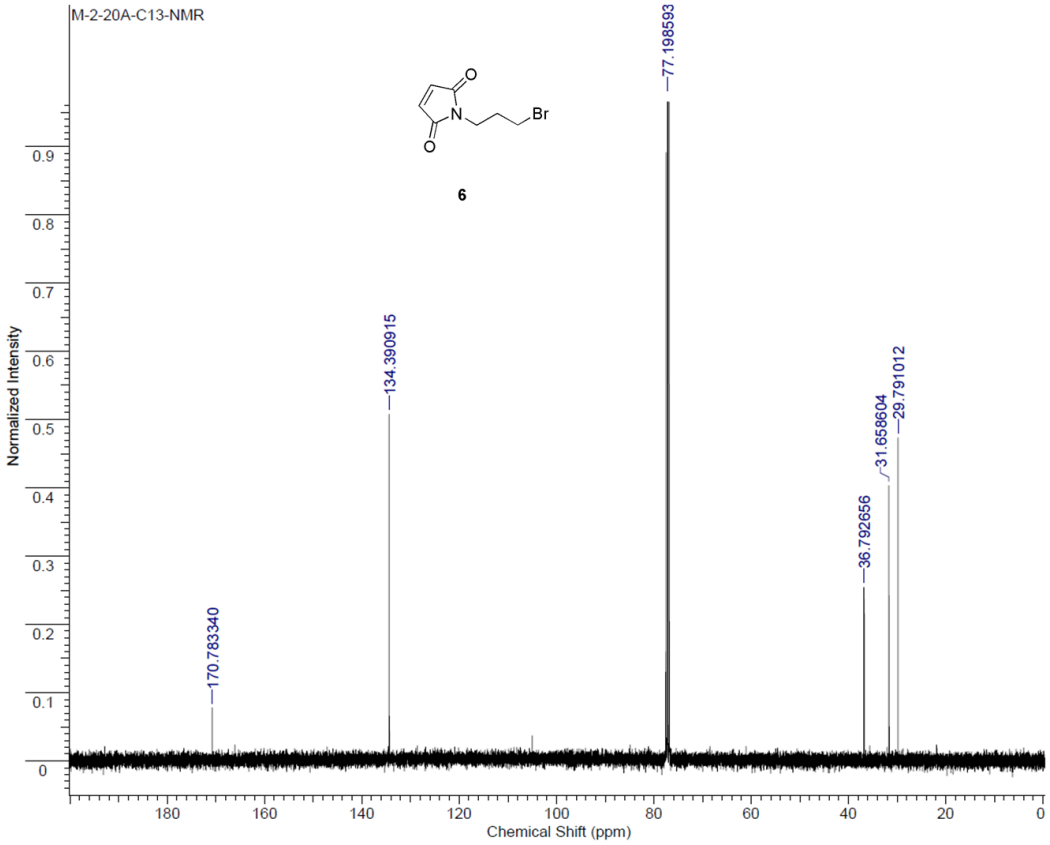
M-2-20A-C13-NMR
77.198593
134.390915
31.658604
29.791012
36.792656
170.783340
Normalized Intensity
Chemical Shift (ppm)
Br
6

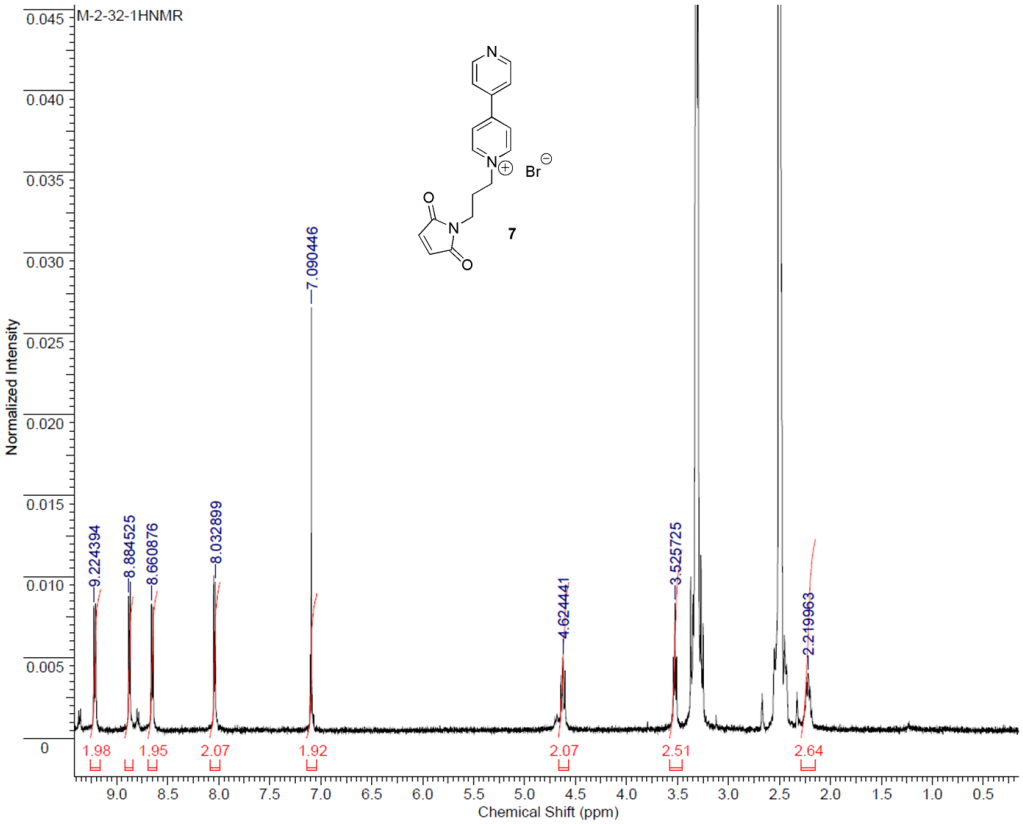
M-2-32-1HNMR
7.090446
9.224394
8.884525
8.660876
8.032899
4.624441
3.525725
2.219963
1.98
1.95
2.07
1.92
2.07
2.51
2.64
Normalized Intensity
Chemical Shift (ppm)
Br
7

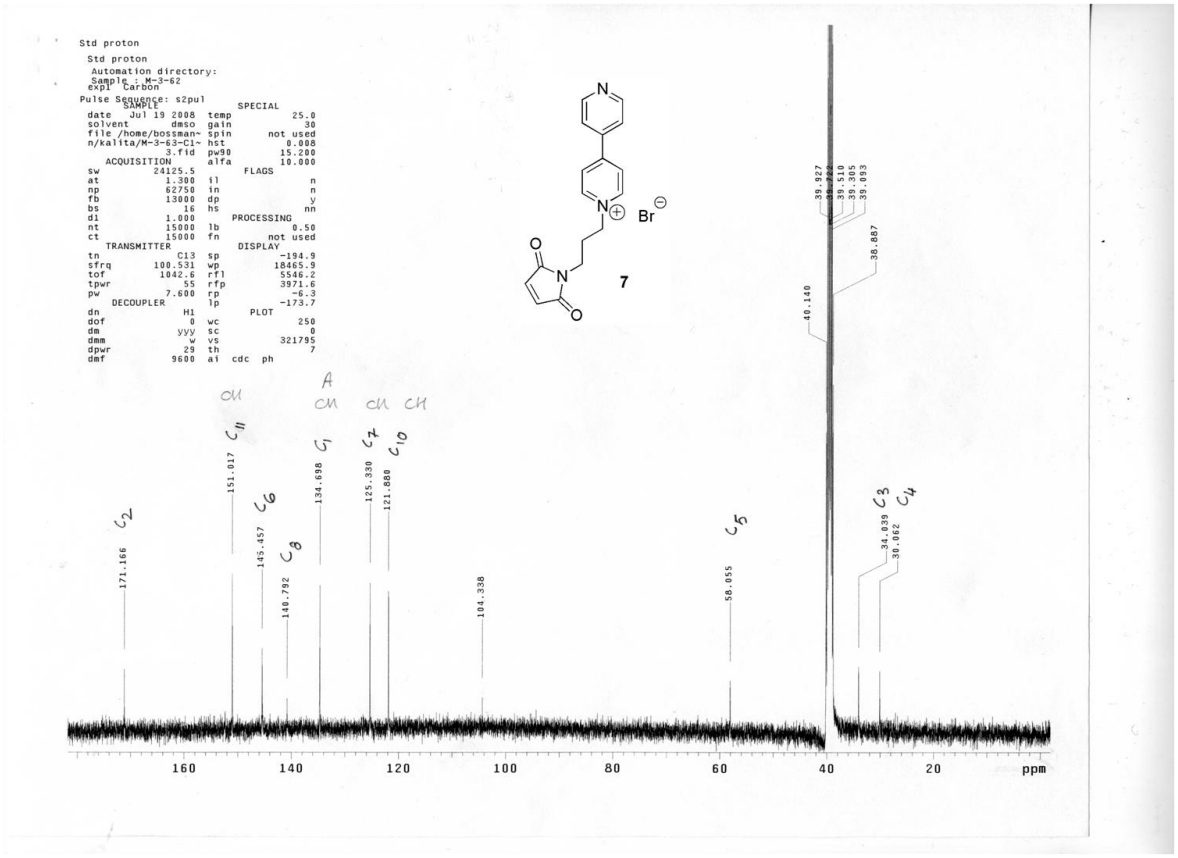
Std proton
Std proton
Automation directory:
Sample : M-3-62
expl Carbon
Pulse Sequence: s2pul
SAMPLE
date Jul 19 2008
solvent dmso
file /home/bossman~
n/kalita/M-3-63-C1~
3.fid
ACQUISITION
sw 24125.5
at 1.300
np 62750
fb 13000
bs 16
d1 1.000
nt 15000
ct 15000
TRANSMITTER
tn C13
tfrq 100.531
tof 1042.6
tpwr 55
pw 7.600
DECOUPLER
dn H1
dof 0
dm yyy
dmm w
dpwr 29
dmf 9600
SPECIAL
temp 25.0
gain 30
spin not used
hst 0.008
pw90 15.200
alfa 10.000
FLAGS
il n
in n
dp y
hs nn
PROCESSING
lb 0.50
fn not used
DISPLAY
sp -194.9
wp 18465.9
rfl 5546.2
rfp 3971.6
rp -6.3
lp -173.7
PLOT
wc 250
sc 0
vs 321795
th 7
al cdc ph
7
C2
C11
C6
C8
C1
C7
C10
C5
C3
C4
171.166
151.017
145.457
140.792
134.698
125.330
121.880
104.338
58.055
39.927
39.718
39.510
39.305
39.093
38.887
40.140
34.039
30.062
160
140
120
100
80
60
40
20
ppm

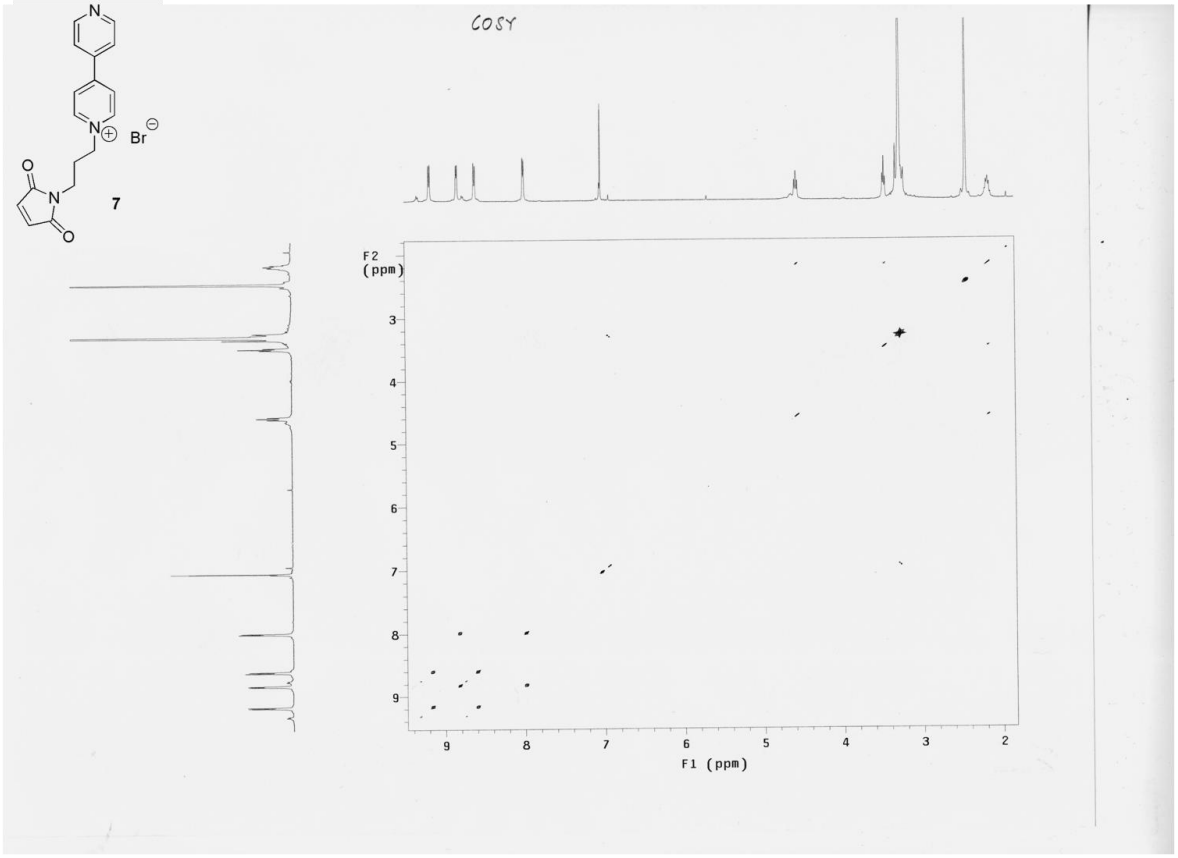
7
COSY
F2 (ppm)
F1 (ppm)
3
4
5
6
7
8
9
2

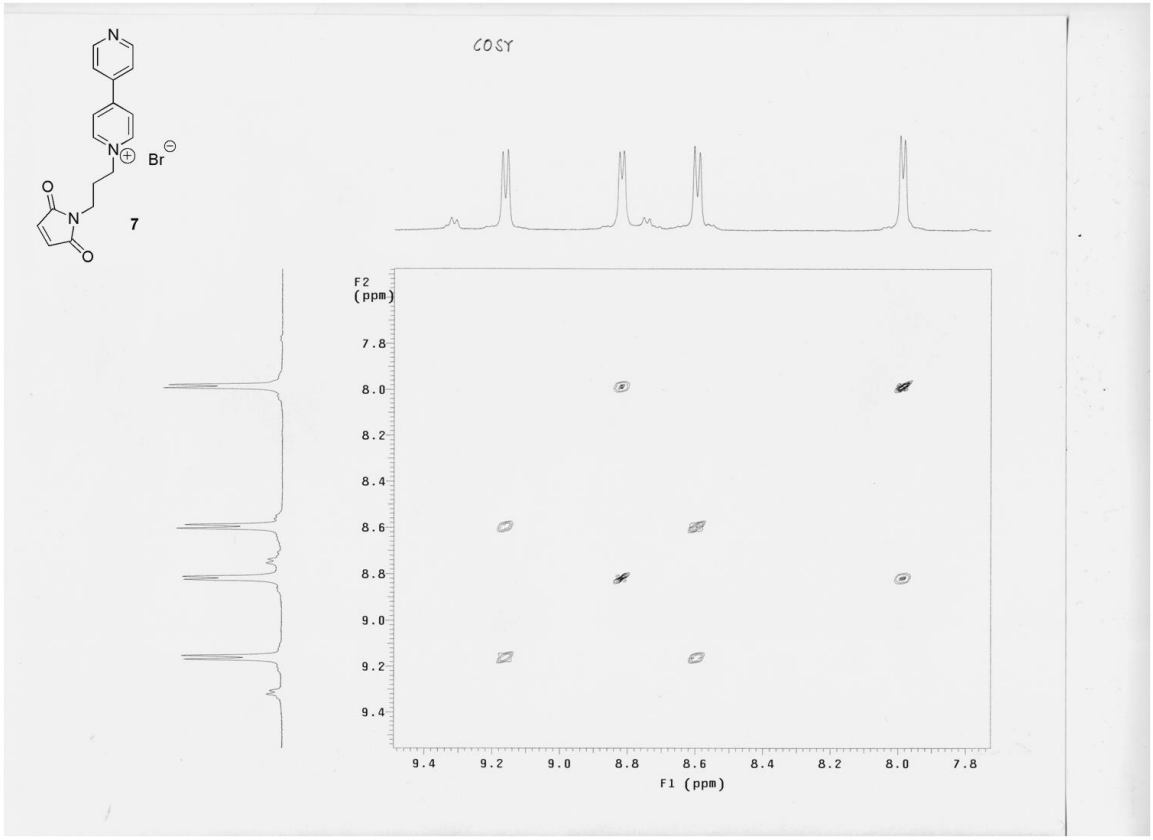
COSY
7
F2 (ppm)
F1 (ppm)

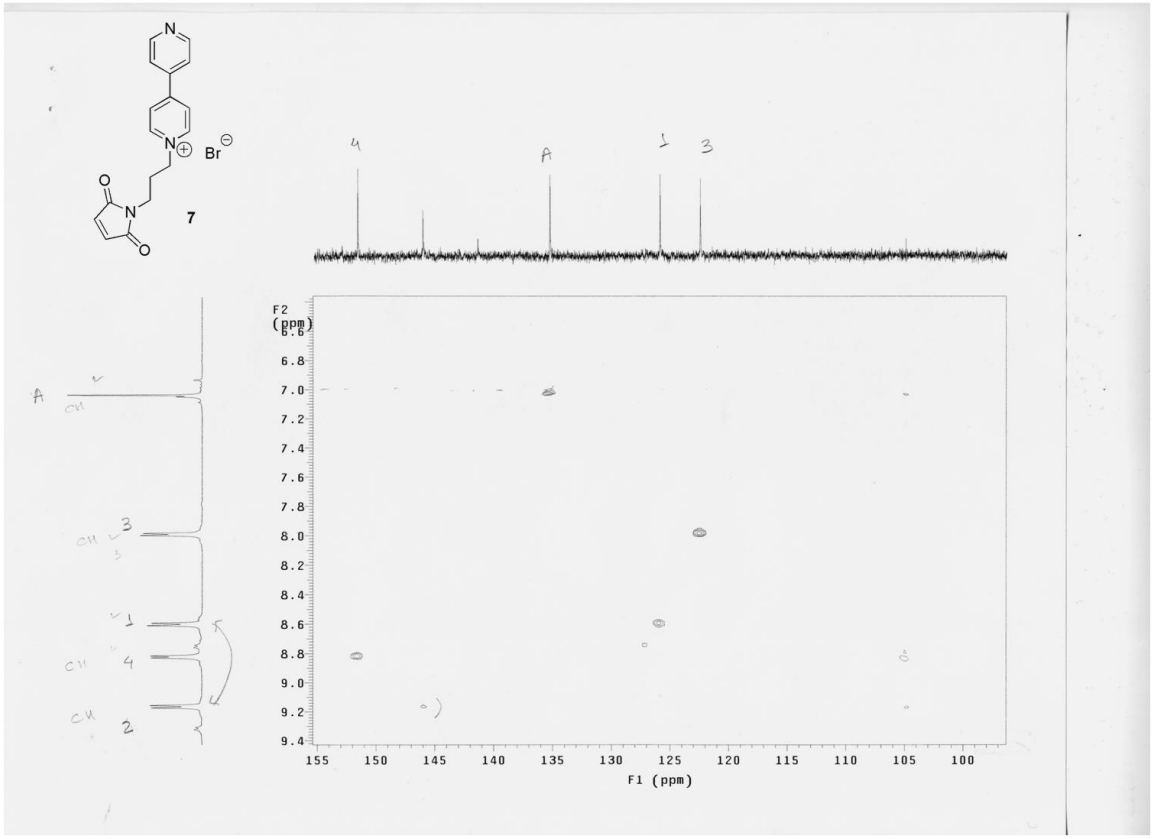
7
F2 (ppm)
F1 (ppm)

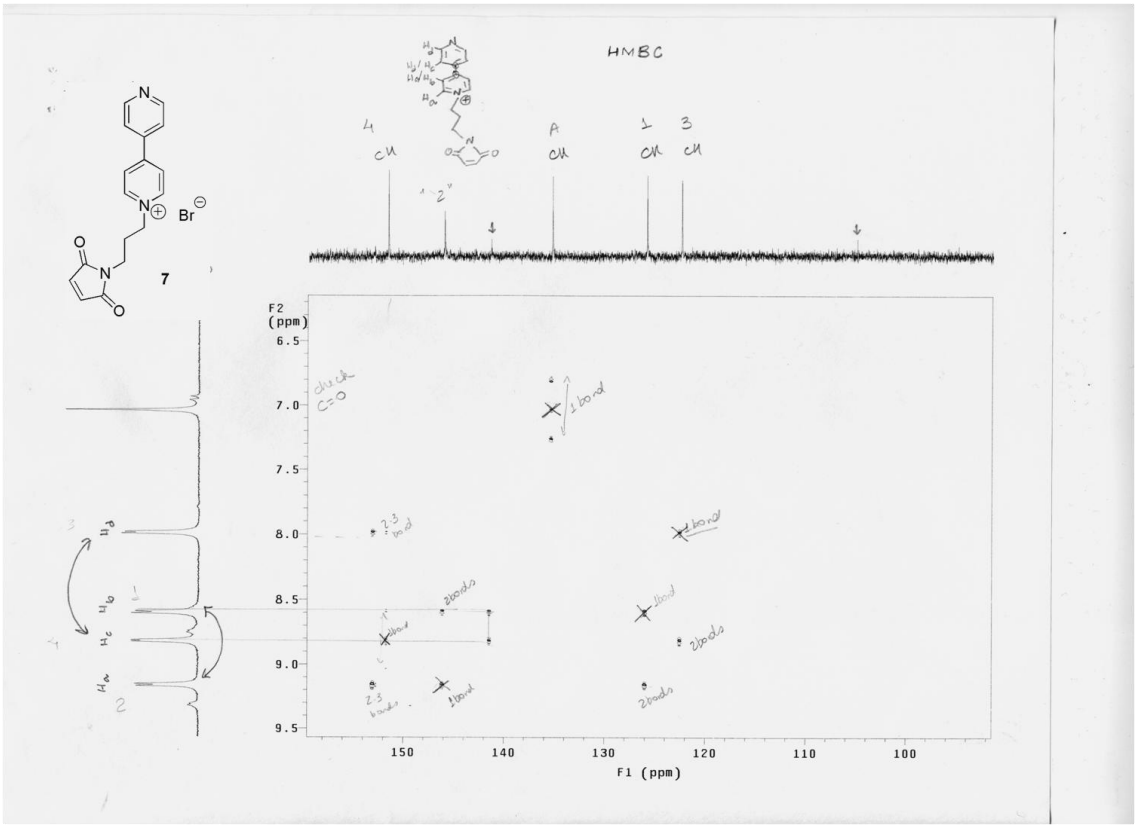

A2. Mass Spectrometry

A2.1. CHAPTER 2

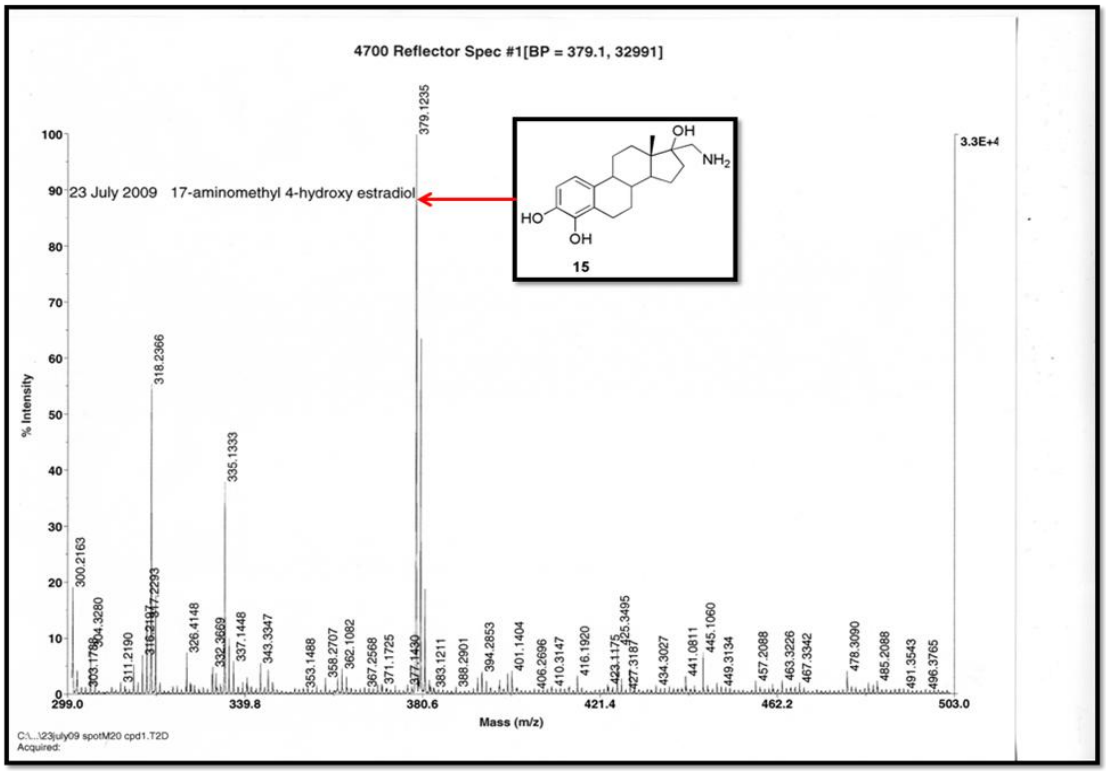

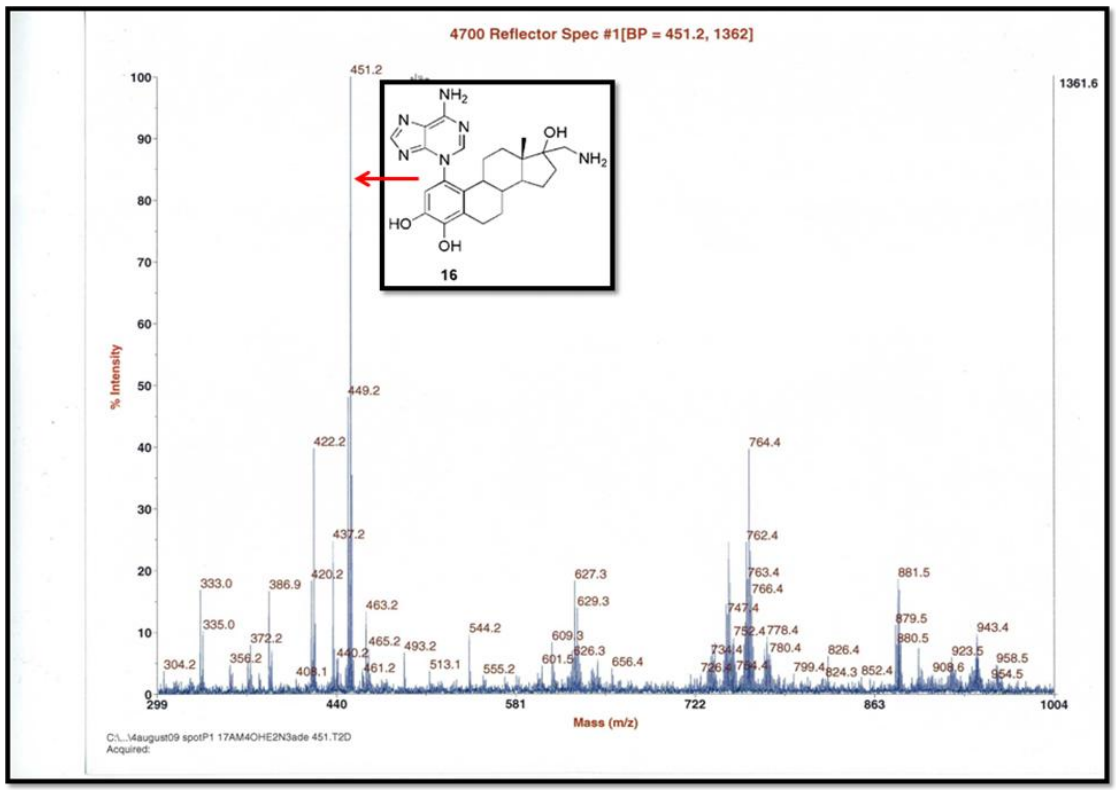
4700 Reflector Spec #1[BP = 451.2, 1362]
451.2
1361.6
NH2
N
N
N
OH
NH2
HO
OH
16
% Intensity
449.2
422.2
764.4
437.2
762.4
333.0
386.9
420.2
627.3
763.4
766.4
629.3
463.2
881.5
335.0
544.2
747.4
879.5
943.4
372.2
465.2
493.2
609.3
752.4
778.4
880.5
923.5
958.5
304.2
356.2
440.2
461.2
513.1
555.2
601.5
626.3
656.4
734.4
780.4
826.4
908.6
954.5
299
440
581
722
863
1004
Mass (m/z)
C:\...\4august09 spotP1 17AM4OHE2N3ade 451.T2D
Acquired:

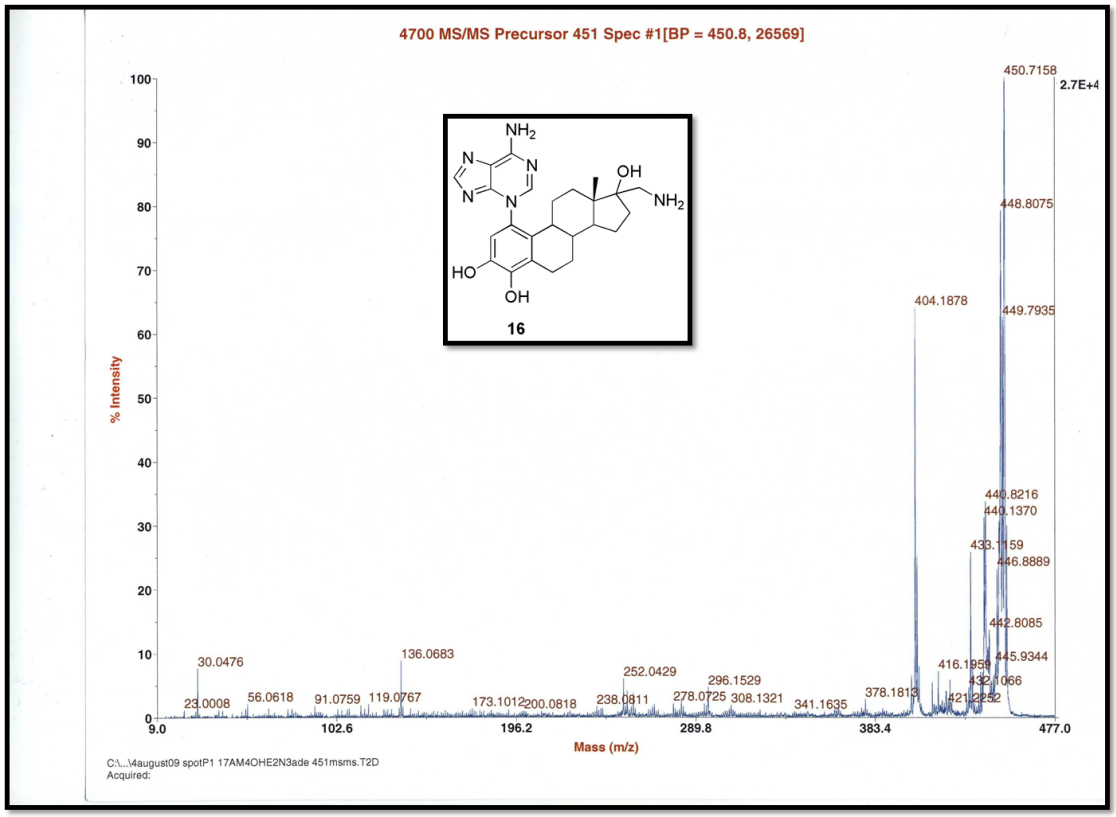
4700 MS/MS Precursor 451 Spec #1[BP = 450.8, 26569]
450.7158
2.7E+4
NH2
N
N
N
OH
NH2
HO
OH
16
448.8075
404.1878
449.7935
% Intensity
440.8216
440.1370
433.1159
446.8889
442.8085
30.0476
136.0683
445.9344
252.0429
416.1958
296.1529
23.0008
56.0618
91.0759
119.0767
173.1012
200.0818
238.0811
278.0725
308.1321
341.1635
378.1813
421.2252
9.0
102.6
196.2
289.8
383.4
477.0
Mass (m/z)
C:\...\4august09 spotP1 17AM4OHE2N3ade 451msms.T2D
Acquired:

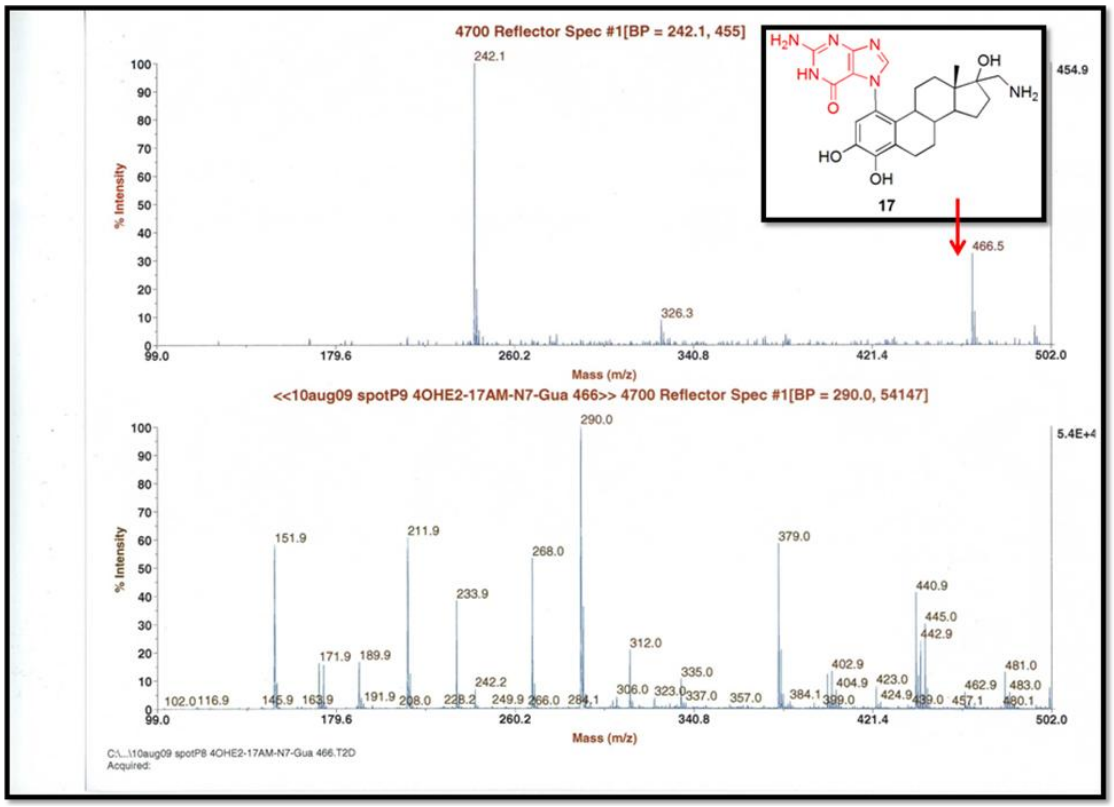
4700 Reflector Spec #1[BP = 242.1, 455]
242.1
454.9
466.5
326.3
% Intensity
Mass (m/z)
17
<<10aug09 spotP9 4OHE2-17AM-N7-Gua 466>> 4700 Reflector Spec #1[BP = 290.0, 54147]
290.0
5.4E+4
151.9
211.9
268.0
233.9
379.0
440.9
445.0
442.9
312.0
171.9
189.9
335.0
402.9
481.0
242.2
423.0
462.9
483.0
C:\...\10aug09 spotP8 4OHE2-17AM-N7-Gua 466.T2D
Acquired:

Appendix B - QD Photostability Experiment

Continuous wave (CW) laser of excitation wavelength 488nm from Spectra-Physics (made in Thiland) equipped with Nikon eclipse T*i* microscope was used.

Glass films of CdTe QDs (approximately 1μM concentration) were prepared from a solution of 20 μL QDs in 1 mL poly(vinylalcohol) in HPLC grade water.

The laser experiment parameters

1. Acquisition Mode- Kinetics
2. Trigger Mode- Internal
3. Exposure Time- 1 second
4. Accumulation cycle time- 1.288 second
5. Number of accumulations- 1
6. Kinetic cycle time- 1.288second
7. Frequency- 0.77639 Hz
8. Readout mode- full resolution image
9. Readout time- 1MHz at 16-bit
10. Pre-amplifier gain- 5.1X
11. Output amplifier- conventional
12. Baseline offset (counts)- 0

Data Processing

Image J and plotted in Igor (modified by Professor Daniel Higgins, Department of Chemistry, Kansas State University)

B 1. QD Population Decay Histograms at Three Laser Powers

B 1.1 Laser Power = 1.9 mW; Frames 300, 500

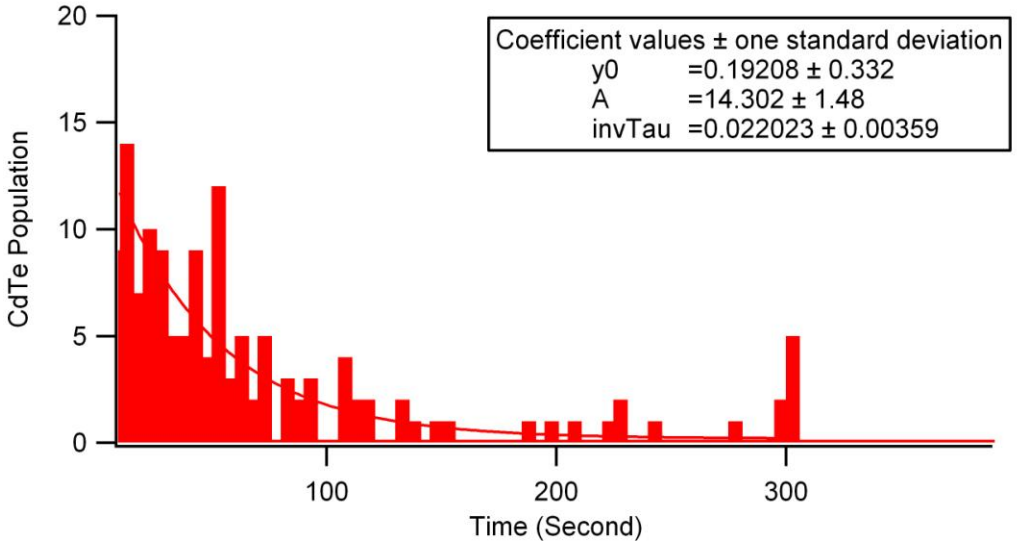

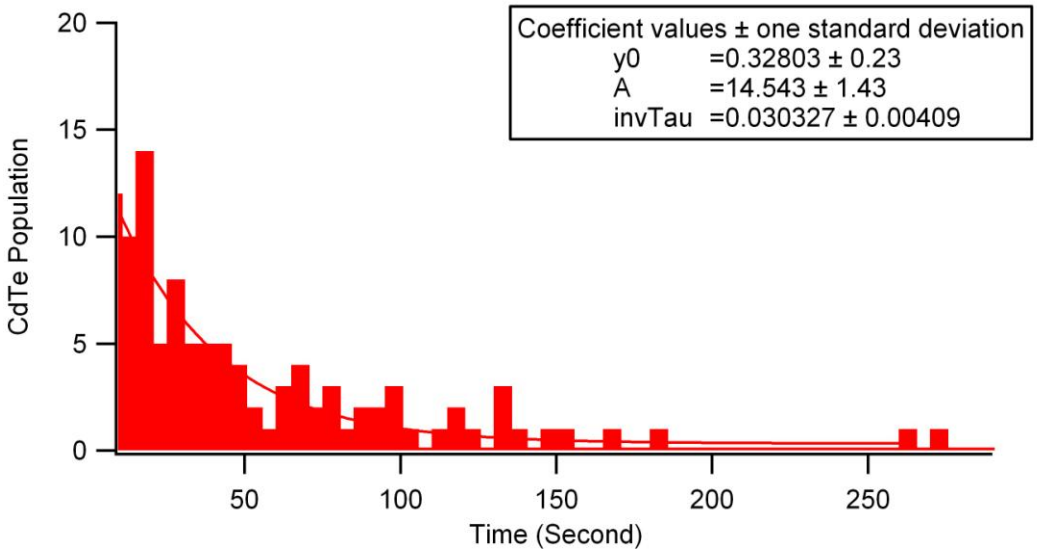

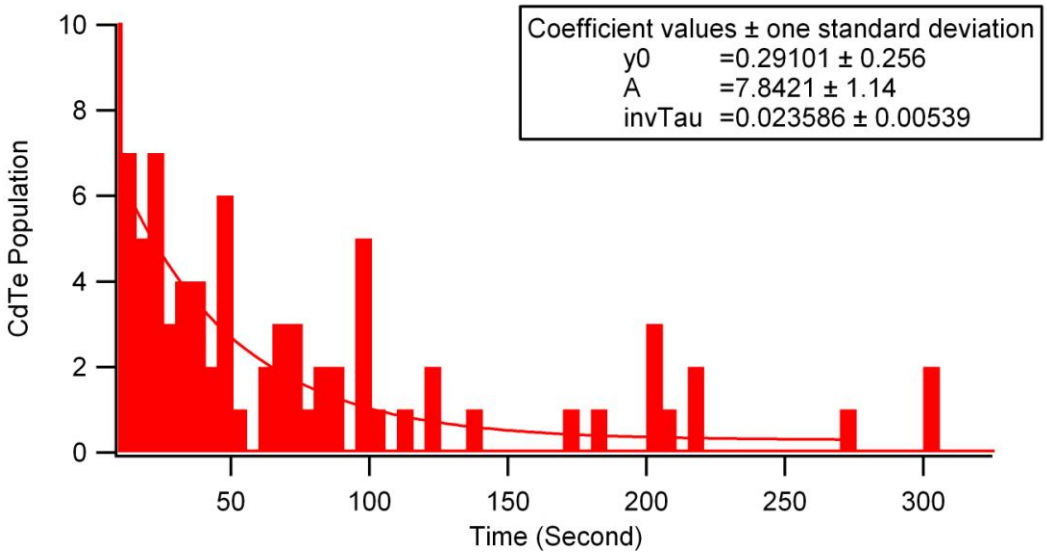

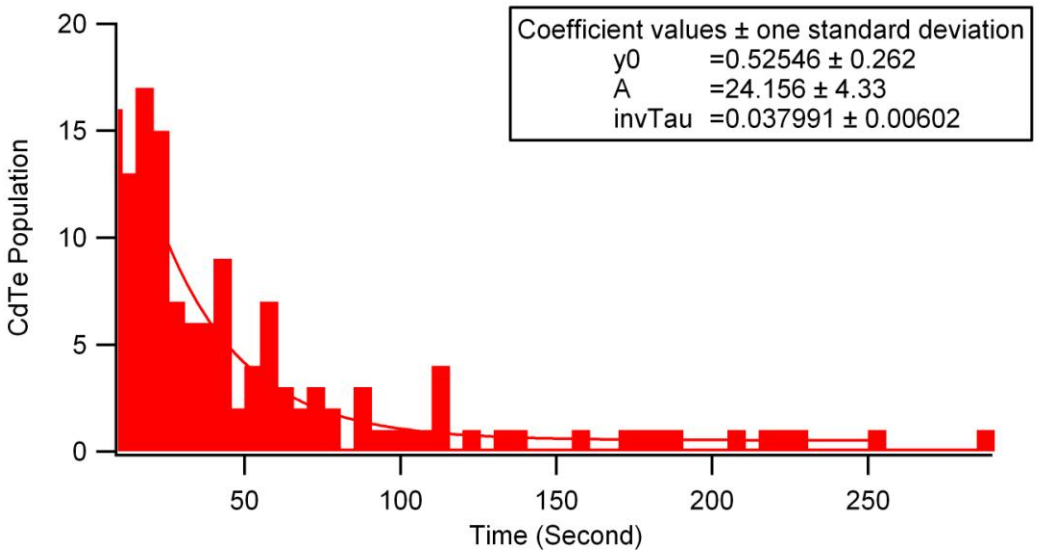

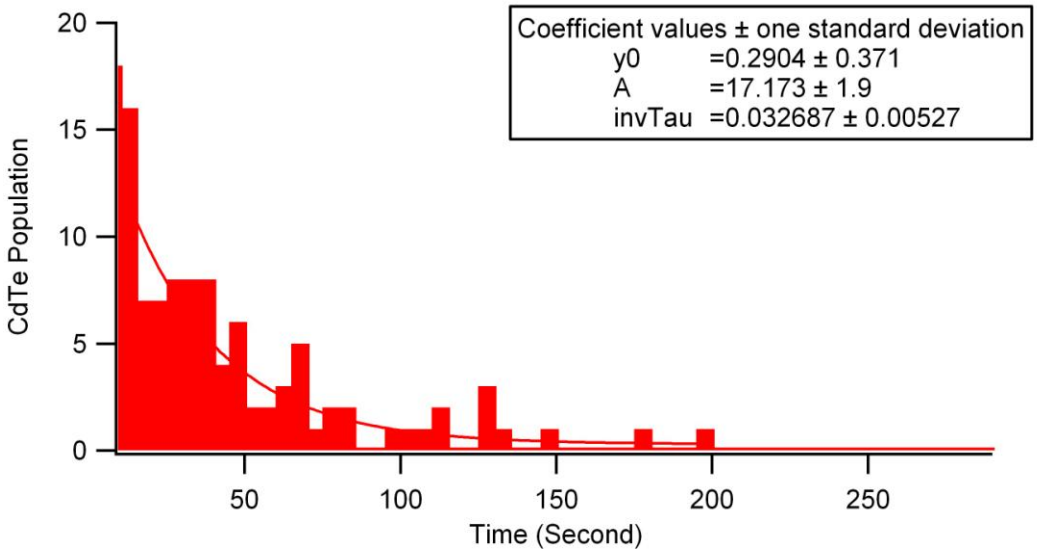

B 1.2 Laser Power = 1.5 mW; Frames 300, 500

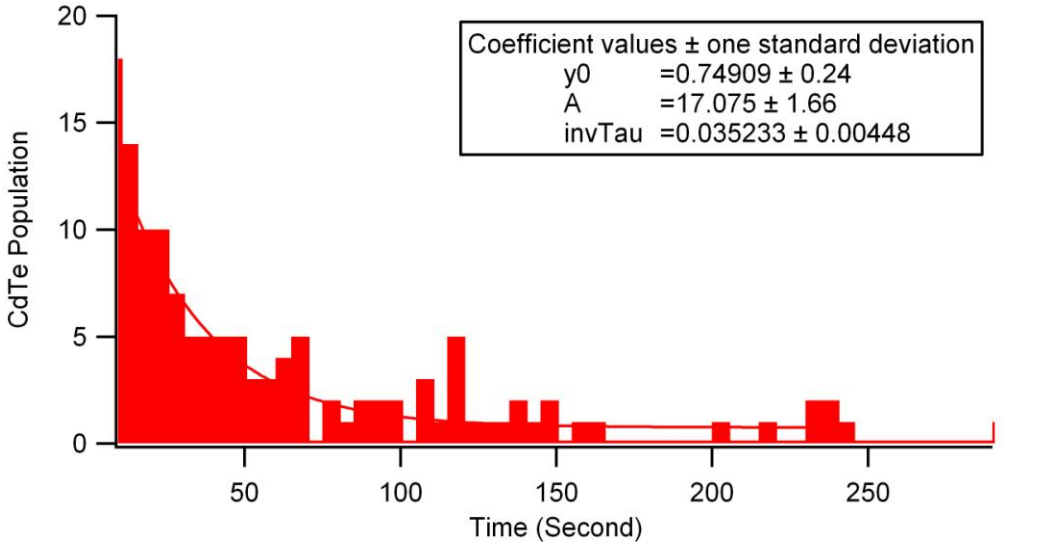

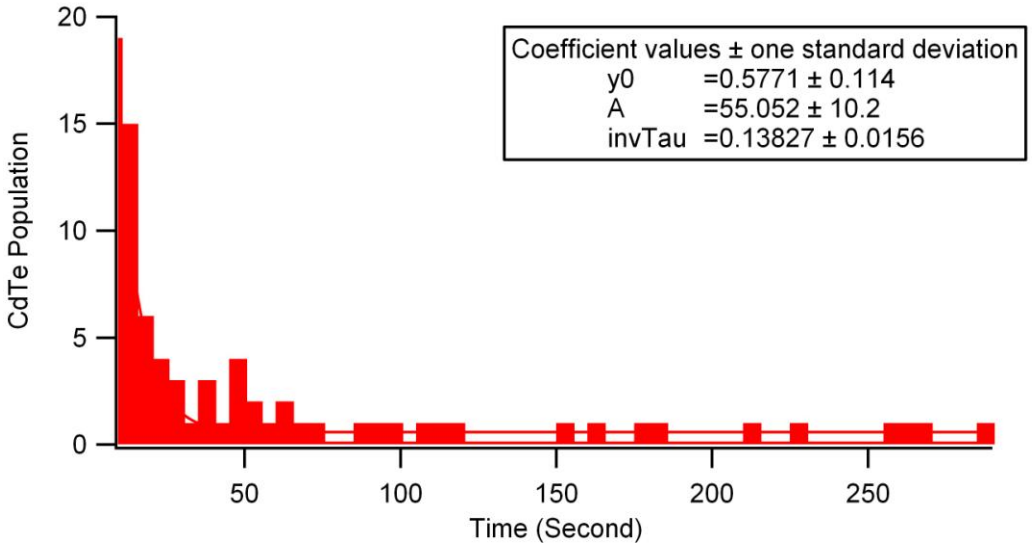
Coefficient values ± one standard deviation
y0 =0.5771 ± 0.114
A =55.052 ± 10.2
invTau =0.13827 ± 0.0156
CdTe Population
Time (Second)

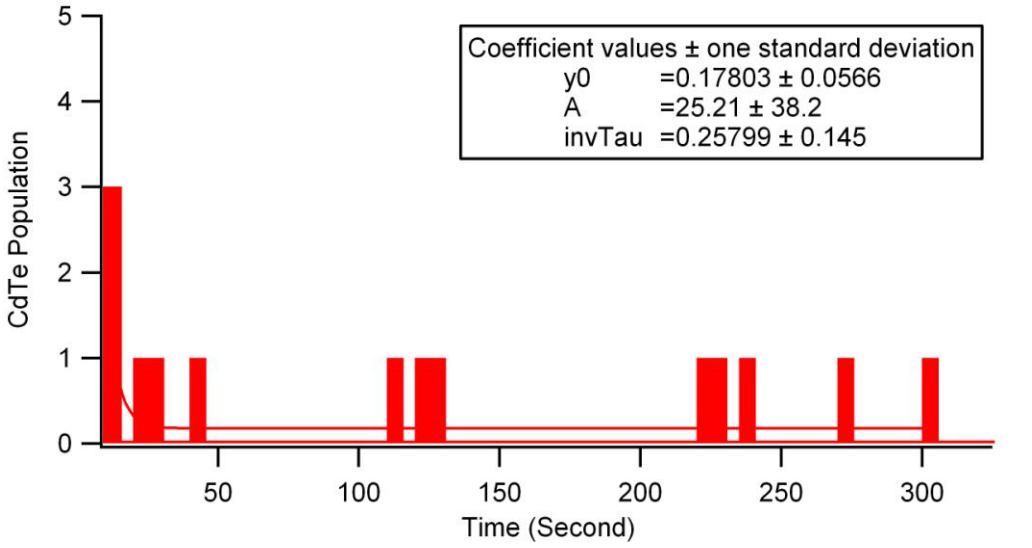
Coefficient values ± one standard deviation
y0 =0.17803 ± 0.0566
A =25.21 ± 38.2
invTau =0.25799 ± 0.145
CdTe Population
Time (Second)

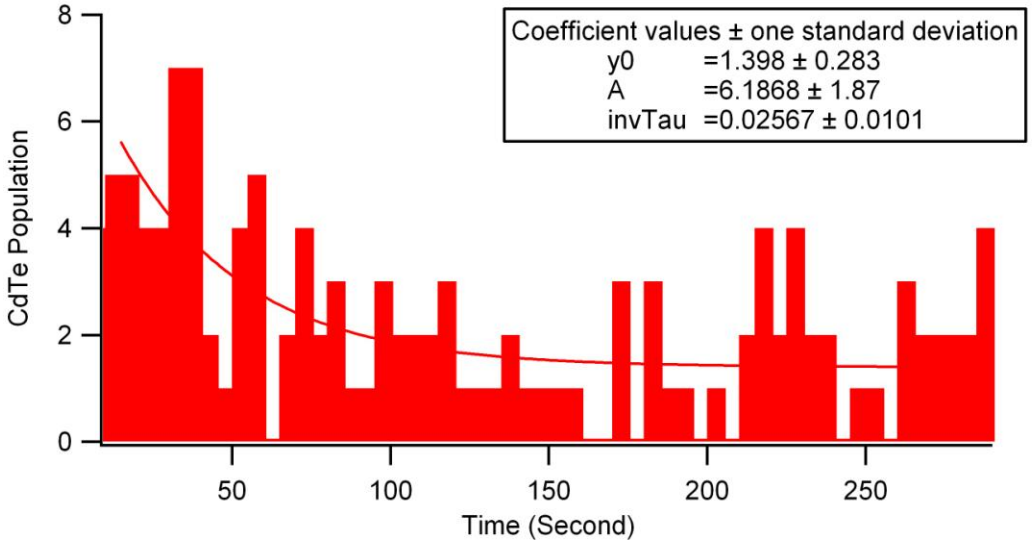
Coefficient values ± one standard deviation
y0 =1.398 ± 0.283
A =6.1868 ± 1.87
invTau =0.02567 ± 0.0101
CdTe Population
Time (Second)

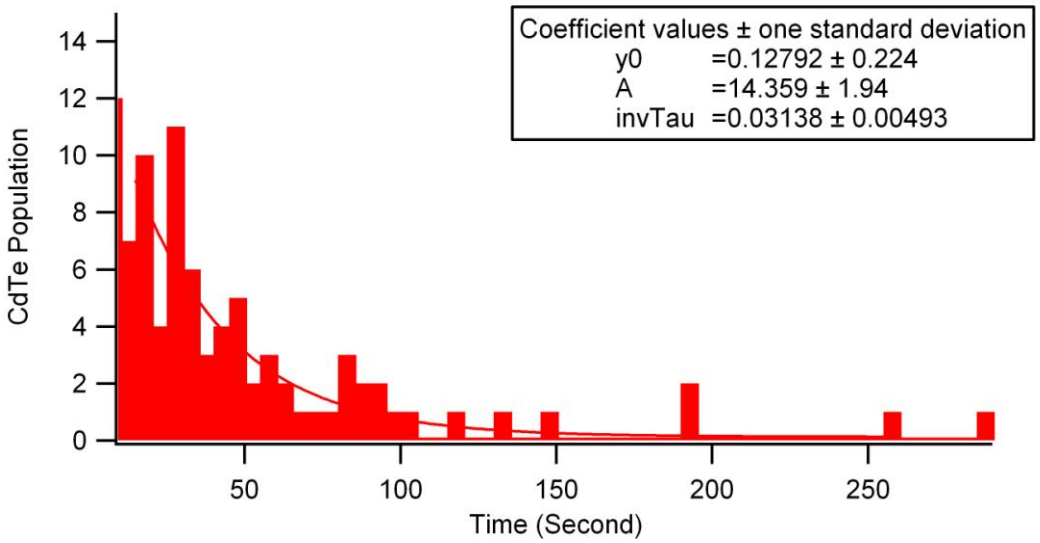

B 1.3 Laser Power = 1.0 mW; Frames 300, 500

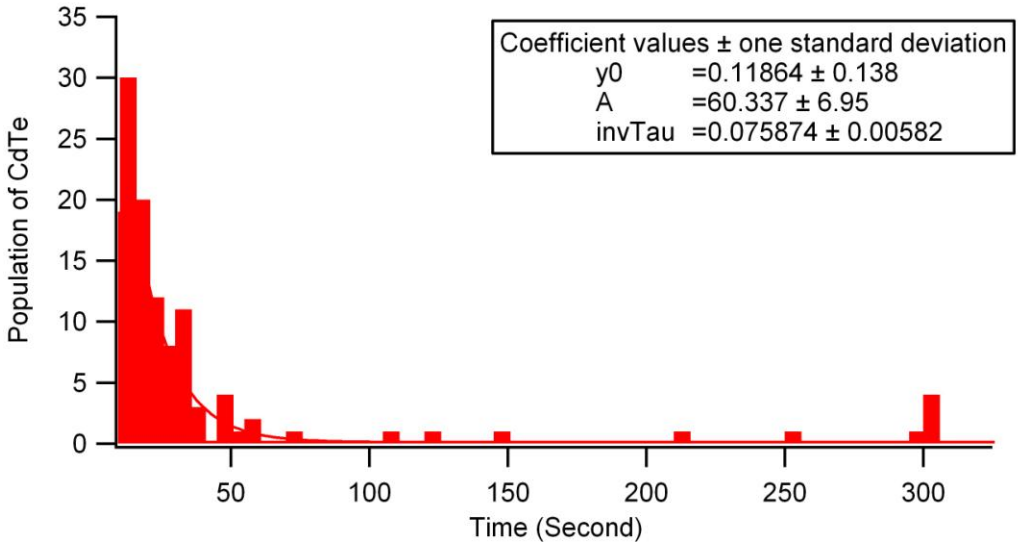

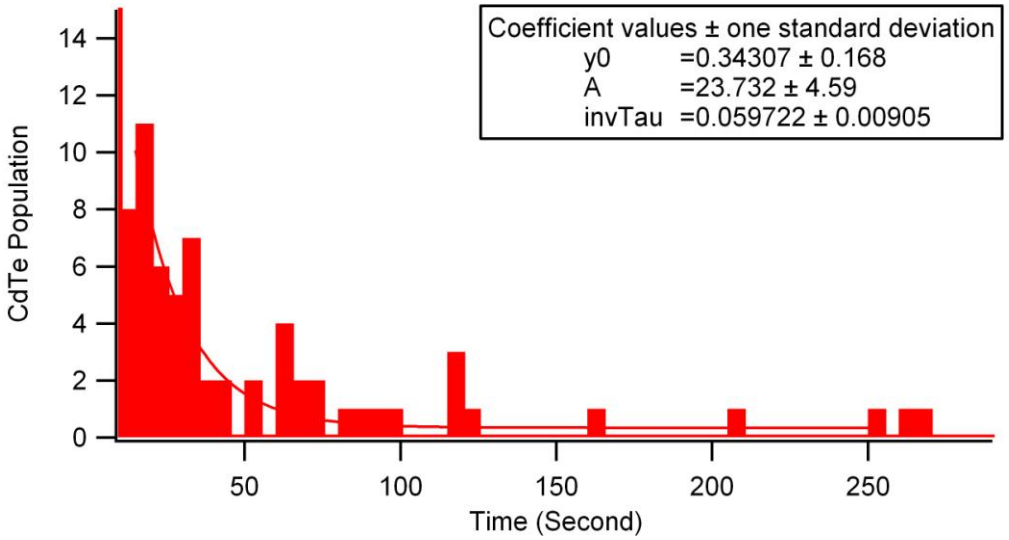
Coefficient values ± one standard deviation
y0 =0.34307 ± 0.168
A =23.732 ± 4.59
invTau =0.059722 ± 0.00905
CdTe Population
Time (Second)

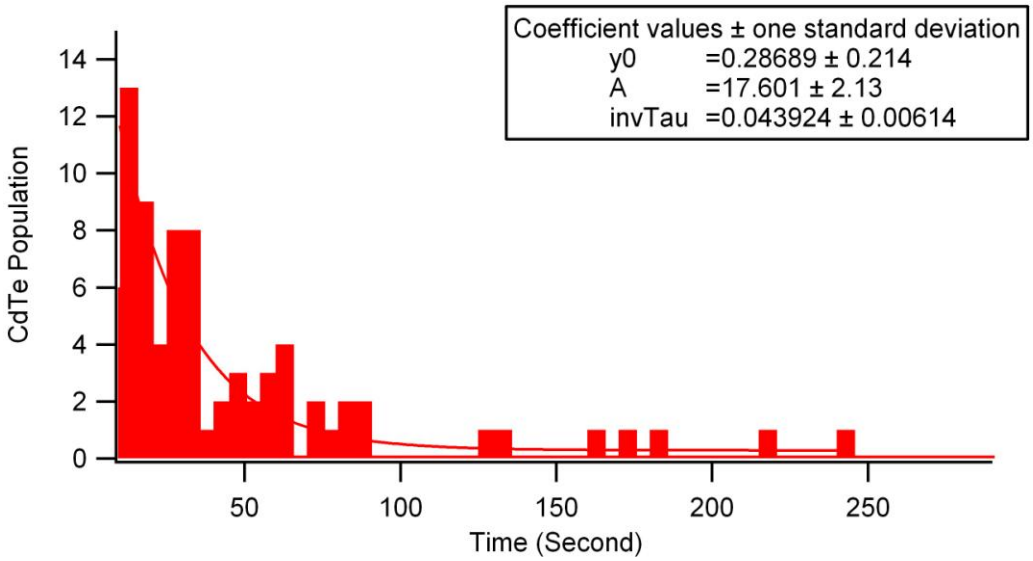
Coefficient values ± one standard deviation
y0 =0.28689 ± 0.214
A =17.601 ± 2.13
invTau =0.043924 ± 0.00614
CdTe Population
Time (Second)

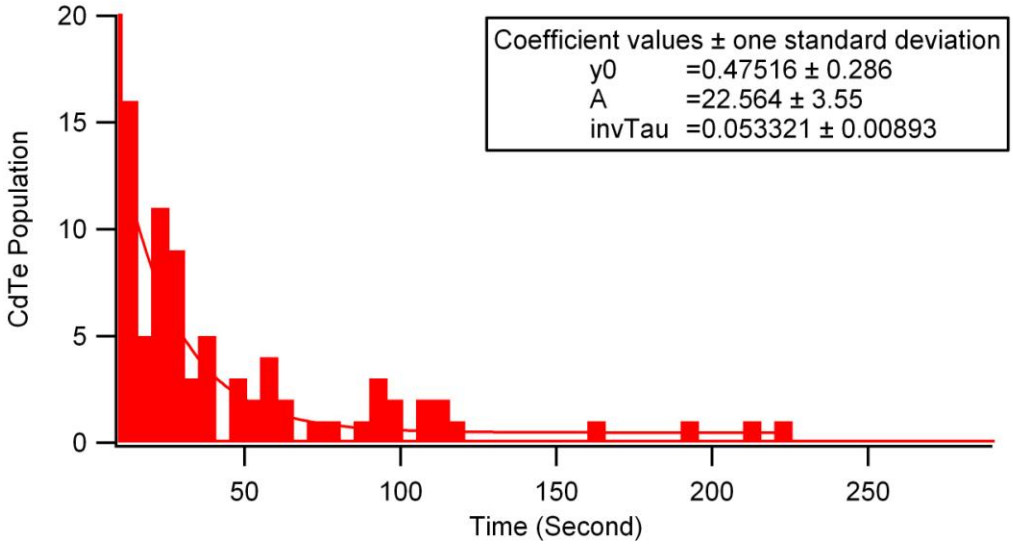
Coefficient values ± one standard deviation
y0 =0.47516 ± 0.286
A =22.564 ± 3.55
invTau =0.053321 ± 0.00893
CdTe Population
Time (Second)

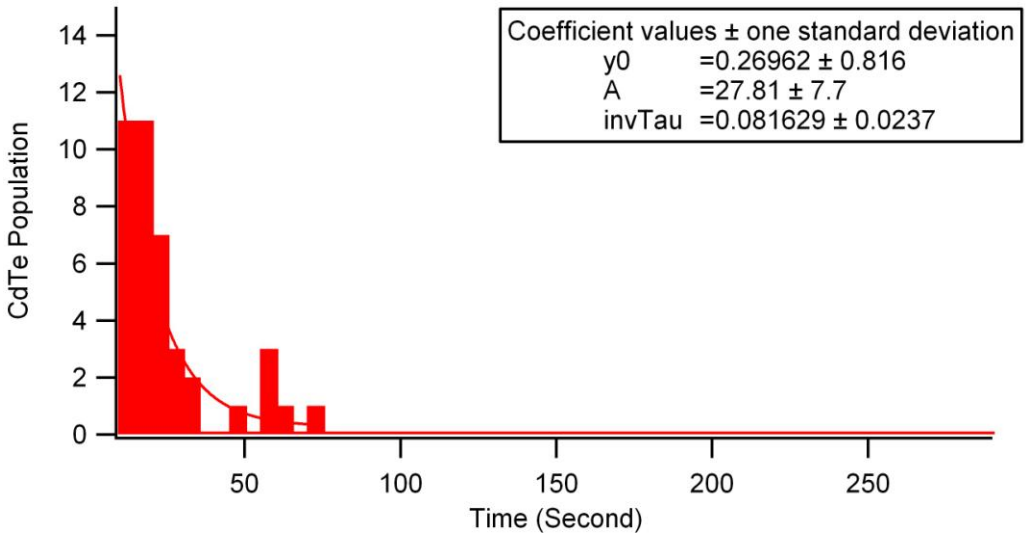

Table B.1 Life Time of aqueous CdTe

1.9 mW	1.9 mW	1.5 mW	1.5 mW	1.0 mW	1.0 mW
Frames (Seconds) 300	500	300	500	300	500
45.4	25	28.6	40	13.3	19
33.3	33.3	7.14	32.2	16.6	12.34
43.4	N/A	5	N/A	23.25	N/A

B 2. Population of Aqueous CdSe Vs Time (Second) at Three Laser Powers

B 2.1. Laser Power = 1.9 mW; Frames 300, 500

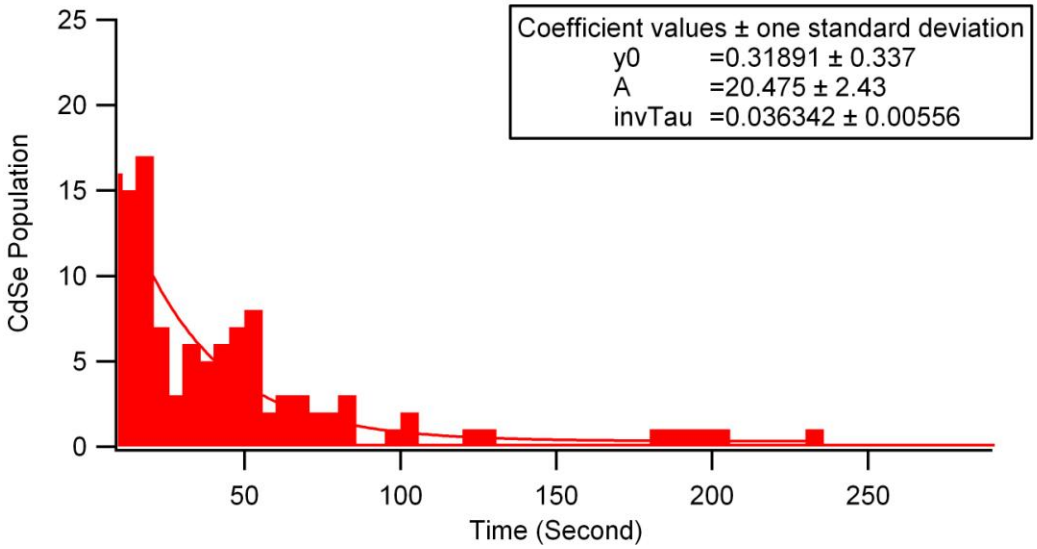

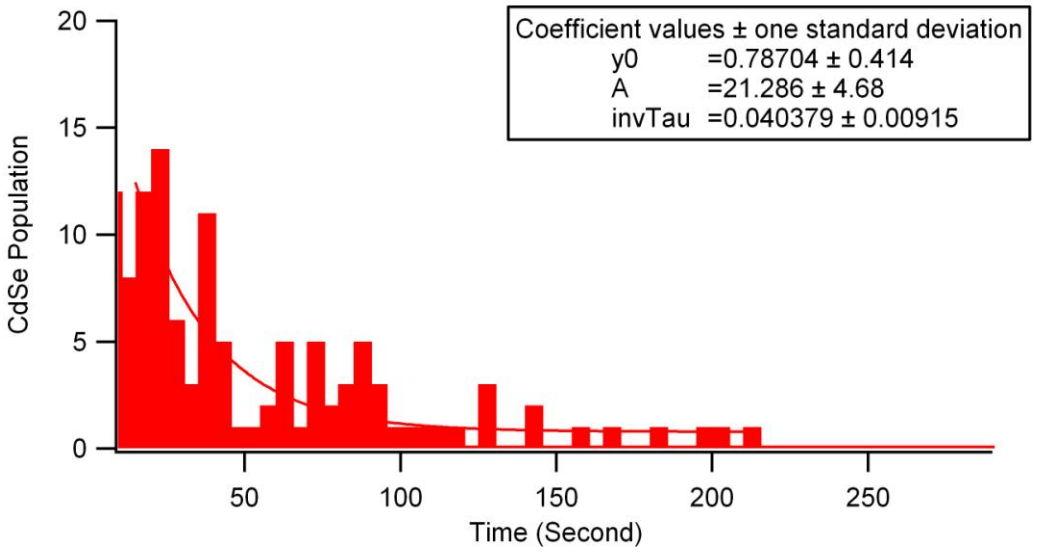
Coefficient values ± one standard deviation
y0 =0.78704 ± 0.414
A =21.286 ± 4.68
invTau =0.040379 ± 0.00915
CdSe Population
Time (Second)

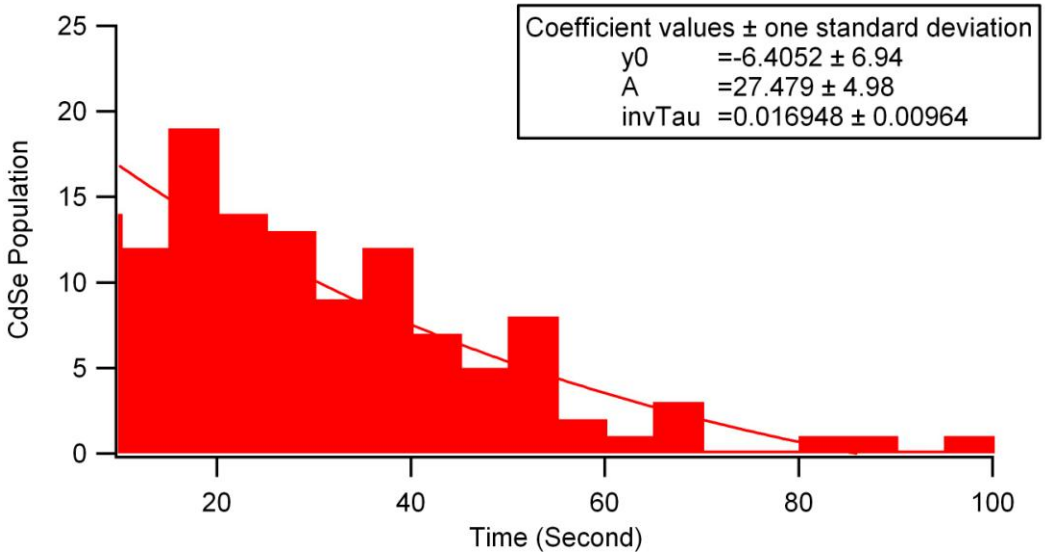
Coefficient values ± one standard deviation
y0 =-6.4052 ± 6.94
A =27.479 ± 4.98
invTau =0.016948 ± 0.00964
CdSe Population
Time (Second)

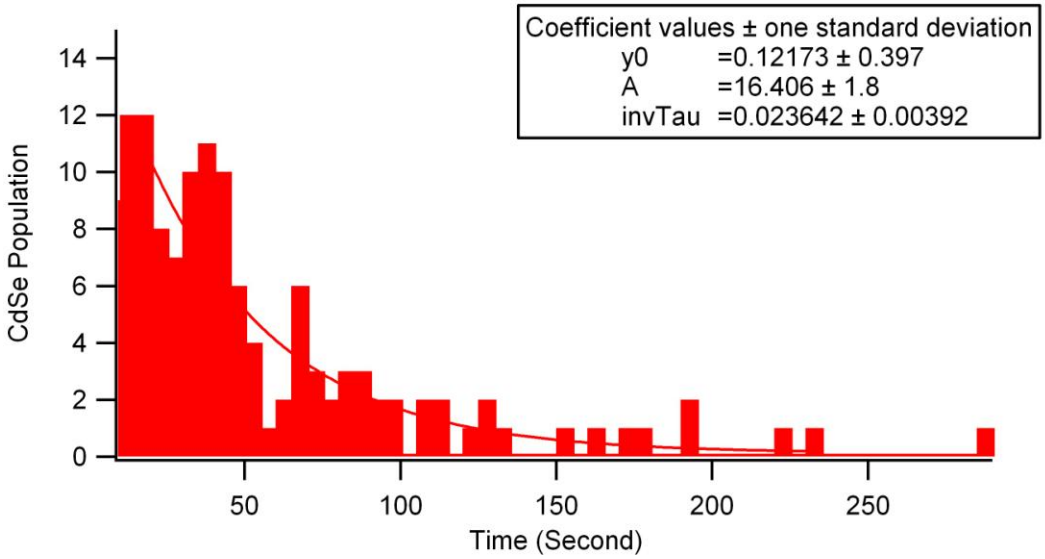
Coefficient values ± one standard deviation
y0 =0.12173 ± 0.397
A =16.406 ± 1.8
invTau =0.023642 ± 0.00392
CdSe Population
Time (Second)

B 2.2 Laser Power = 1.5 mW; Frames 300, 500

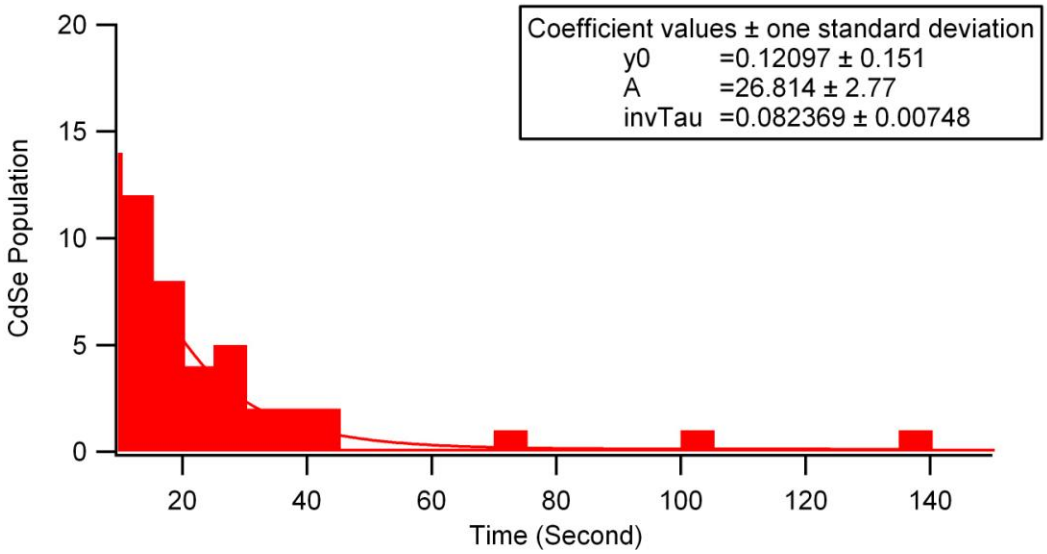

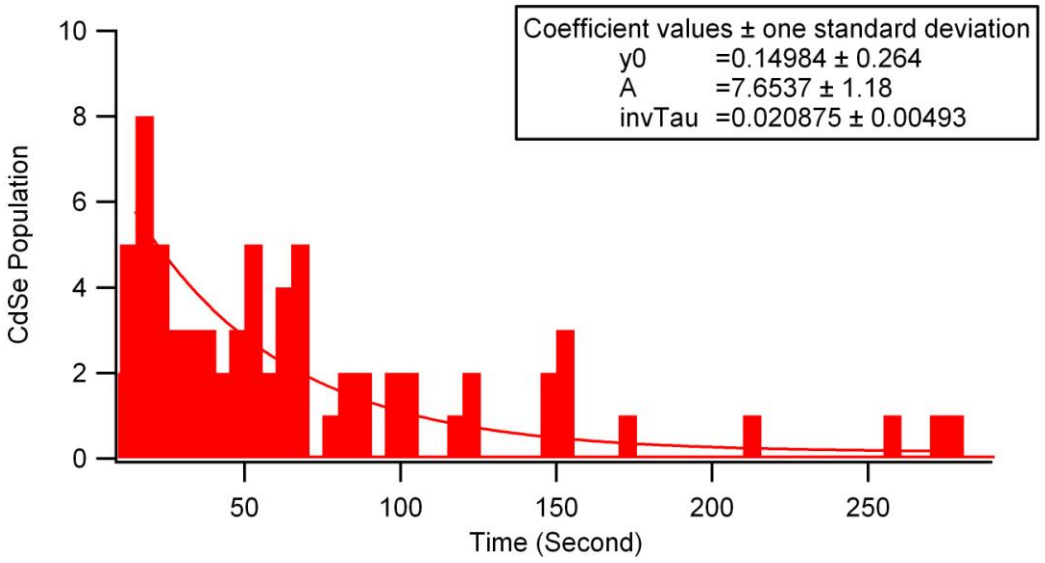

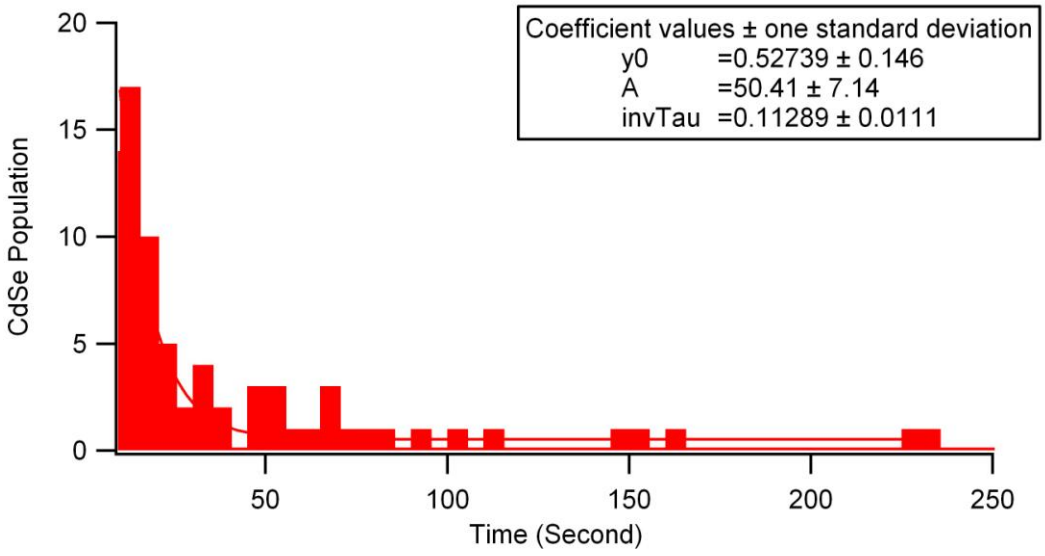

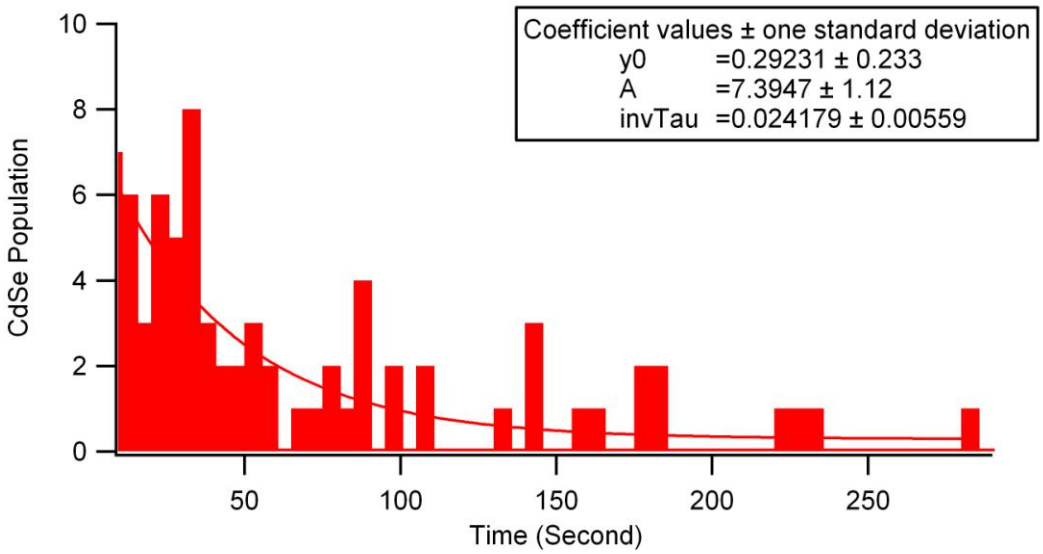

B 2.3 Laser Power = 1.0 mW; Frames 300, 500

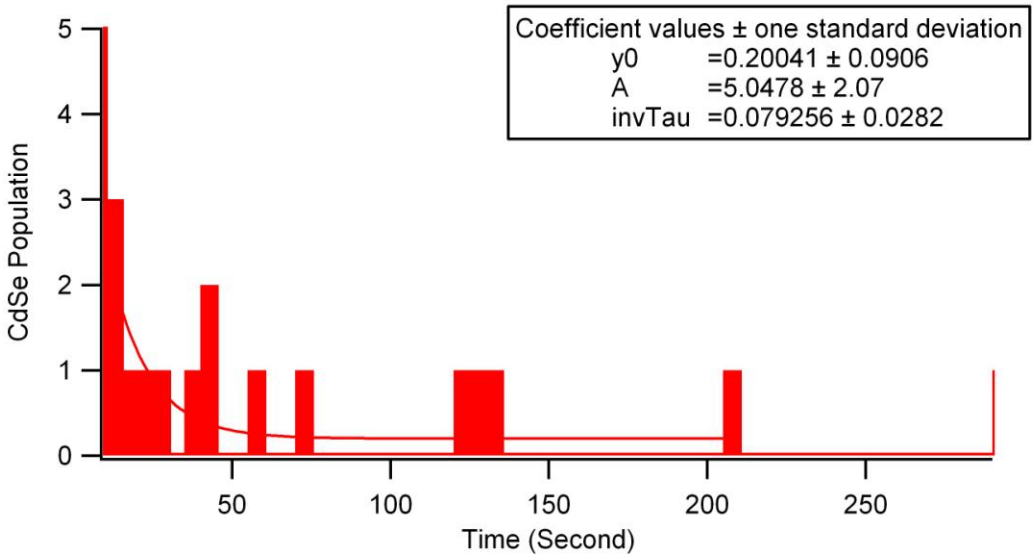

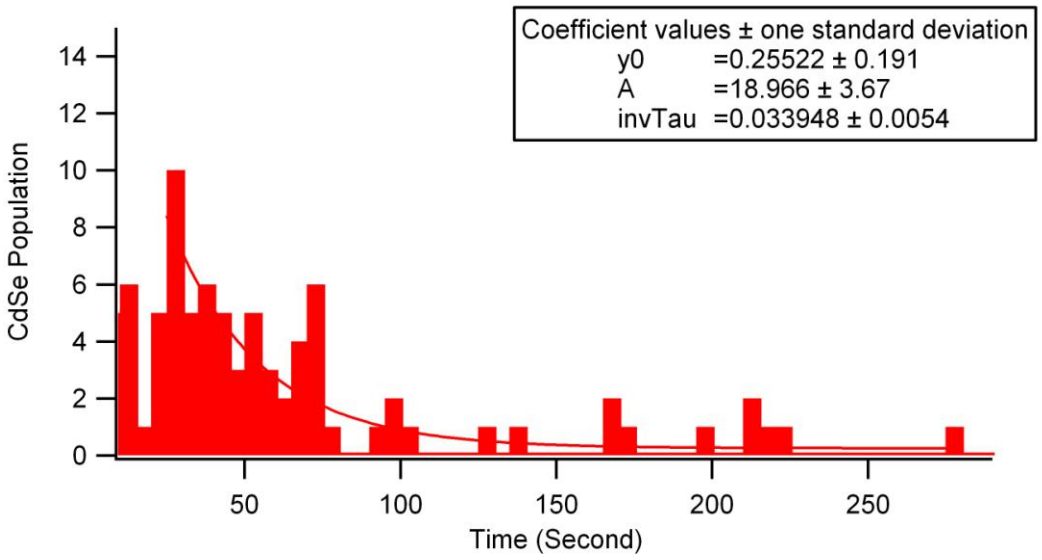
Coefficient values ± one standard deviation
y0 =0.25522 ± 0.191
A =18.966 ± 3.67
invTau =0.033948 ± 0.0054
CdSe Population
Time (Second)

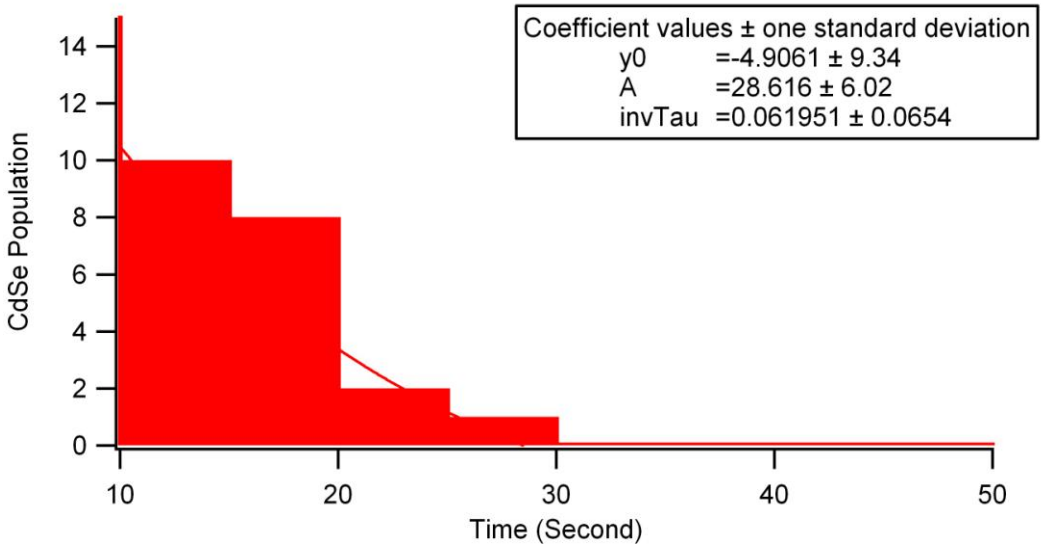
Coefficient values ± one standard deviation
y0 =-4.9061 ± 9.34
A =28.616 ± 6.02
invTau =0.061951 ± 0.0654
CdSe Population
Time (Second)

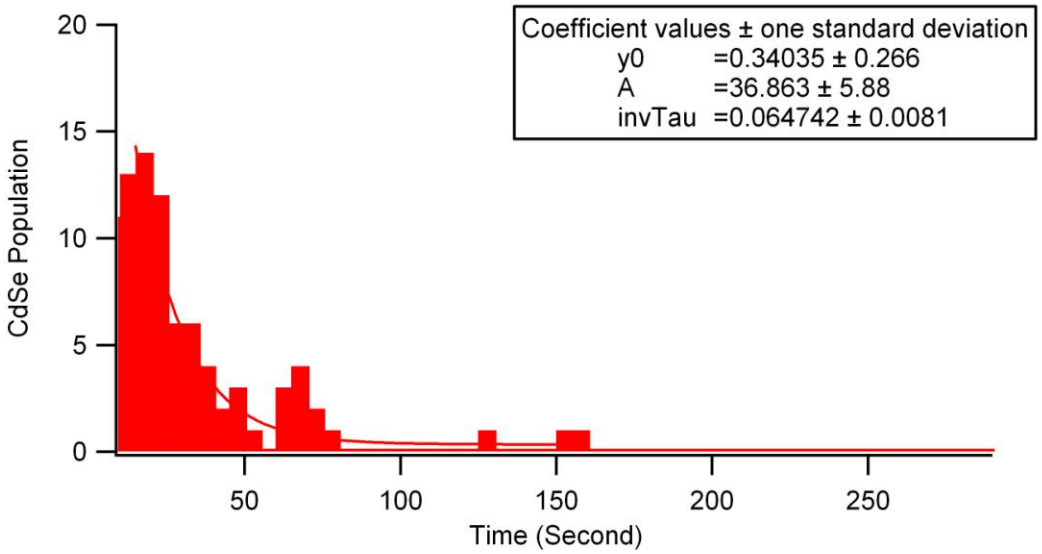
Coefficient values ± one standard deviation
y0 =0.34035 ± 0.266
A =36.863 ± 5.88
invTau =0.064742 ± 0.0081
CdSe Population
Time (Second)

Table B.2 Life Time of aqueous CdSe

1.9 mW	1.9 mW	1.5 mW	1.5 mW	1.0 mW	1.0 mW
Frames (Seconds) 300	500	300	500	300	500
27.7	58.8	12.5	9.1	12.5	16.6
25	43.48	50	41.6	33.3	16.6

B 3. Population of Toluene-Dissolved CdTe Vs Time (Second) at Three Laser Powers

B 3.1. Laser Power = 1.9 mW; Frames 300, 500

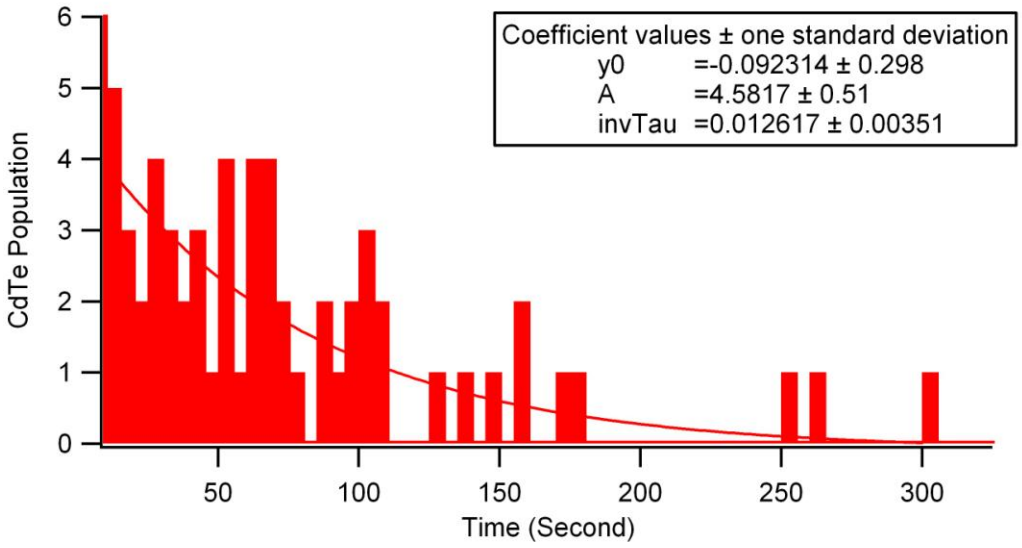

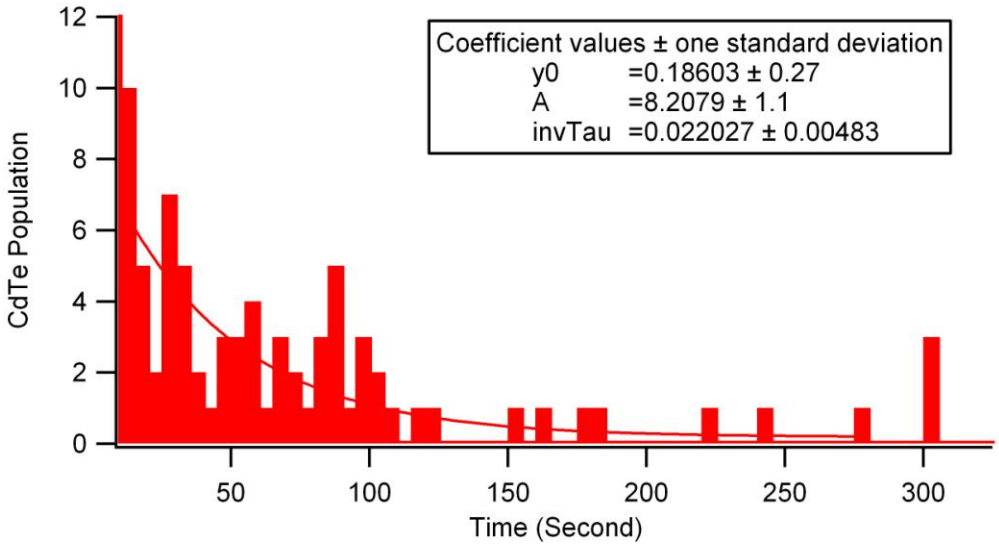

B 3.2 Laser Power = 1.5 mW; Frames 300, 500

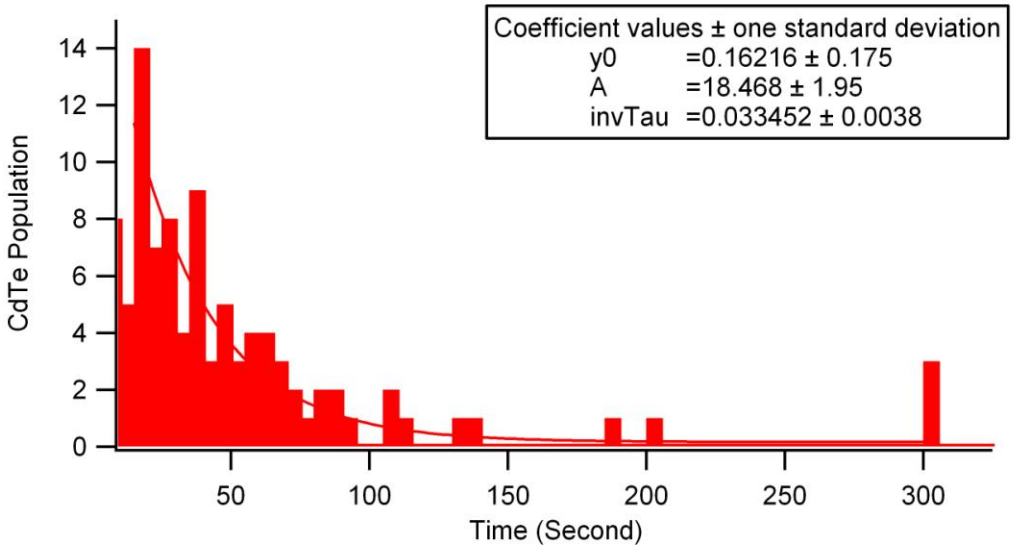

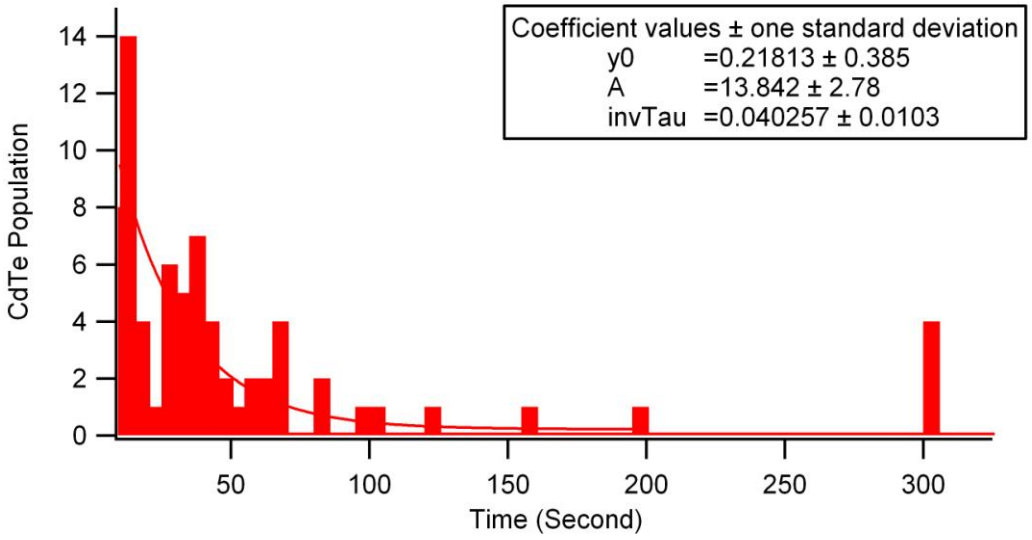

B 3.3 Laser Power = 1.0 mW; Frames 300, 500

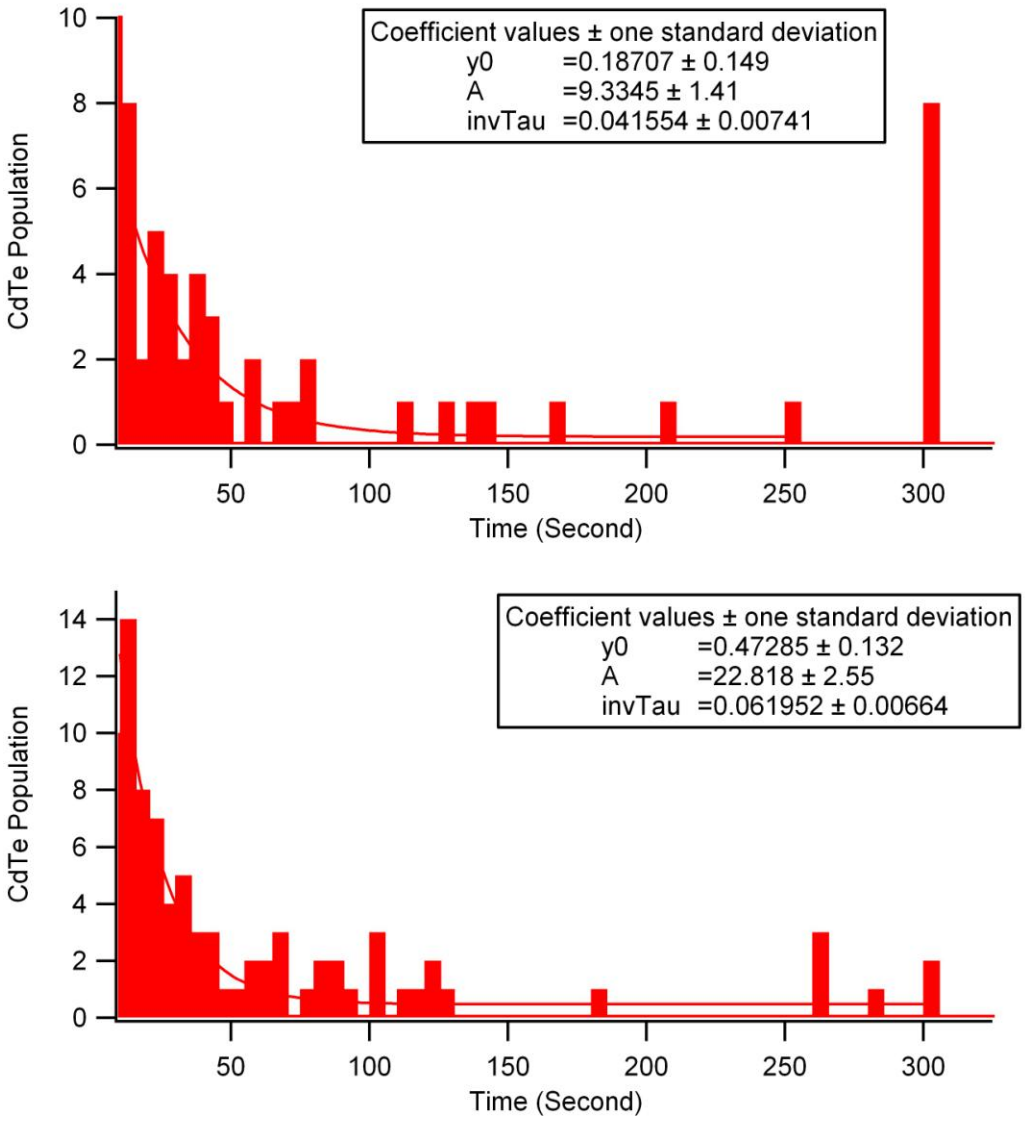

Table B.3 Life time of organic CdTe

1.9 mW	1.9 mW	1.5 mW	1.5 mW	1.0 mW	1.0 mW
Frames (Seconds) 300	500	300	500	300	500
77	50	33.3	25	25	16.13

B4. Still Images from Videos at 0 s and 4s

Aq. CdTe, 1.5mW, Time 0s

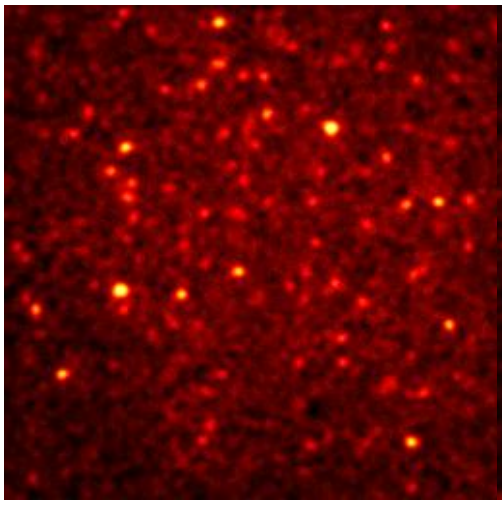

Aq. CdTe, 1.5 mW, Time 4s

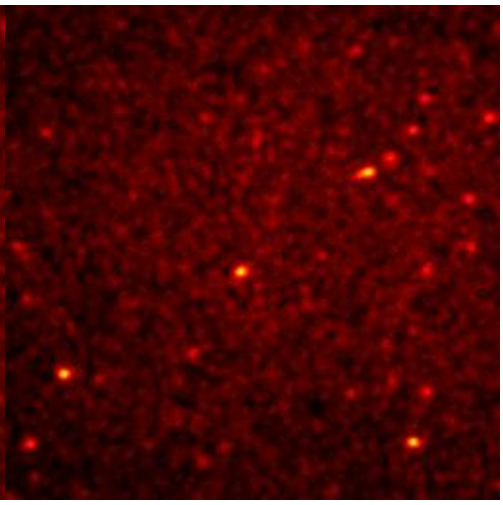

CdTe-TOPO, 1.5mW, Time 0s

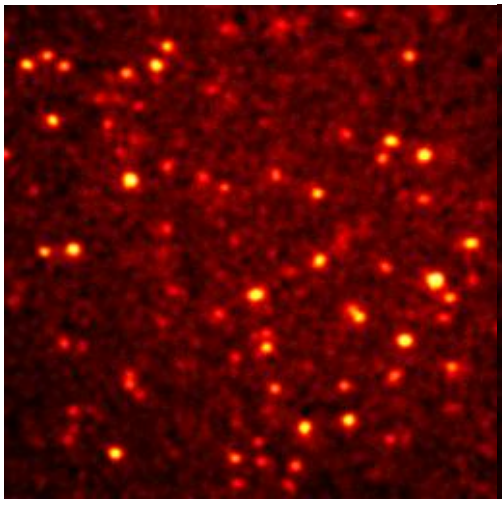

CdTe-TOPO, 1.5mW, Time 4s

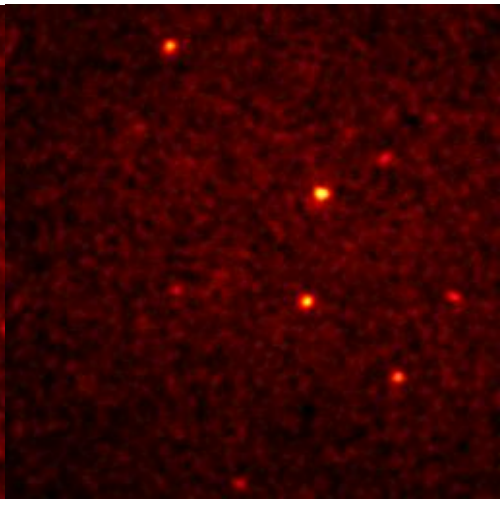

Aq. CdTe, 1.0 mW, Time 0s

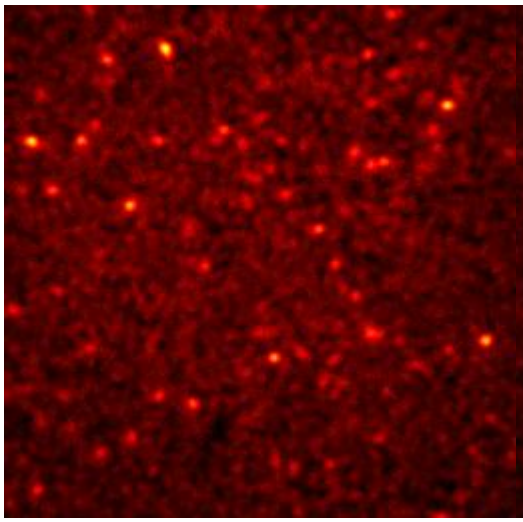

Aq. CdTe, 1.0 mW, Time 4s

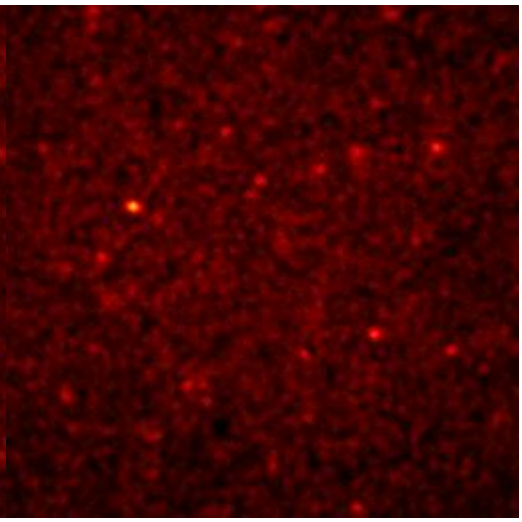

CdTe-TOPO, 1.0mW, Time 0s

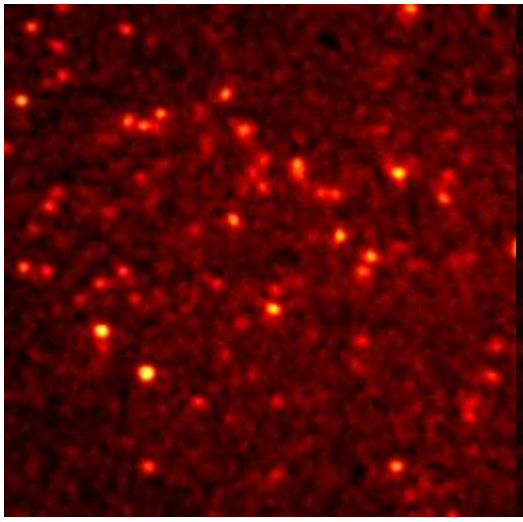

CdTe-TOPO, 1.0mW, Time 4s

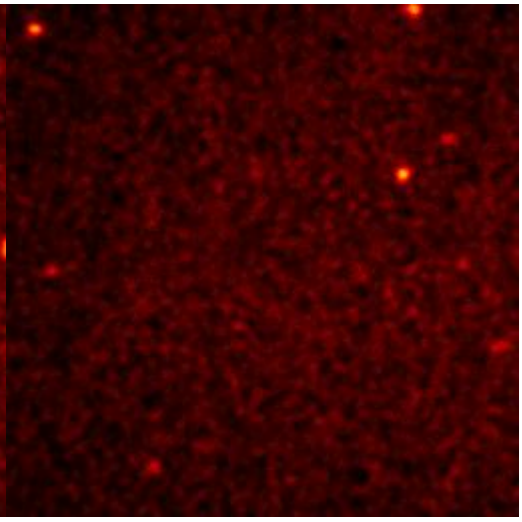

Appendix C - Images from and Confocal and TEM

C.1 Confocal Images of 4,4'-bipyridinium salt based ligands

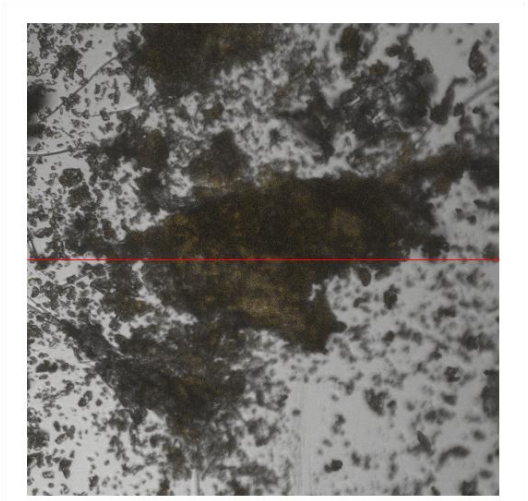

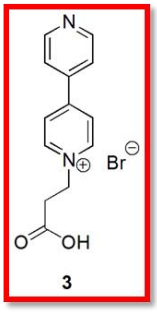

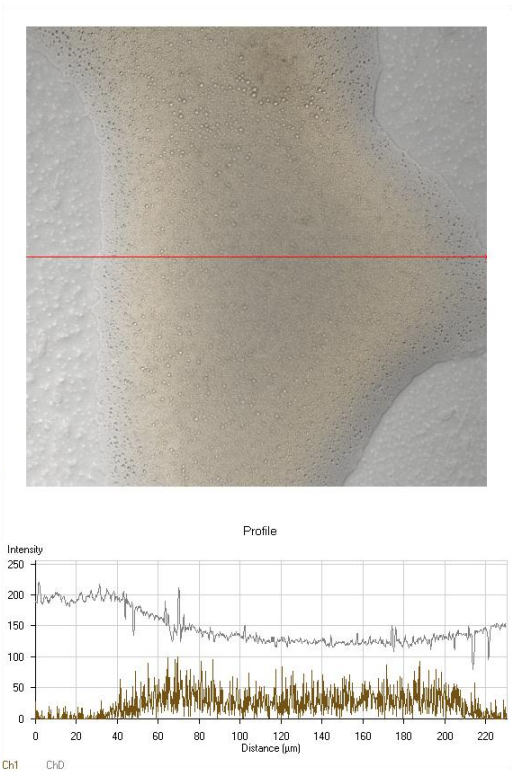

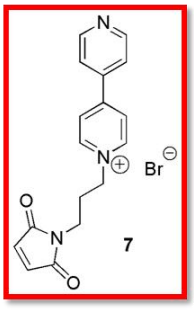

C2. TEM images of CdTe labeled estrogen-derived DNA adducts

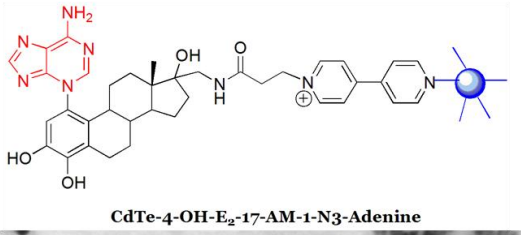

CdTe-4-OH-E_2-17-AM-1-N3-Adenine

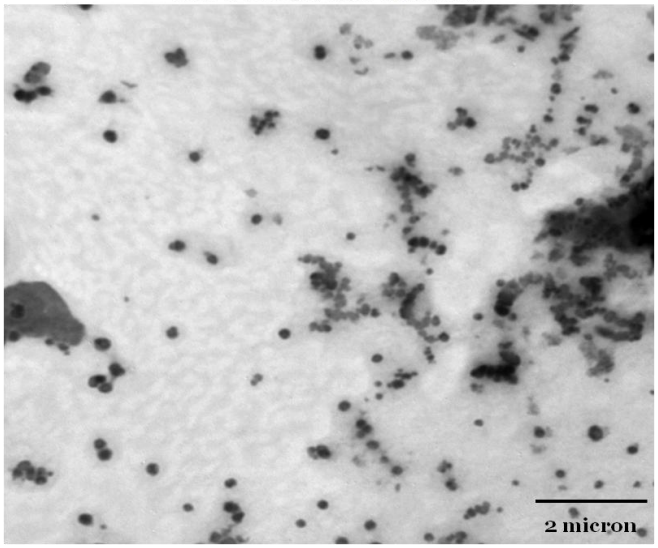

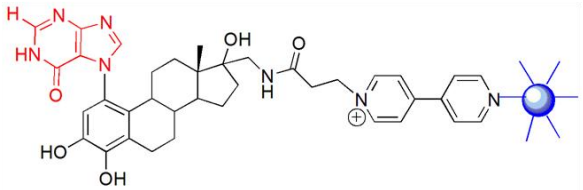

CdTe-4-OH-E_2-17-AM-1-N_7-Guanine